Supporting Information

A multilayer fluorogenic material for the ultrasensitive detection of TATP in air, suitable for implementation on a mechanized semi-autonomous robotic platform.

*Irene Abajo-Cuadrado,[a] Andrea Revilla-Cuesta,[a] Ricardo Fernández-Ordóñez,[a] J. Rafael Santana-Tejada,[a] Yeray Moreno-Macías,[a] Cristian Almeida-Estévez,[a] Carla Hernando-Muñoz,[a] José García-Calvo,[a#] Manuel Avella,[b] Tomás Torroba,[a,]**

[a]Department of Chemistry, Faculty of Science, University of Burgos, 09001 Burgos, Spain.

[b]Electron Microscopy Lab, IMDEA Materials Institute, Eric Kandel, 2, Tecnogetafe, 28906 Getafe (Madrid), Spain.

*E-mail: ttorroba@ubu.es

[#]Permanent Address: Department of Organic Chemistry, Faculty of Science, Autonomous University of Madrid, 28049 Madrid, Spain.

Synthesis of chemical probe.

General methods: Melting points were determined on an electrothermal melting point Gallenkamp apparatus and are uncorrected. Infrared Spectra were recorded with the potassium bromide pellet method, with a JASCO FT/IR-4200 spectrometer. Nuclear magnetic resonance (NMR) spectra were recorded with Varian Mercury-300 and Varian Unity Inova-400 spectrometers at room temperature (25ºC), with $CDCl_3$, CD_3CN and CD_3OD as solvents. Chemical shifts (δ) were reported in parts per million (*ppm*) relative to the residual solvent peaks, rounded to the nearest 0.01 for ^{1}H-NMR and 0.1 for ^{13}C-NMR. Spin-spin coupling constants (*J*) in ^{1}H-NMR were given in Hz, rounded to the nearest 0.1 Hz. Peak multiplicity was indicated as follows: *s* (singlet), *d* (doublet), *t* (triplet), *q* (quartet), *m* (multiplet) and *br* (broad). Relative integrals were given in ^{1}H-NMR too. All ^{13}C NMR were recorded with complete proton decoupling. Carbon types, structure assignments and attribution of peaks were determined from ^{13}C-DEPT-NMR. NMR spectra were analyzed using MestReNova NMR data processing software. MALDI-TOF mass spectra were measured with a MALDI-TOF Bruker Autoflex Mass Spectrometry instrument, using DCTB (*trans*-2-[3-(4-tert-butylphenyl)-2-methyl-2-propenylidene]malononitrile) or DIT (dithranol) as matrixes, in modes positive or negative. The atomic mass of the molecular ion (and/or fragments) per elementary charge were reported in dimensionless quantities. Absorption spectra were acquired with a Hitachi U-3900 spectrometer, in one-centimeter quartz cells at 25ºC. Emission spectra were recorded with a Hitachi F-7000 FL or a modular Edinburgh Instruments FLS980 spectrofluorometers, in one-centimeter quartz cells at 25ºC. Solvatochromism Tests: All samples were freshly prepared in each different solvent. Photos were taken with a Canon (EOS M3) camera with a 22 mm lens. Absorption spectra were acquired with a Hitachi U-3900 spectrometer, in one-centimeter quartz cells at 25ºC. Emission spectra were recorded with Hitachi F-7000 FL spectrofluorometer, in one-centimeter quartz cells at 25ºC. The solvents were, if it is not said otherwise: 1: H_2O, 2: MeOH (methanol), 3: DMSO (dimethyl sulfoxide), 4: DMF (*N*,*N'*-dimethylformamide), 5: MeCN (acetonitrile), 6: Acetone, 7: AcOEt (ethyl acetate), 8: THF (tetrahydrofuran), 9: $CHCl_3$, 10: CH_2Cl_2 (dichloromethane), 11: Toluene, 12: Et_2O (diethyl ether), 13: *n*-Hx (hexane), 14: *c*-Hx (cyclohexane). Fluorescence Lifetime Decays: Chromophore solutions were freshly prepared in a concentration of 1-10 μM in the corresponding solvent. The decay was fitted (black) with a sum of two exponentials by convolution with the instrumental response function (red). The quality of the fit was judged by $\chi 2$ values and the plot of the weighted residues. Measurements were made with a modular spectrometer Edinburgh Instruments FLS980, with a source excitation pulsed lasers of picosecond diode: 366-380 nm, 398-410 nm, 437-446 nm, 470-478 nm, 505-515 nm and 635 nm. One-centimeter quartz cells, at 25 ºC, were employed. Quantum Yields: Fresh solutions made from high-purity dyes (or mixtures of dye with an additive) and solvent were used. Integrating sphere was used as the method and three measurements were performed for each sample in order to calculate the average. Solutions were prepared in a concentration of 1-10 μM in the corresponding solvent. The excitation wavelength is indicated in each case. Measurements were made with a modular spectrometer Edinburgh Instruments FLS980. One-centimeter quartz cells, at 25ºC, were employed.

Synthesis of *N*-(*N'*-Boc-piperidin-4-yl)-4-bromonaphthalene-1,8-dicarboxylmonoimide (AR43p)

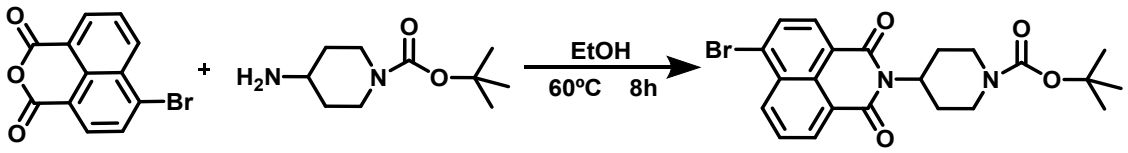

In a 100 ml flask, provided with a magnetic stirrer, 2 g of 4-bromo-1,8-naphtalic anhydride (7.22 mmol) and 2.9 g of 4-amino-1-Boc-piperidine (14.44 mmol) were dissolved in 40 ml of ethanol and the mixture was stirred 8 hours at 60ºC. After that, the mixture was filtered, cooling to room temperature and the solvent was evaporated under reduced pressure. The organic solid was purified by column chromatography (SiO_2, CH_2Cl_2), getting 3.15 g of AR43p, white solid, 95% yield. m.p.: 148 – 150ºC. IR (ATR, cm^{-1}): 2977 – 2849, 1689 (C=O), 1649 (C=O), 1419 (C-O), 1359, 1344, 1244, 1173 (C-N), 1143 (-CH_3), 1101, 1032 (C-Br), 981, 894, 774, 747, 424. ^{1}H-NMR (300 MHz, $CDCl_3$) δ (ppm): 8.48 (d, *J* = 7.1 Hz, 1H, H_{Ar}), 8.35 (d, *J* = 8.4 Hz, 1H, H_{Ar}), 8.23 (d, *J* = 7.9 Hz, 1H, H_{Ar}), 7.86 (d, *J* = 7.9 Hz, 1H, H_{Ar}), 7.70 (t, *J* = 7.9 Hz, 1H, H_{Ar}), 5.17 – 5.02 (m, 1H, CH), 4.26 (s, 2H, CH_2), 2.69 (m, 4H, 2×CH_2), 1.64 (m, 2H, CH_2), 1.45 (s, 9H, 3×CH_3). ^{13}C-NMR (75MHz, $CDCl_3$) δ (ppm): 163.3 (C=O), 163.2 (C=O), 154.3 (C=O), 132.4 ($C_{Ar}H$), 131.5 ($C_{Ar}H$), 130.7 ($C_{Ar}H$), 130.6 ($C_{Ar}H$), 129.8 (C_{Ar}), 129.5 (C_{Ar}), 128.3 (C_{Ar}), 127.6 ($C_{Ar}H$), 122.9 (C_{Ar}), 122.0 (C_{Ar}), 79.2 (Cq), 51.6 (CH), 43.8 (CH_2), 28.2 (CH_3), 27.9 (CH_2). HRMS (MALDI, DCTB-) m/z: calculated for $C_{22}H_{23}BrN_2O_4$: 458.0836 (M^-); found 458.0802.

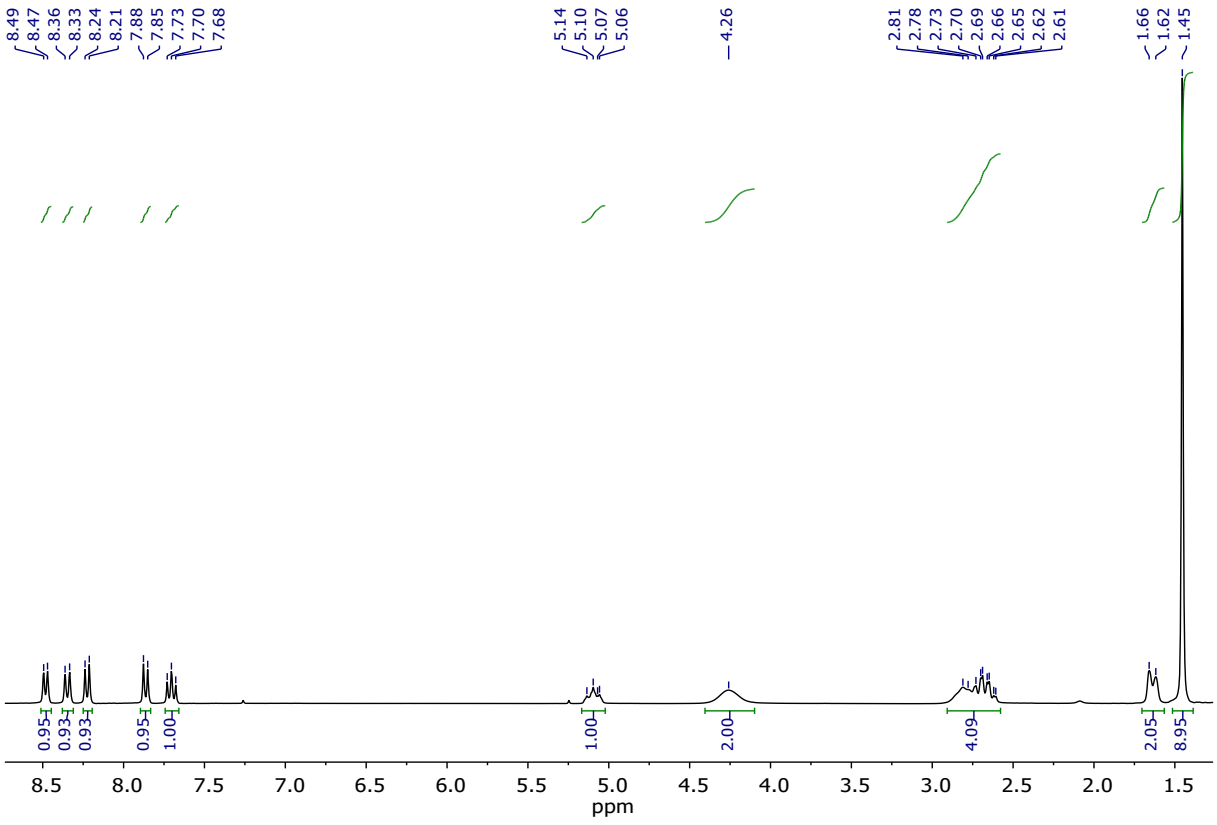

Figure S01. ^{1}H-NMR ($CDCl_3$, 300 MHz) of AR43p.

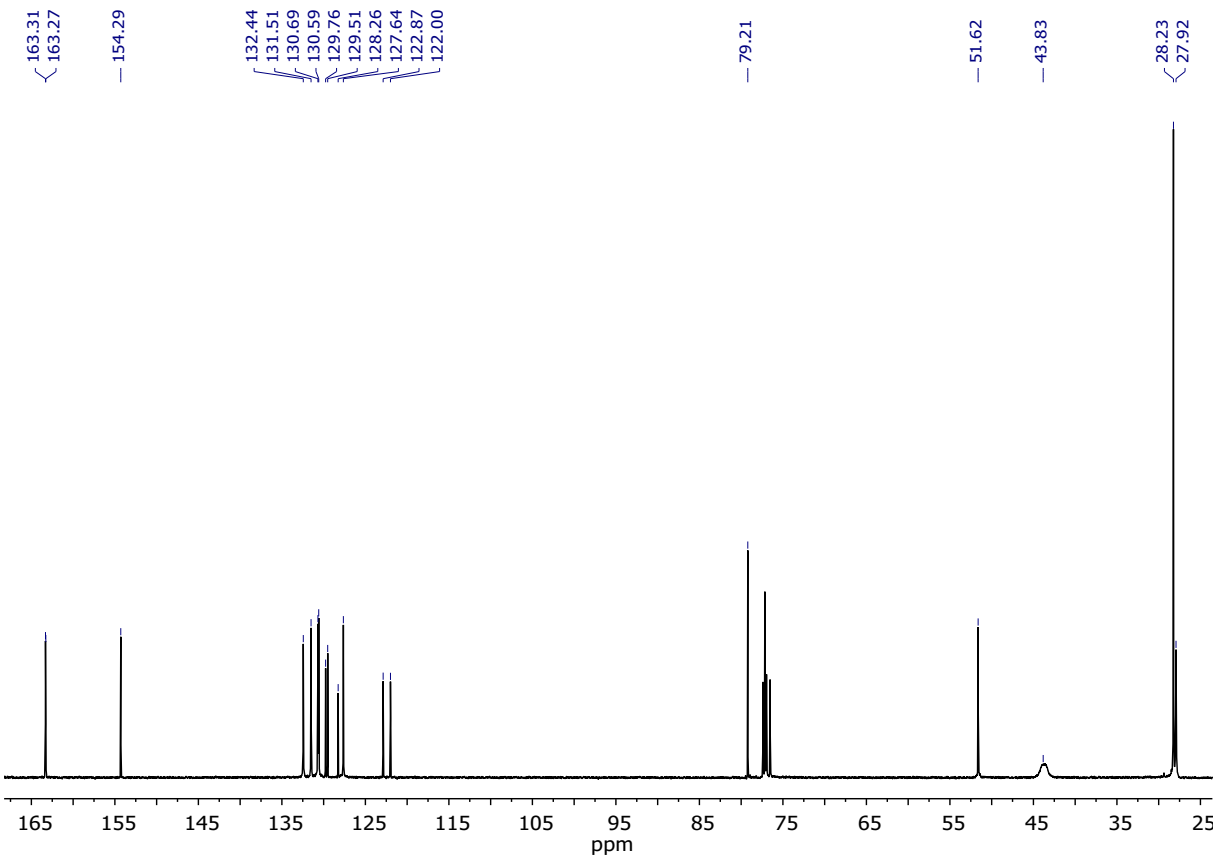

Figure S02. ^{13}C-NMR ($CDCl_3$, 75 MHz) of AR43p.

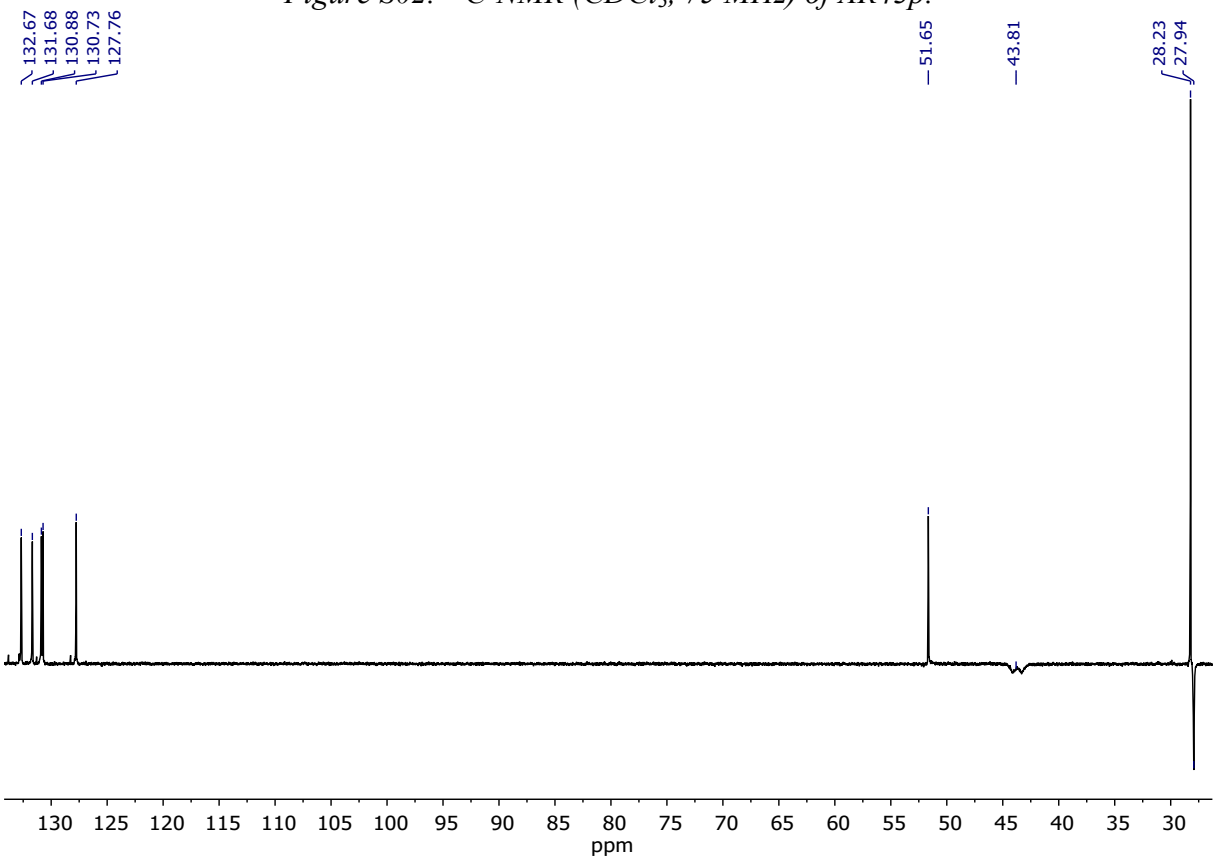

Figure S03. DEPT NMR ($CDCl_3$, 75 MHz) of AR43p.

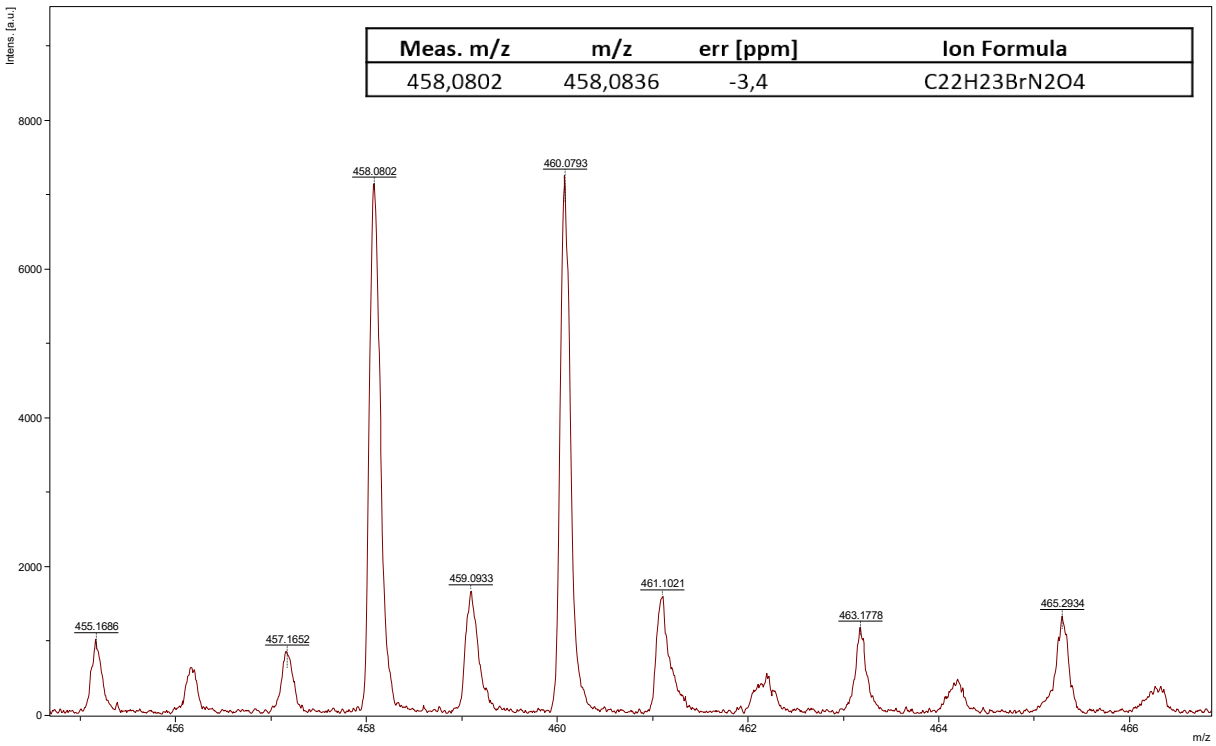

Figure S04. HRMS (MALDI, DCTB-) of AR43p.

Synthesis of *N*-(piperidin-4-yl)-4-bromonaphthalene-1,8-dicarboxylmonoimide (AR43d)

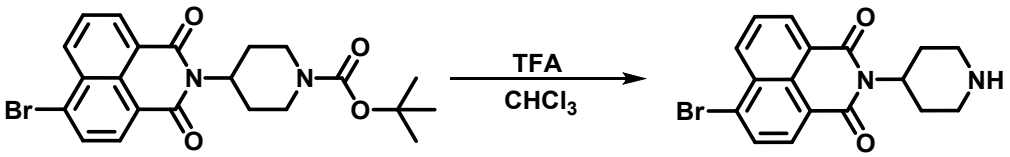

In a 50 ml flask with a magnetic stirrer, 150 mg of *N*-(*N'*-Boc-piperidin-4-yl)-4-bromonaphthalene-1,8-dicarboxylmonoimide (AR43, 0.33 mmol) were dissolved in 15 ml of chloroform and 2 ml of trifluoroacetic acid (26 mmol) were added, and the mixture was stirred for 4 hours at room temperature. Afterwards, 10 ml of water were poured into the flask and the mixture was neutralized employing a 40% sodium hydroxide solution until it reached a neutral pH. Then, 20 ml of water were added and the mixture was extracted with chloroform (3×30 ml). The organic extracts were combined, dried over anhydrous Na_2SO_4 and the solvent was evaporated under reduced pressure. The product AR43d was obtained quantitatively as a white solid, 100% yield (117 mg). m.p.: 88 – 89ºC. IR (ATR, cm^{-1}): 3359 (N-H), 2973 – 2830, 1686 (C=O), 1579, 1477, 1417, 1390, 1357, 1238, 1162 (C-N), 1121, 1097, 1076, 1049, 998 (C-Br), 932, 861, 807, 761, 642, 543, 511, 462, 408. ^{1}H-NMR (300 MHz, CD_3OD) δ (ppm): 8.61 – 8.55 (m, 2H, 2×H_{Ar}), 8.36 (d, *J* = 7.9 Hz, 1H, H_{Ar}), 8.10 (d, *J* = 7.9 Hz, 1H, H_{Ar}), 7.90 (dd, *J* = 8.5, 7.3 Hz, 1H, H_{Ar}), 5.31 (m, 1H, CH), 3.60 – 3.52 (m, 2H, NH y ½CH_2), 3.27 – 2.93 (m, 5H, 2×CH_2 y ½CH_2), 2.04 – 1.95 (m, 2H, CH_2). ^{13}C-NMR (75MHz, $CDCl_3$) δ (ppm): 163.7 (C=O), 133.1 ($C_{Ar}H$), 132.1 ($C_{Ar}H$), 131.3 ($C_{Ar}H$), 131.1 ($C_{Ar}H$), 128.9 (C_{Ar}), 128.1 ($C_{Ar}H$), 123.3 (C_{Ar}), 122.4 (C_{Ar}), 53.4 (Cq), 50.6 (CH), 45.5 (CH_2), 27.7 (CH_2). HRMS (MALDI, DCTB+) m/z: calculated for $C_{17}H_{15}BrN_2O_2$: 359.0390 (M^+ + H); found 359.0391.

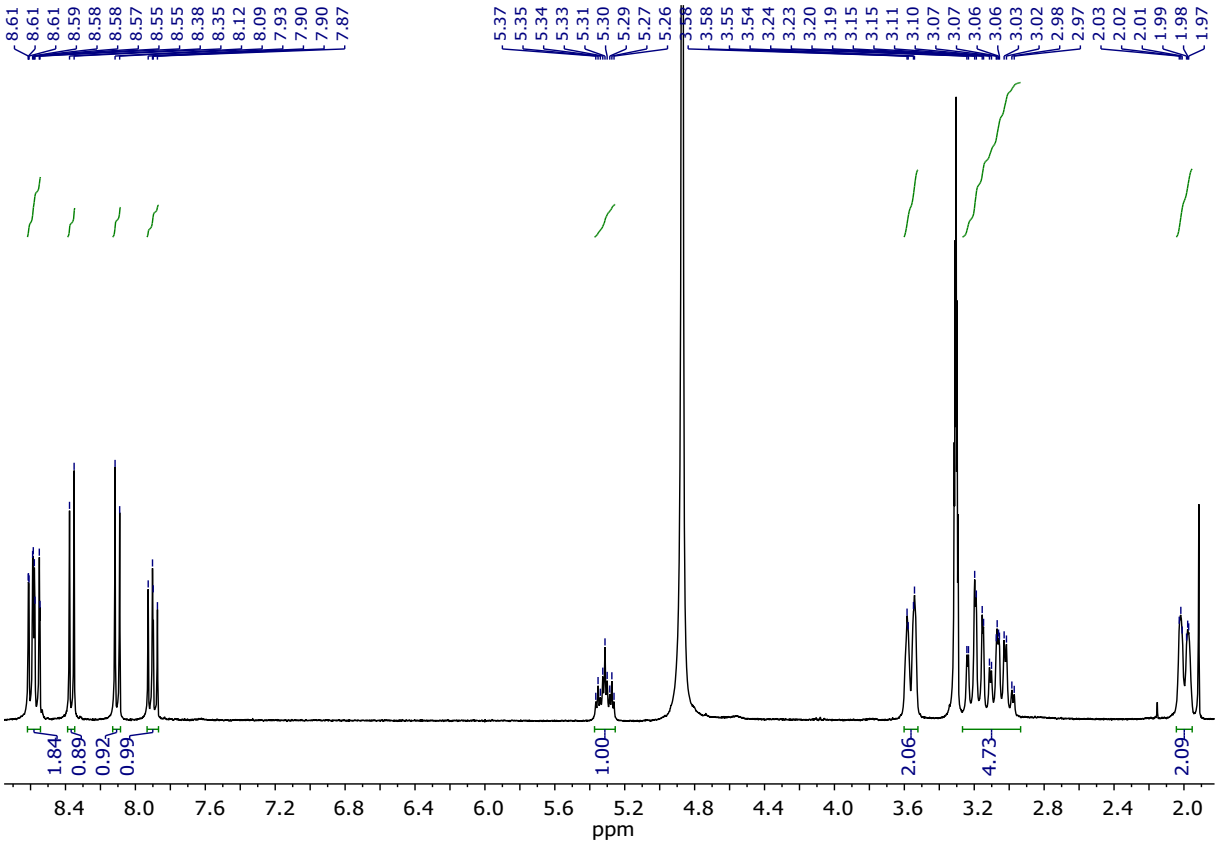

Figure S05. [1]H-NMR (CD_3OD, 300 MHz) of AR43d.

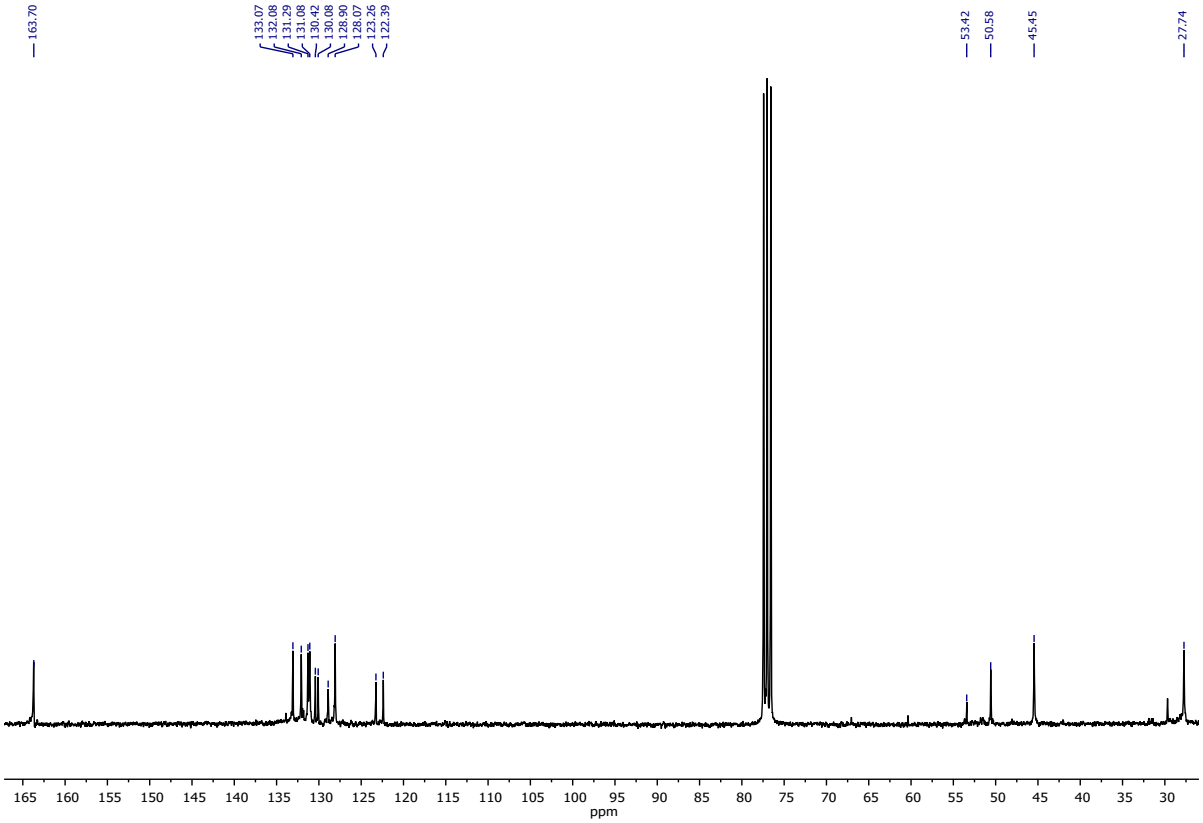

Figure S06. [13]C-NMR ($CDCl_3$, 75 MHz) of AR43d.

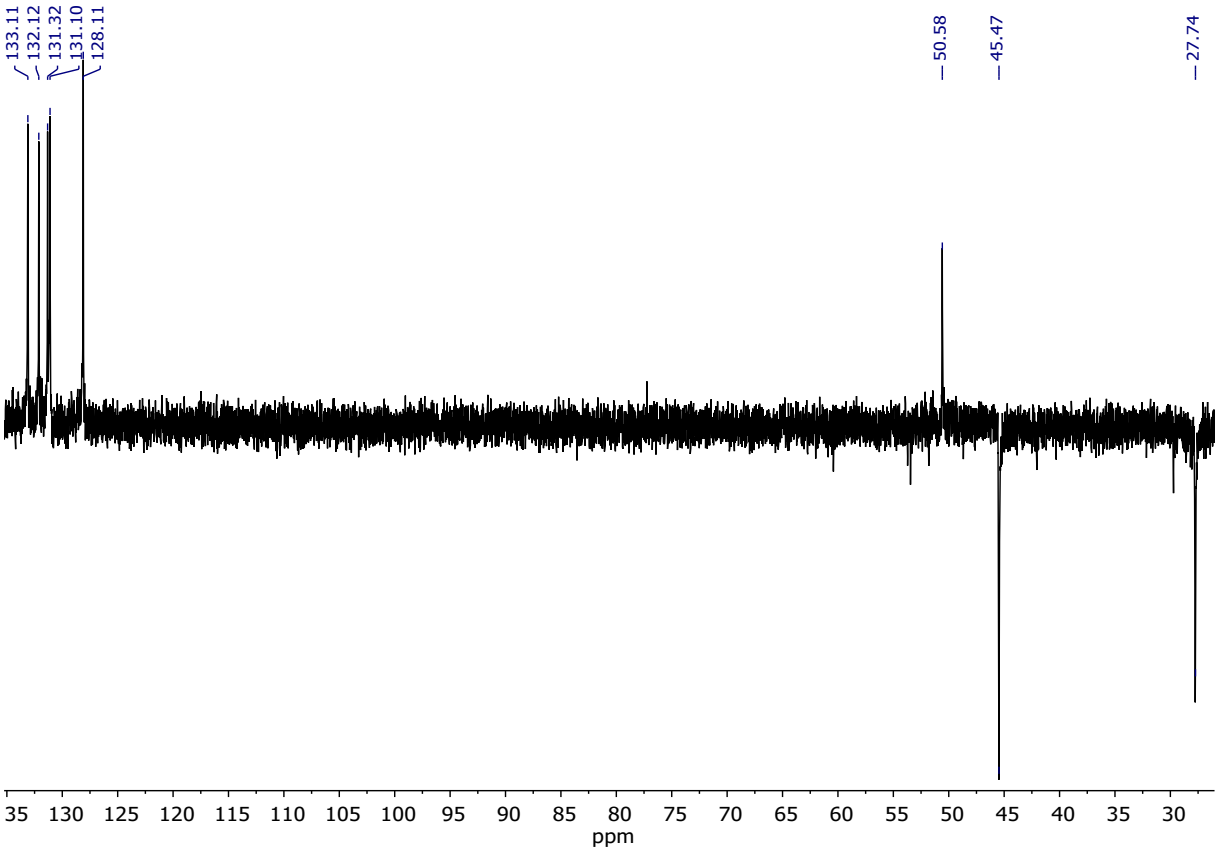

Figure S07. DEPT NMR ($CDCl_3$, 75 MHz) of AR43d.

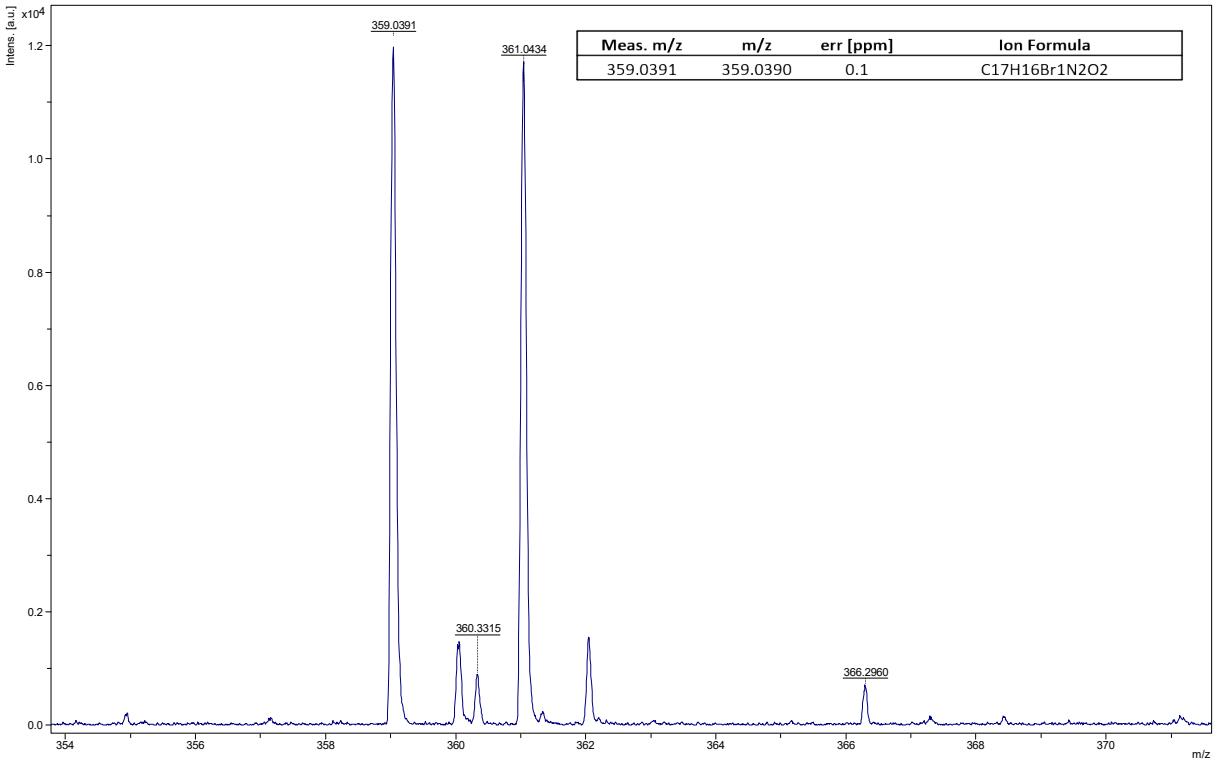

Figure S08. HRMS (MALDI, DCTB+) of AR43d.

Synthesis of *N*-(piperidin-4-yl)-4-[2-(4-Boc-piperazin-1-yl)pyrimidin-5-yl]naphthalene-1,8-dicarboxylmonoimide (ACTD)

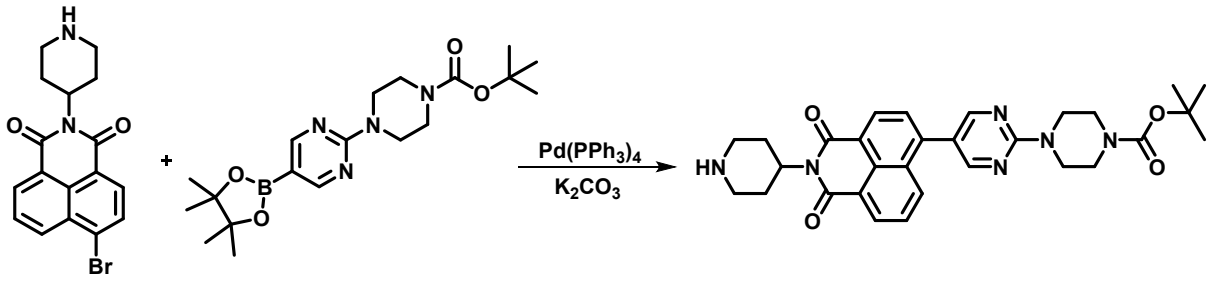

150 mg of *N*-(piperidin-4-yl)-4-bromonaphthalene-1,8-dicarboxylmonoimide (AR43d, 0.42 mmol), 172 mg of 2-(4-Boc-piperazin-1-yl)pyrimidin-5-yl boronic acid pinacol ester (0.44 mmol) and 451 mg of potassium carbonate (3.26 mmol) were dissolved in a mixture of toluene:butanol:water (4:1:2 ml) under nitrogen atmosphere and, then, the $Pd(PPh_3)_4$ (5% mmol) was added. The resulting mixture was stirred overnight at 110ºC, the solvent was evaporated under reduce pressure. The solid was dissolved in CH_2Cl_2 and washed with water (3×100 ml). The organic extracts were combined, dried over anhydrous Na_2SO_4 and the solvent was evaporated under reduce pressure. The organic solid was purified by column chromatography (SiO_2, CH_2Cl_2:MeOH 50:1) getting 87 mg of ACTD, yellow solid, 38% yield. m.p.: 302 – 304ºC (decomposition). IR (ATR, cm^{-1}): 3440 (N-H), 2922 – 2480, 1693 (C=O), 1650 (C=O), 1585, 1509, 1450 (C-O), 1402, 1351, 1238, 1162 (C-N), 1121, 998, 947, 780, 753, 687, 642, 508. ^{1}H-NMR (300 MHz, $CDCl_3$) δ (ppm): 8.62 (dd, *J* = 7.4, 1.7 Hz, 2H, 2×H_{Ar}), 8.50 (s, 2H, 2×H_{Ar}), 8.25 (dd, *J* = 8.5, 1.1 Hz, 1H, H_{Ar}), 7.73 (dd, *J* = 8.5, 7.4 Hz, 1H, H_{Ar}), 7.64 (d, *J* = 7.4 Hz, 1H, H_{Ar}), 5.26 – 5.13 (m, 1H, CH), 3.93 (m, 4H, 2×CH_2), 3.56 (m, 4H, 2×CH_2), 3.29 (m, 2H, CH_2), 2.89 – 2.65 (m, 4H, 2×CH_2), 2.13 (s, 1H, NH), 1.73 (m, 2H, CH_2), 1.51 (s, 9H, 3×CH_3). ^{13}C-NMR (75 MHz, $CDCl_3$) δ (ppm): 164.5 (C=O), 164.3 (C=O), 164.1 (C=O), 158.2 (C_{Ar}H), 154.9 (C_{Ar}), 140.7 (C_{Ar}), 132.1 (C_{Ar}), 131.9 (C_{Ar}H), 131.8 (C_{Ar}), 131.7 (C_{Ar}), 131.5 (C_{Ar}), 131.4 (C_{Ar}), 130.1 (C_{Ar}), 129.0 (C_{Ar}), 127.8 (C_{Ar}H), 127.5 (C_{Ar}H), 123.3 (C_{Ar}), 122.2 (C_{Ar}), 121.0 (C_{Ar}), 80.4 (Cq), 44.1 (CH_2), 28.6 (CH_3), 25.8 (CH_2). HRMS (MALDI, DCTB+) m/z: calculated for $C_{30}H_{34}N_6O_4$: 543.2714 (M^+ + H); found 543.2689. UV-Vis ($CHCl_3$), λ_{max} nm (log ε): 385 (4.9). Ø ($CHCl_3$, %): 73.00. τ (375 nm, $CHCl_3$, ns): 3.962 (χ^2: 1.072).

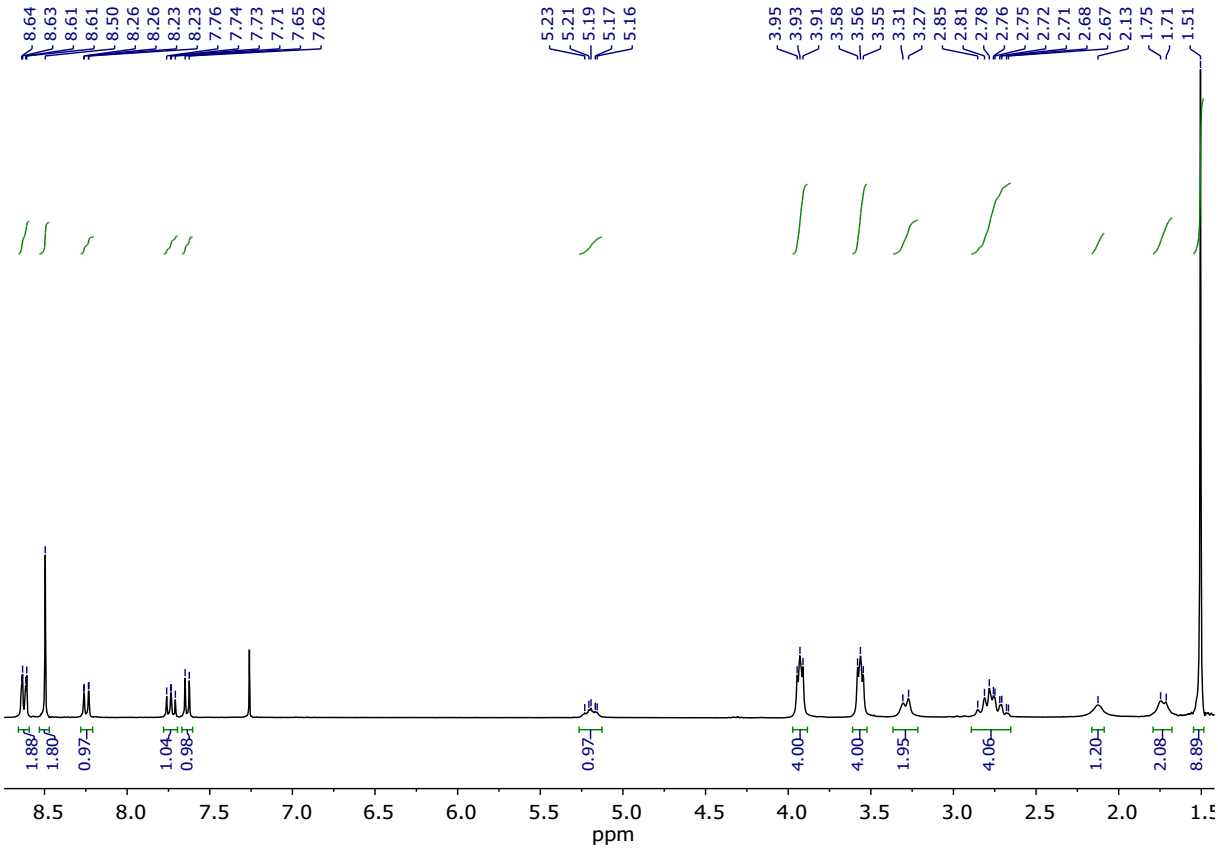

Figure S09. ^{1}H-NMR ($CDCl_3$, 300 MHz) of ACTD.

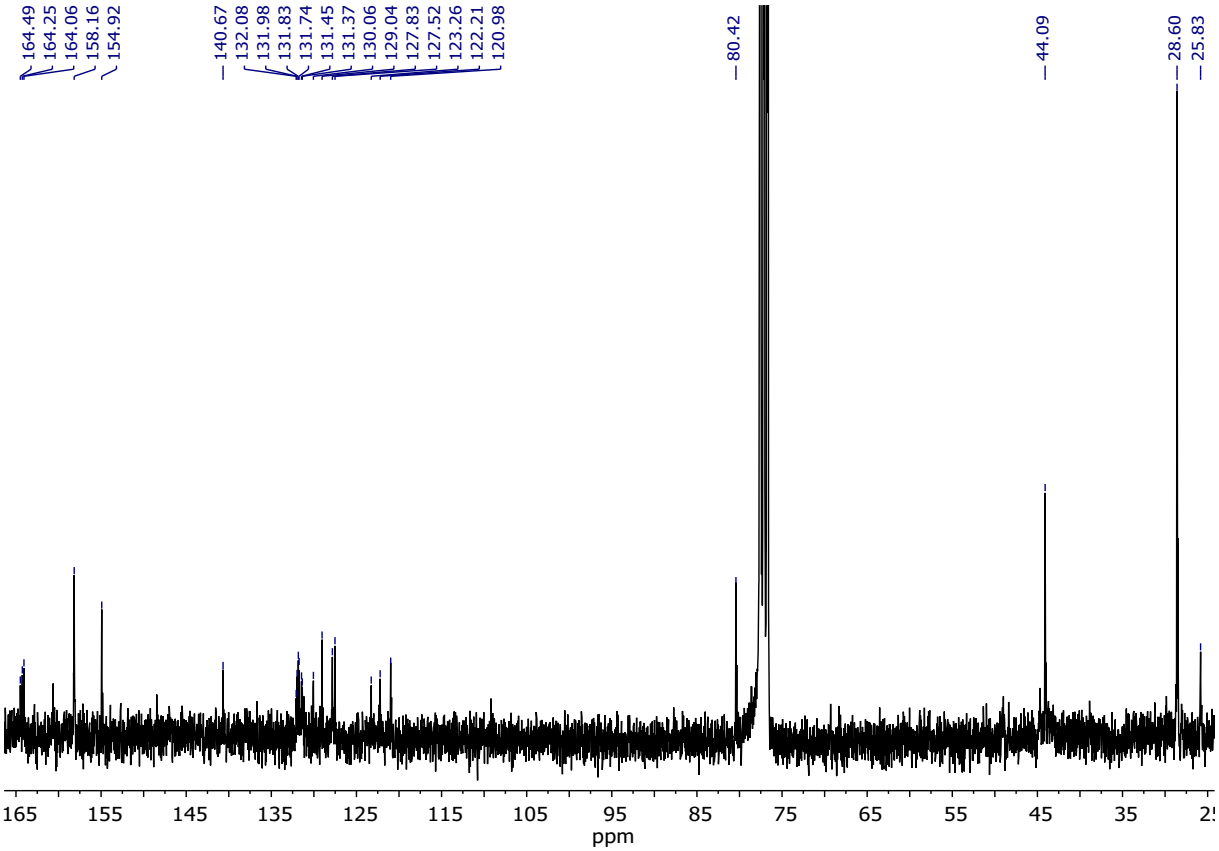

Figure S10. ^{13}C-NMR ($CDCl_3$, 75 MHz) of ACTD.

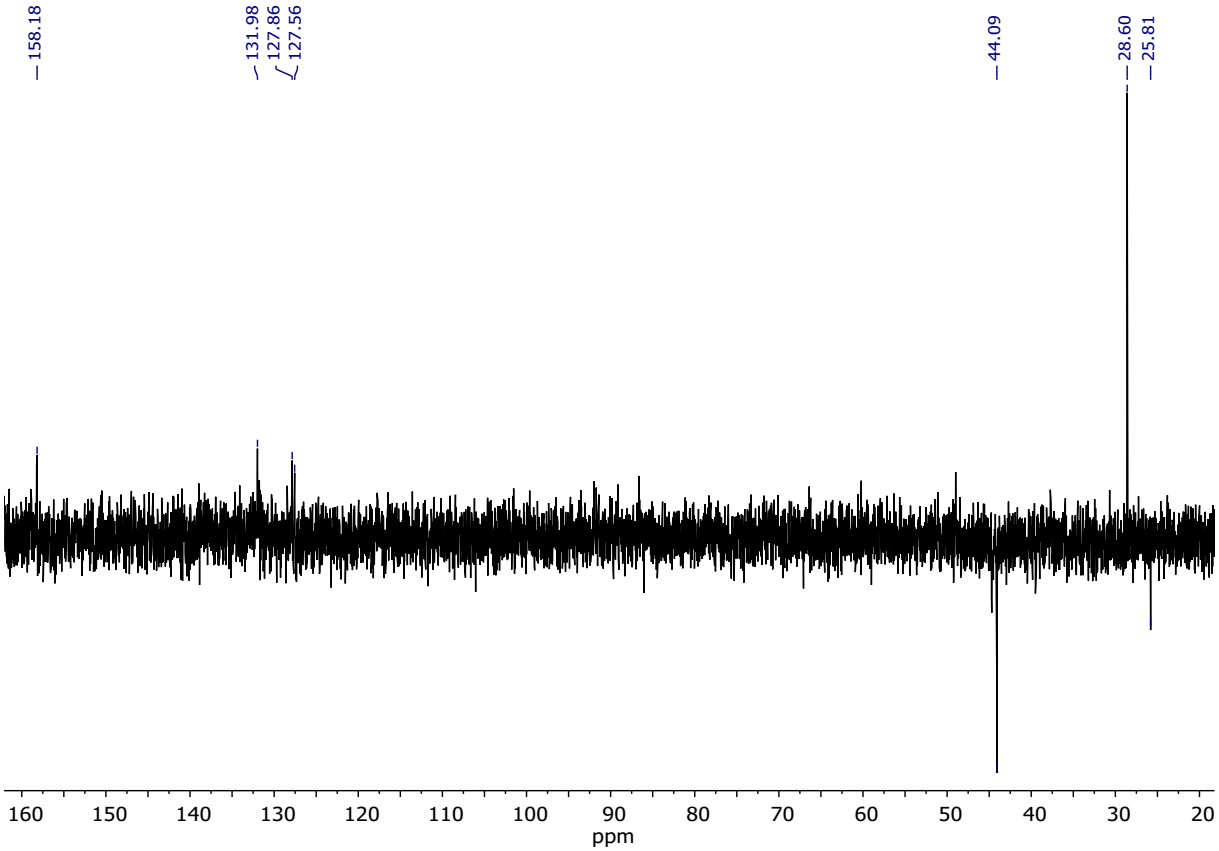

Figure S11. DEPT NMR ($CDCl_3$, 75 MHz) of ACTD.

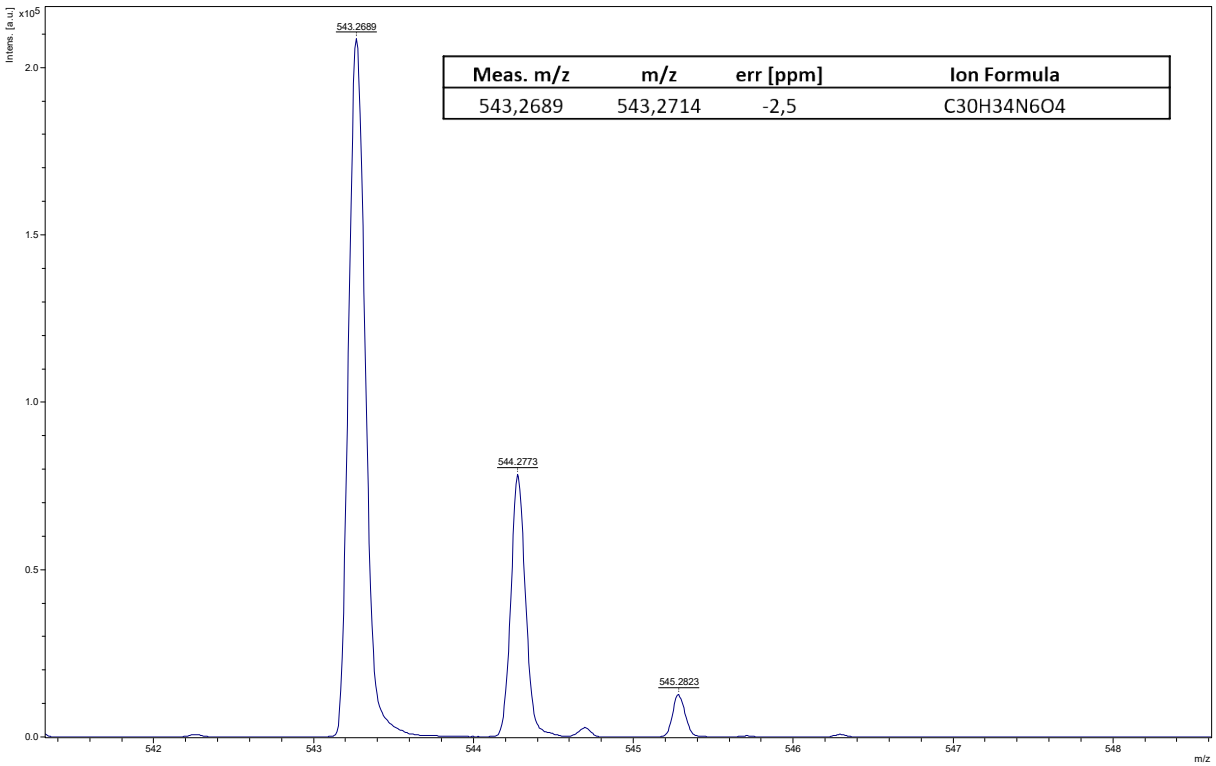

Figure S12. HRMS (MALDI, DCTB+) of ACTD.

Solvatochromism: The concentration of the compound was 20 μM and the excitation wavelength was 370 nm.

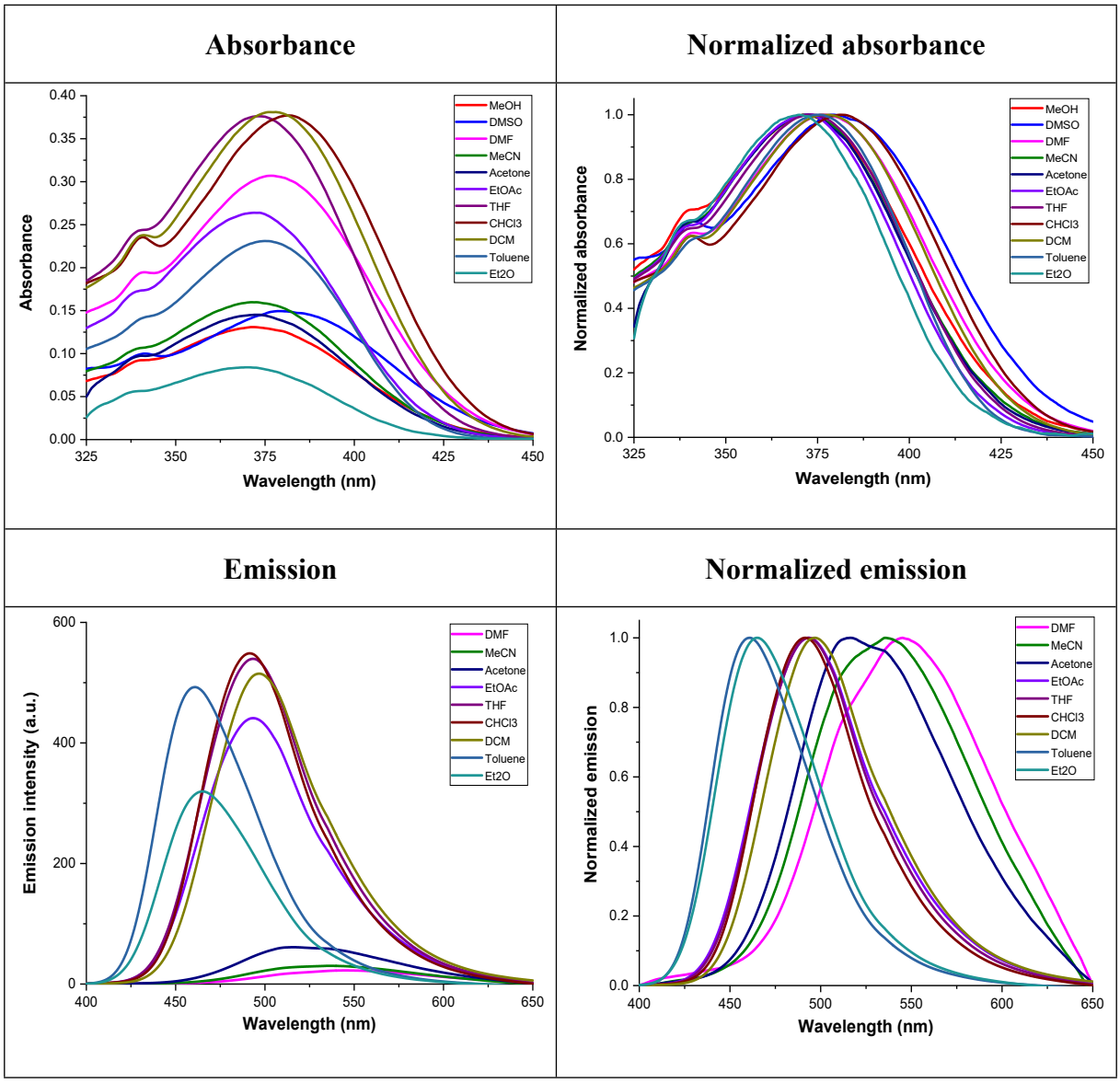

Figure S13. Solvatochromism of ACTD.

Fluorescence decay lifetime (τ): The solvent used was $CHCl_3$. The concentration of the compound was 20 μM.

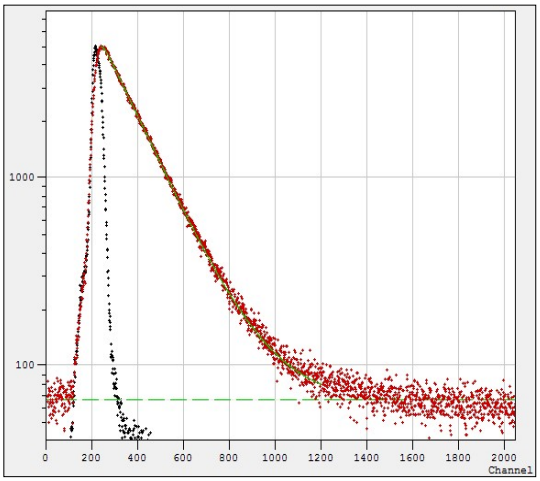

Figure S14. Fluorescence decay lifetime of ACTD.

DETECTION OF AIRBORNE TAPT BY TABLETOP EXPERIMENTS:

Figure S15. The LED/Mini-fluorometer/laptop experiments.

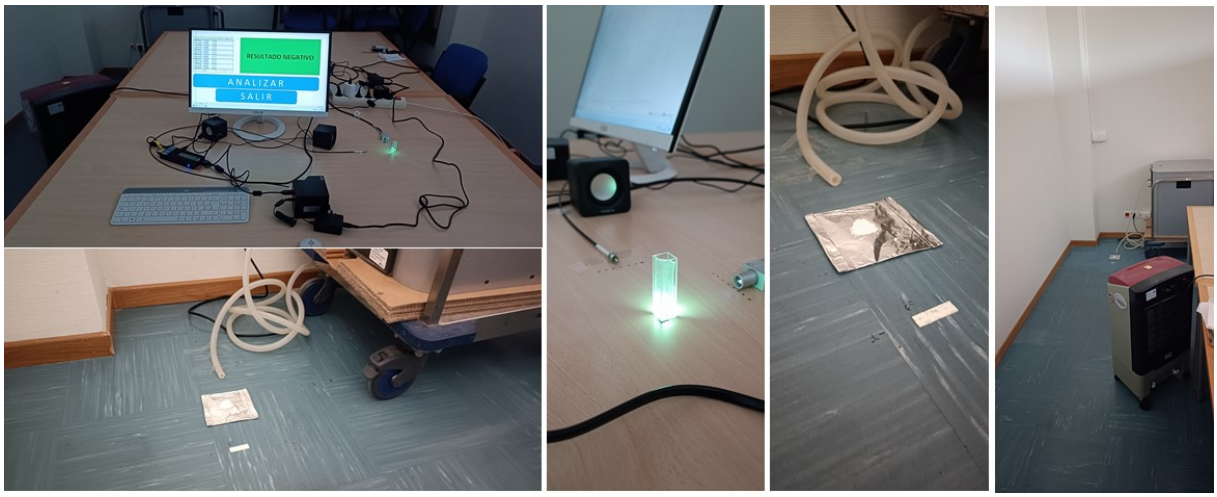

Figure S16. The LED/Mini-fluorometer/Mini-PC experiments.

1. Experiment 1: 24-26°C_30 minutes (DAY 1)

6 mg of TATP were evaporated over a 30-minute period under a temperature of 24 – 26°C. The emission spectra of the particles before and after exposure to TATP vapors were measured using both Hamamatsu C10082CA mini-spectrometer and Edimburgh FLS980 Spectrometer in order to evaluate the performance of the Hamamatsu C10082CA mini-spectrometer and verify that the results are comparable to those obtained in the experiments carried out to date. The experimental conditions in the case of the Hamamatsu devise were acquisition time = 100000 μs (default value) and LED intensity = 2 %. Edimburgh instrument parameters were λexc = 370 nm, Δλexc = 0.30 nm, Δλem = 0.15 nm, integration time 0.3 s/step and step of 1 nm for all samples. A comparative table of the results is shown below in **Table S1**, in order of increasing distance from the TATP source (10 – 25 – 50 – 75 – 100 – 150 – 200 – 300 cm).

HAMAMATSU C10082CA MINI-SPECTROMETER	EDIMBURGH FLS980 SPECTROMETER
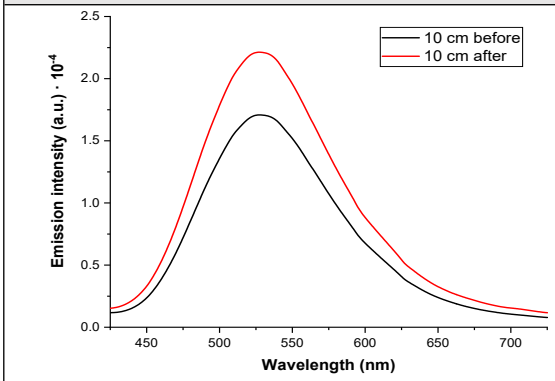	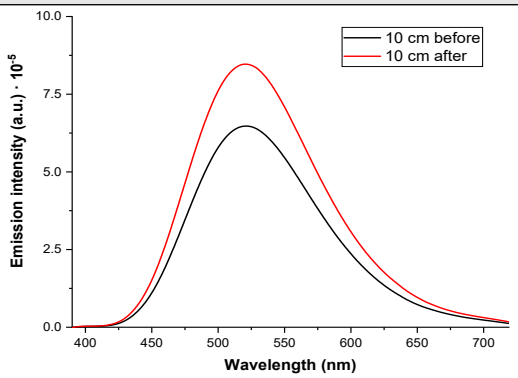
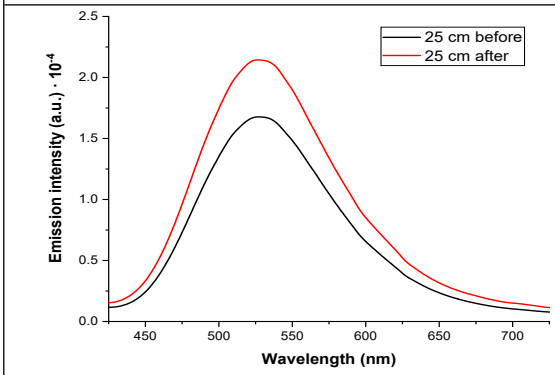	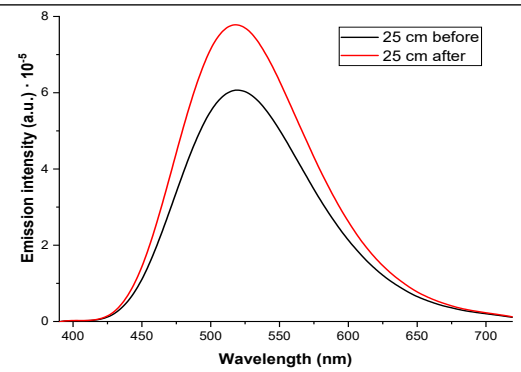
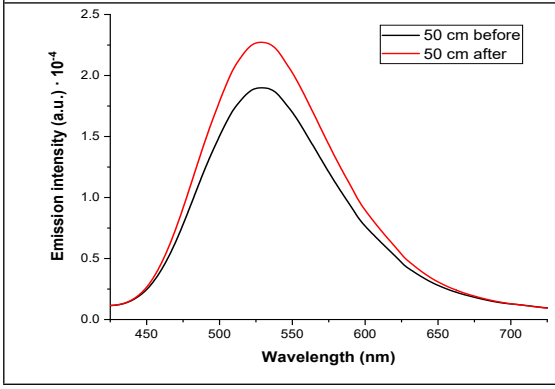	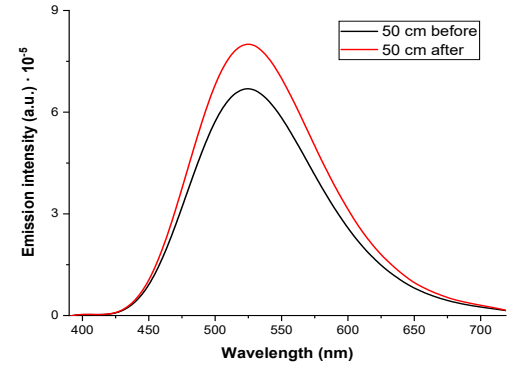

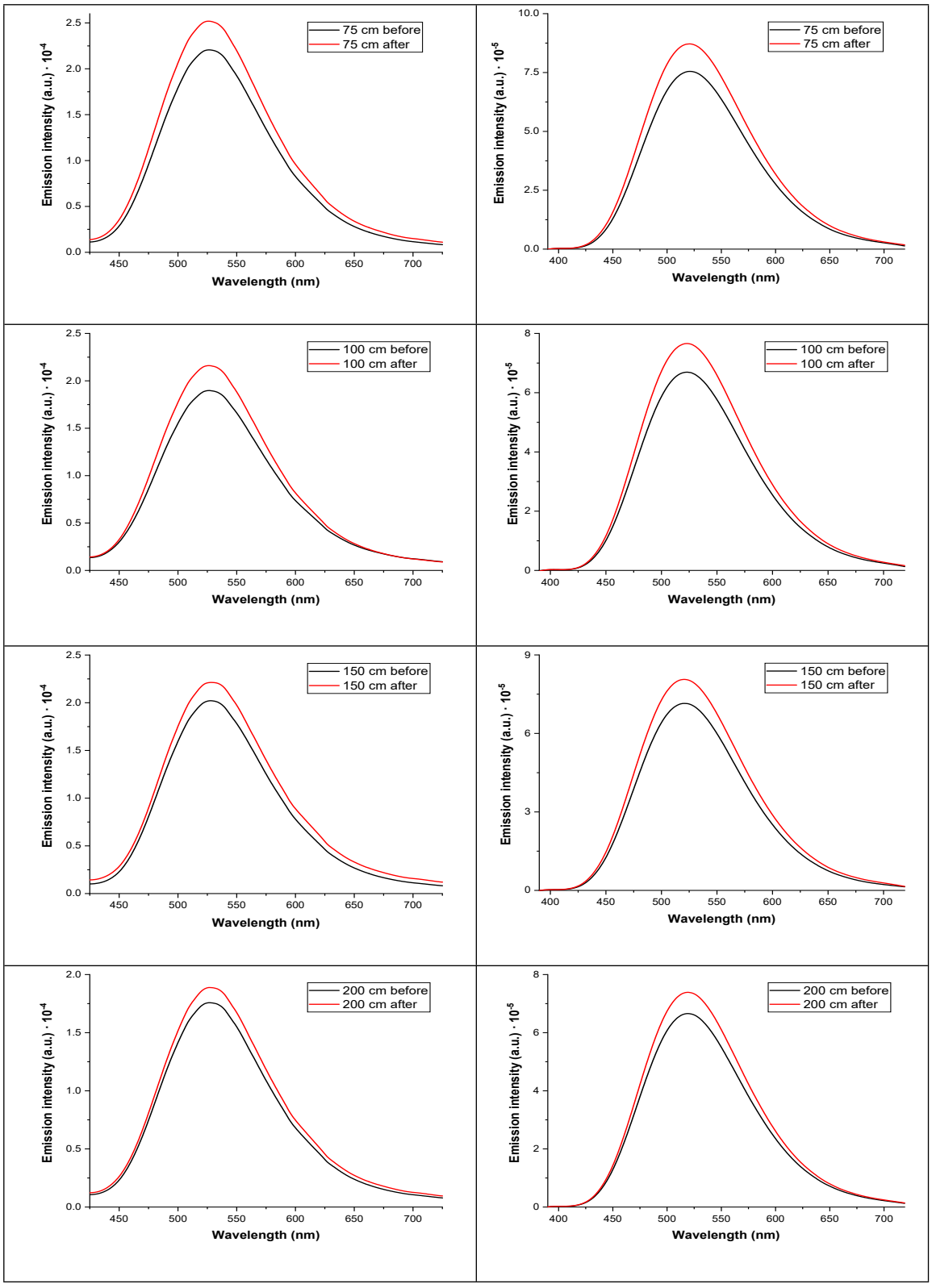
75 cm before
75 cm after
Emission intensity (a.u.) · 10⁻⁴
Wavelength (nm)
75 cm before
75 cm after
Emission intensity (a.u.) · 10⁻⁵
Wavelength (nm)
100 cm before
100 cm after
Emission intensity (a.u.) · 10⁻⁴
Wavelength (nm)
100 cm before
100 cm after
Emission intensity (a.u.) · 10⁻⁵
Wavelength (nm)
150 cm before
150 cm after
Emission intensity (a.u.) · 10⁻⁴
Wavelength (nm)
150 cm before
150 cm after
Emission intensity (a.u.) · 10⁻⁵
Wavelength (nm)
200 cm before
200 cm after
Emission intensity (a.u.) · 10⁻⁴
Wavelength (nm)
200 cm before
200 cm after
Emission intensity (a.u.) · 10⁻⁵
Wavelength (nm)

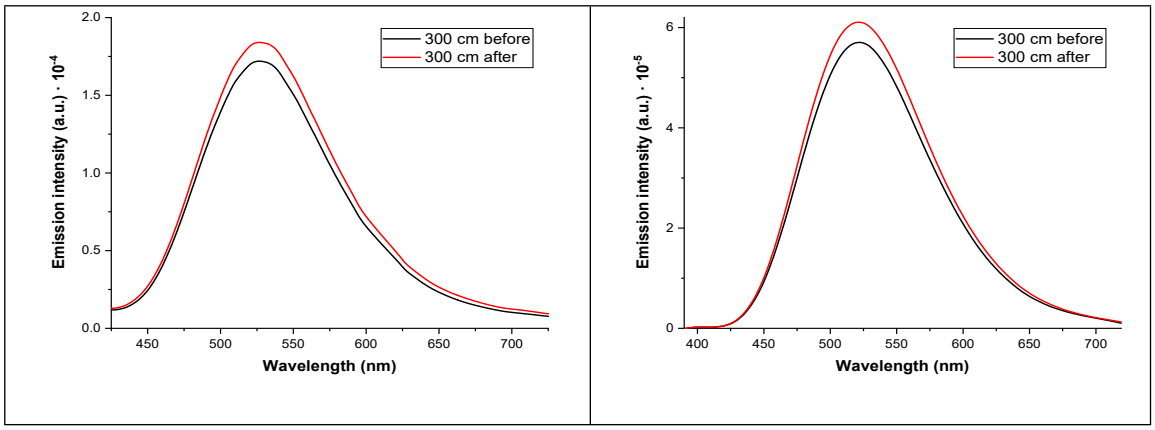

***Table S1**. Emission spectra of the particles before and after a 30-minute exposure to TATP vapors in order of increasing distance from the TATP source measured by a Hamamatsu C10082CA mini-spectrometer (left) and an Edimburgh FLS980 Spectrometer (right).*

In both cases the maximum emission is placed around 525 nm. The histogram in the **Table S2** represents the maximum emission peak (λem max = 525 nm) before and after exposure to TATP vapors as a function of distance from the TATP source, once again comparing both spectrometers.

HAMAMATSU C10082CA MINI-SPECTROMETER	EDIMBURGH FLS980 SPECTROMETER
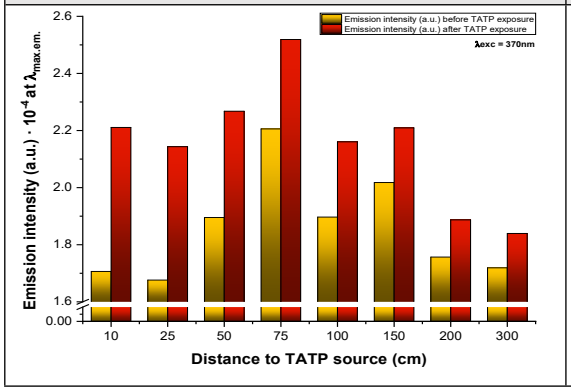	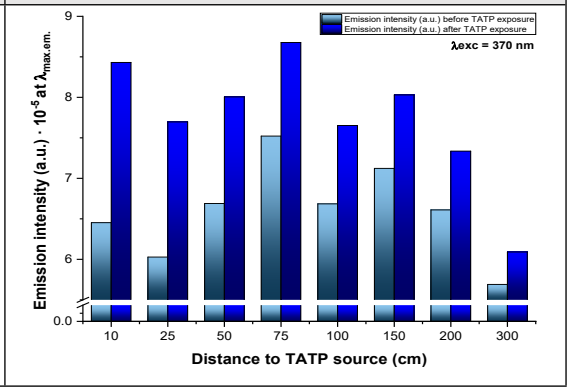

***Table S2**. Histogram plotting the peak emission before and after a 30-minute exposure to TATP vapors as a function of distance from the TATP source measured by a Hamamatsu C10082CA mini-spectrometer (left) and an Edimburgh FLS980 Spectrometer (right).*

Photographs under UV light before and after exposure to TATP vapors were also taken and are shown below (Figure S17).

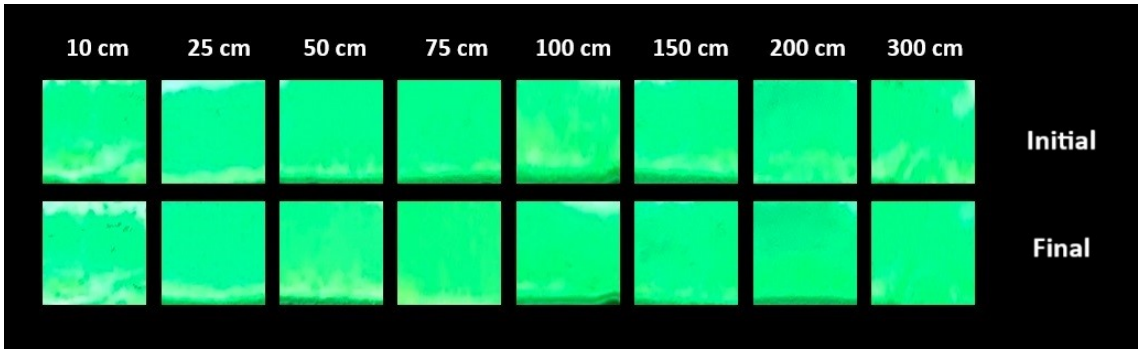

***Figure S17**. Comparative photograph taken under UV light before and after a 30-minute exposure to TATP vapors.*

2. Experiment 2: 24-26°C_30 minutes (DAY 1)

6.5 mg of TATP were evaporated over a 30-minute period under a temperature of 24 – 26°C. The emission spectra of the particles before and after exposure to TATP vapors were measured using both

Hamamatsu C10082CA mini-spectrometer and Edimburgh FLS980 Spectrometer in order to evaluate the performance of the Hamamatsu C10082CA mini-spectrometer and verify that the results are comparable to those obtained in the experiments carried out to date. The experimental conditions in the case of the Hamamatsu devise were acquisition time = 100000 μs (default value) and LED intensity = 2 %. Edimburgh instrument parameters were λexc = 370 nm, Δλexc = 0.30 nm, Δλem = 0.15 nm, integration time 0.3 s/step and step of 1 nm for all samples. A comparative table of the results is shown below in **Table S3**, in order of increasing distance from the TATP source (10 – 25 – 50 – 75 – 100 – 150 – 200 – 300 cm).

HAMAMATSU C10082CA MINI-SPECTROMETER	EDIMBURGH FLS980 SPECTROMETER
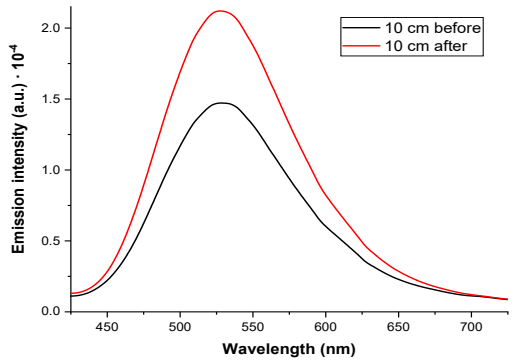	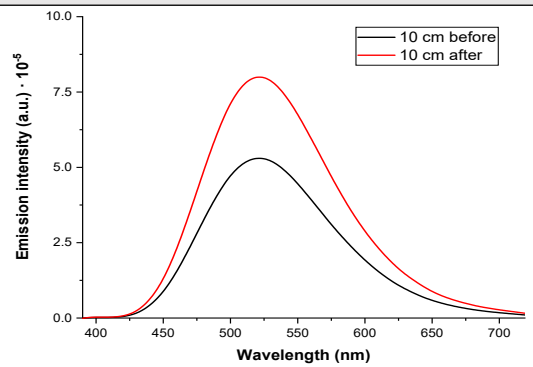
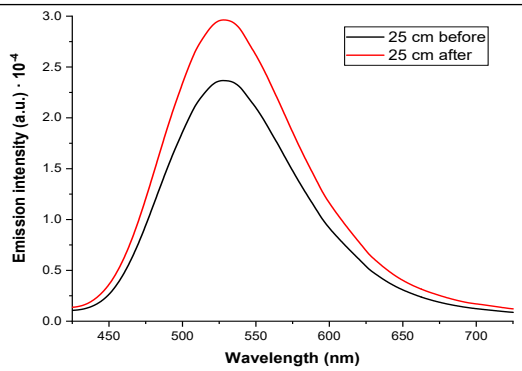	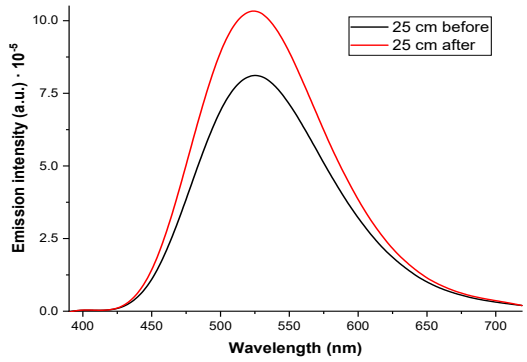
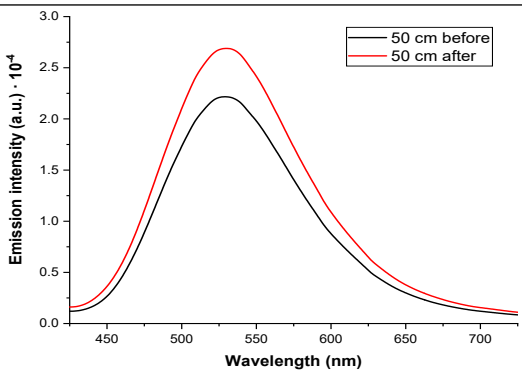	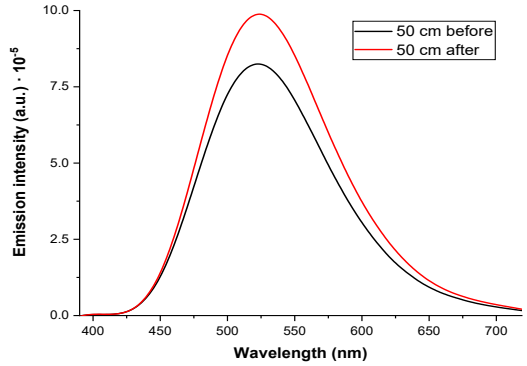

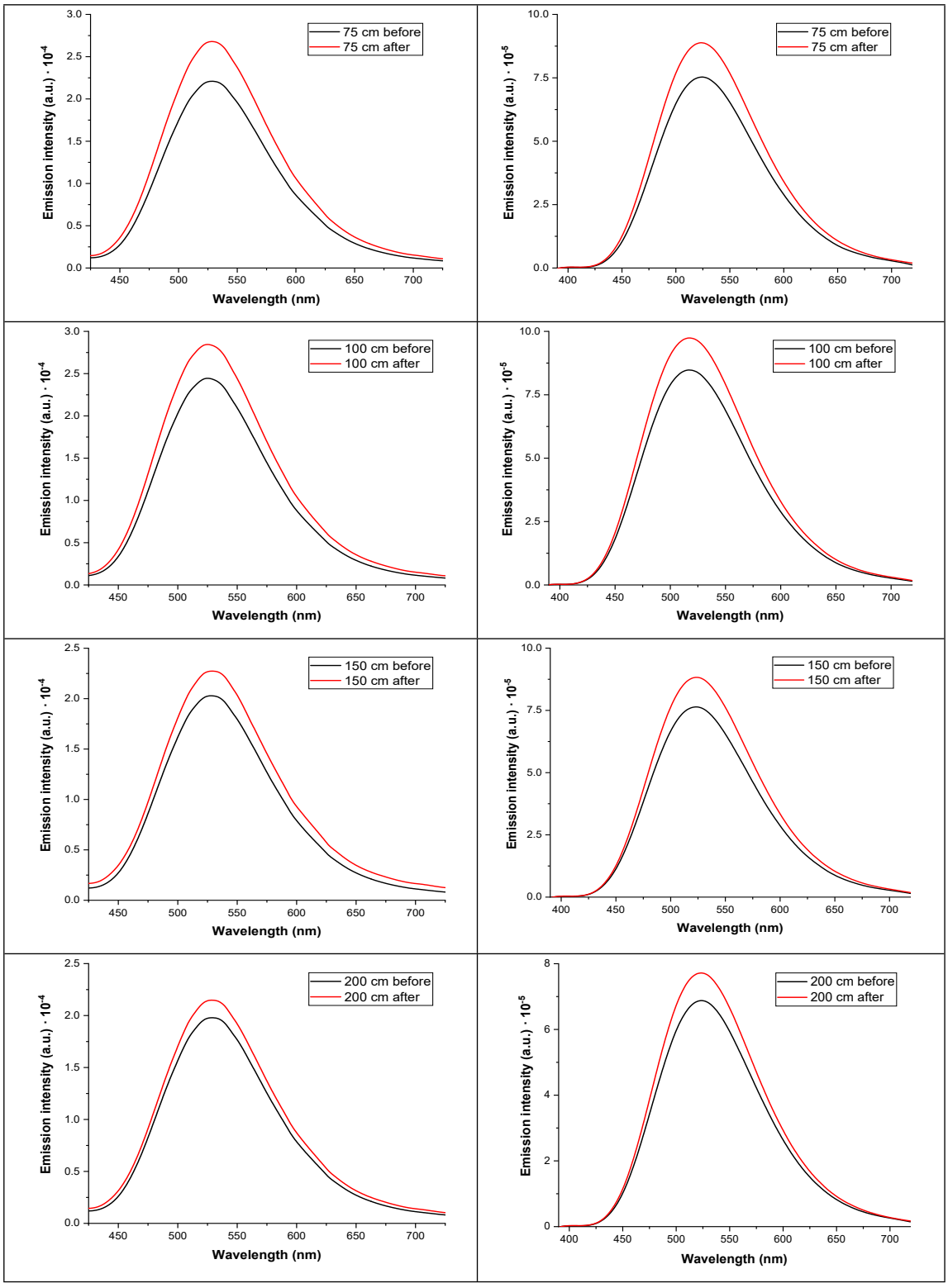
75 cm before
75 cm after
Emission intensity (a.u.) · 10⁻⁴
Wavelength (nm)
75 cm before
75 cm after
Emission intensity (a.u.) · 10⁻⁵
Wavelength (nm)
100 cm before
100 cm after
Emission intensity (a.u.) · 10⁻⁴
Wavelength (nm)
100 cm before
100 cm after
Emission intensity (a.u.) · 10⁻⁵
Wavelength (nm)
150 cm before
150 cm after
Emission intensity (a.u.) · 10⁻⁴
Wavelength (nm)
150 cm before
150 cm after
Emission intensity (a.u.) · 10⁻⁵
Wavelength (nm)
200 cm before
200 cm after
Emission intensity (a.u.) · 10⁻⁴
Wavelength (nm)
200 cm before
200 cm after
Emission intensity (a.u.) · 10⁻⁵
Wavelength (nm)

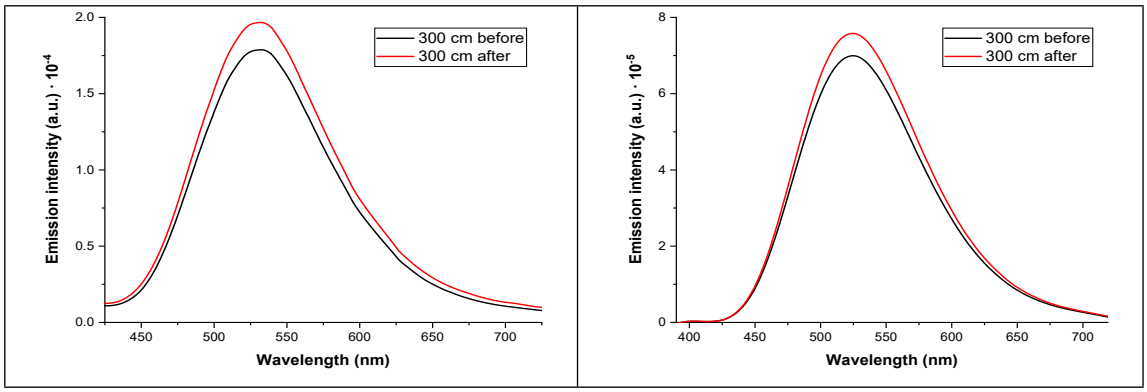

***Table S3**. Emission spectra of the particles before and after a 30-minute exposure to TATP vapors in order of increasing distance from the TATP source measured by a Hamamatsu C10082CA mini-spectrometer (left) and an Edimburgh FLS980 Spectrometer (right).*

In both cases the maximum emission is placed around 525 nm. The histogram in the **Table S4** represents the maximum emission peak (λem max = 525 nm) before and after exposure to TATP vapors as a function of distance from the TATP source, once again comparing both spectrometers.

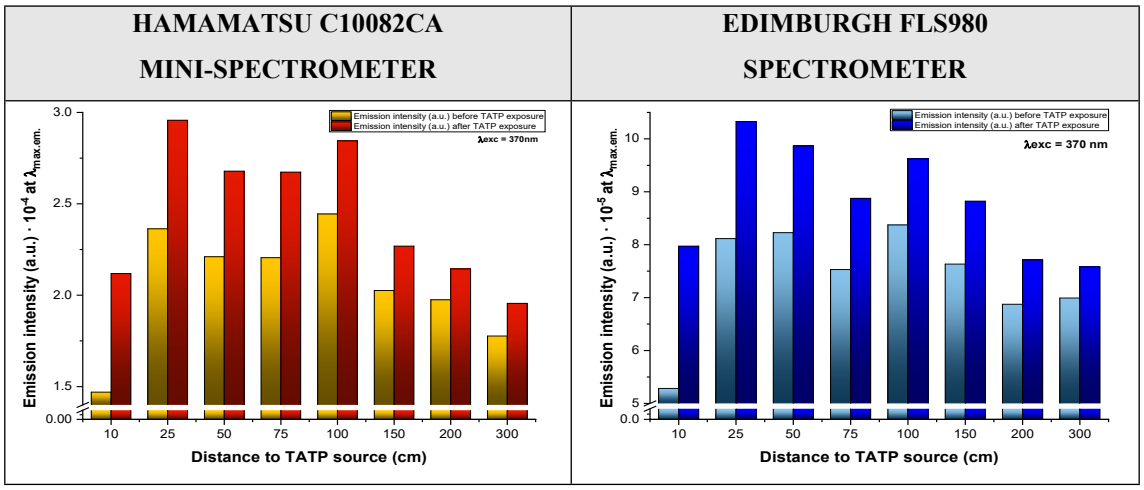

***Table S4**. Histogram plotting the peak emission before and after a 30-minute exposure to TATP vapors as a function of distance from the TATP source measured by a Hamamatsu C10082CA mini-spectrometer (left) and an Edimburgh FLS980 Spectrometer (right).*

Photographs under UV light before and after exposure to TATP vapors were also taken and are shown below (Figure S18).

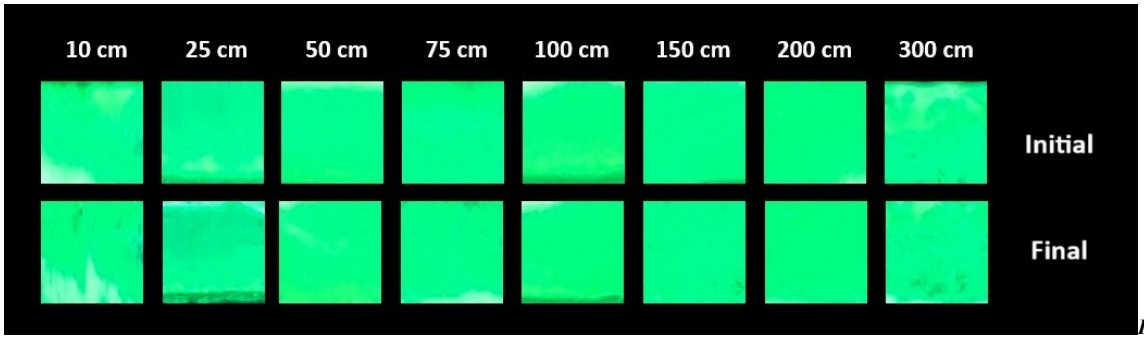

***Figure S18**. Comparative photograph taken under UV light before and after a 30-minute exposure to TATP vapors.*

3. Experiment 3: 25°C_30 minutes (DAY 2)

7.4 mg of TATP were evaporated over a 30-minute period under a temperature of 25°C. The emission spectra of the particles before and after exposure to TATP vapors were measured using both Hamamatsu C10082CA mini-spectrometer and Edimburgh FLS980 Spectrometer in order to evaluate the performance of the Hamamatsu C10082CA mini-spectrometer and verify that the results are comparable to those obtained in the experiments carried out to date. The experimental conditions in the case of the Hamamatsu devise were acquisition time = 100000 μs (default value) and LED intensity = 2 %. Edimburgh instrument parameters were λexc = 370 nm, Δλexc = 0.30 nm, Δλem = 0.15 nm, integration time 0.3 s/step and step of 1 nm for all samples. A comparative table of the results is shown below in **Table S5**, in order of increasing distance from the TATP source (10 – 25 – 50 – 75 – 100 – 150 – 200 – 300 cm).

HAMAMATSU C10082CA MINI-SPECTROMETER	EDIMBURGH FLS980 SPECTROMETER
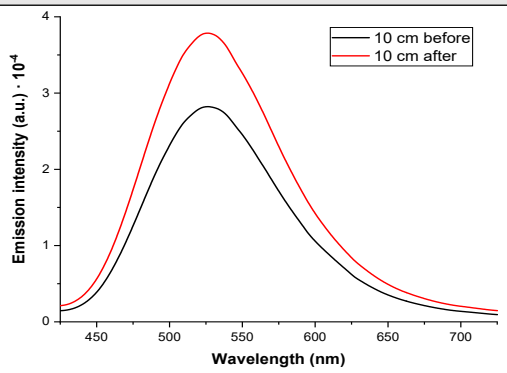	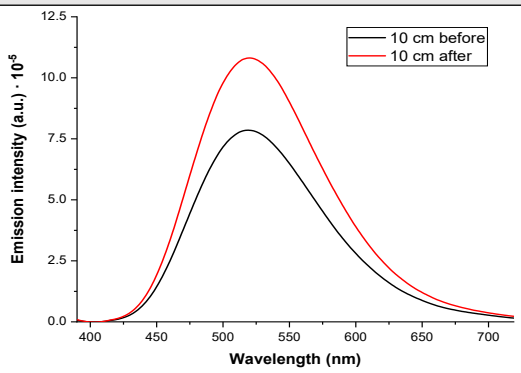
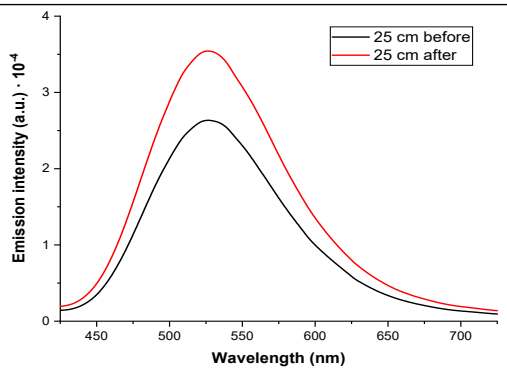	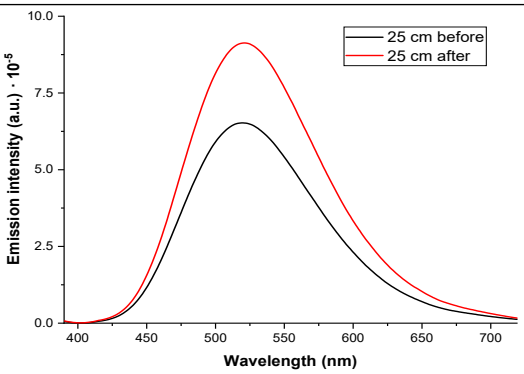

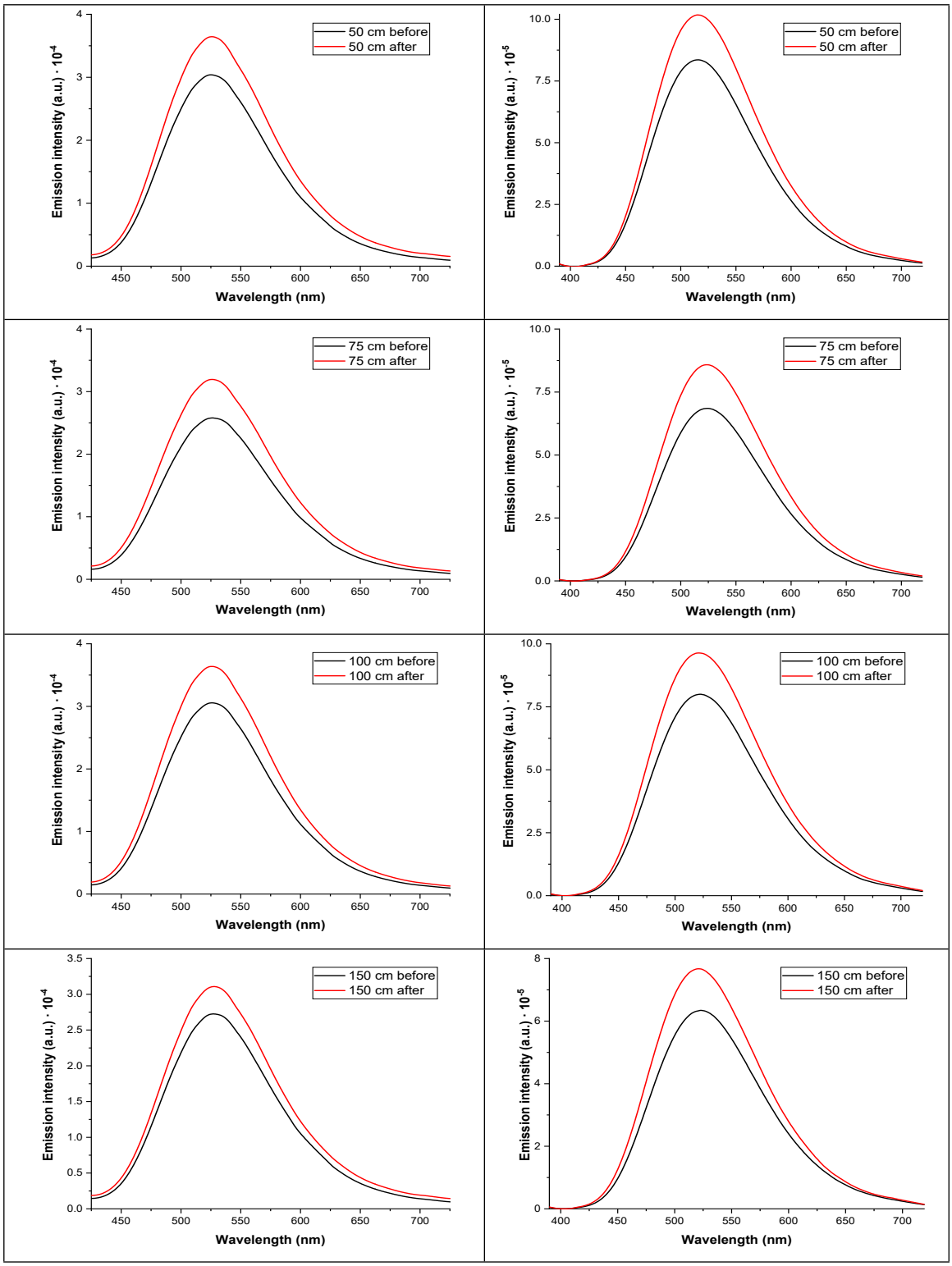
50 cm before
50 cm after
Emission intensity (a.u.) · 10⁻⁴
Wavelength (nm)
50 cm before
50 cm after
Emission intensity (a.u.) · 10⁻⁵
Wavelength (nm)
75 cm before
75 cm after
Emission intensity (a.u.) · 10⁻⁴
Wavelength (nm)
75 cm before
75 cm after
Emission intensity (a.u.) · 10⁻⁵
Wavelength (nm)
100 cm before
100 cm after
Emission intensity (a.u.) · 10⁻⁴
Wavelength (nm)
100 cm before
100 cm after
Emission intensity (a.u.) · 10⁻⁵
Wavelength (nm)
150 cm before
150 cm after
Emission intensity (a.u.) · 10⁻⁴
Wavelength (nm)
150 cm before
150 cm after
Emission intensity (a.u.) · 10⁻⁵
Wavelength (nm)

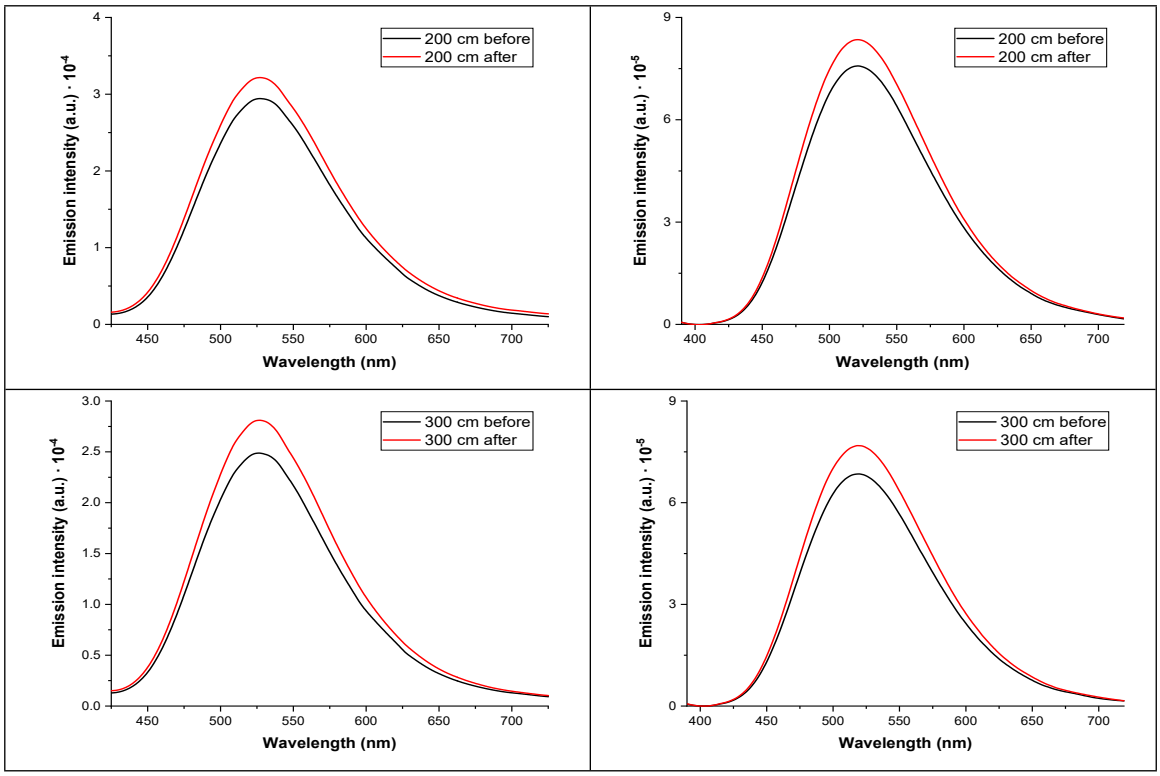

***Table S5**. Emission spectra of the particles before and after a 30-minute exposure to TATP vapors in order of increasing distance from the TATP source measured by a Hamamatsu C10082CA mini-spectrometer (left) and an Edimburgh FLS980 Spectrometer (right).*

In both cases the maximum emission is placed around 525 nm. The histogram in the **Table S6** represents the maximum emission peak (λem max = 525 nm) before and after exposure to TATP vapors as a function of distance from the TATP source, once again comparing both spectrometers.

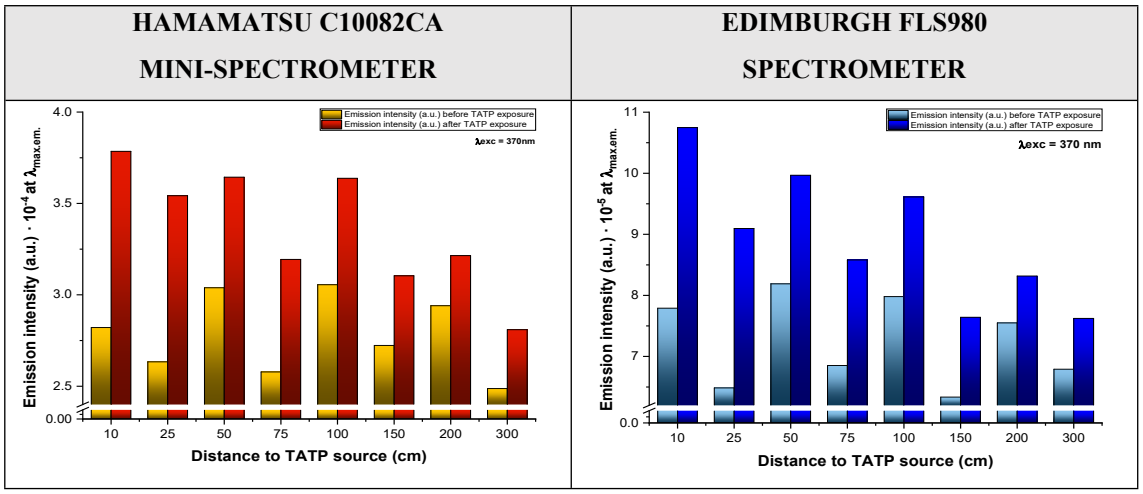

***Table S6**. Histogram plotting the peak emission before and after a 30-minute exposure to TATP vapors as a function of distance from the TATP source measured by a Hamamatsu C10082CA mini-spectrometer (left) and an Edimburgh FLS980 Spectrometer (right).*

Photographs under UV light before and after exposure to TATP vapors were also taken and are shown below (Figure S19).

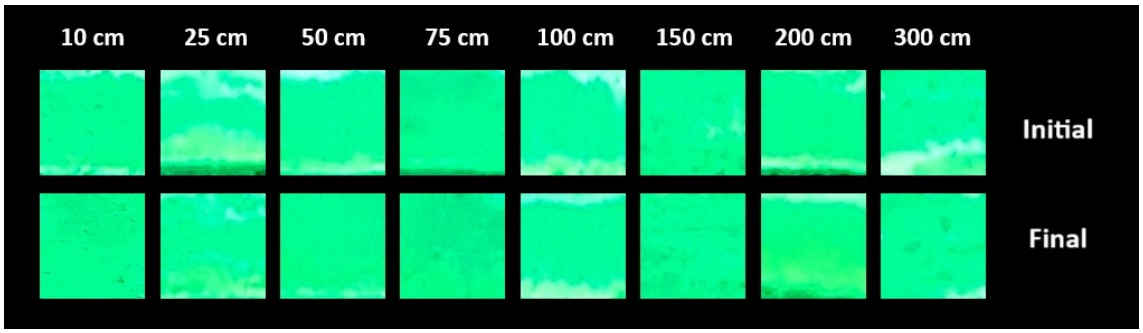

***Figure S19**. Comparative photograph taken under UV light before and after a 30-minute exposure to TATP vapors.*

4. Experiment 4: 25°C_30 minutes (DAY 2)

5.7 mg of TATP were evaporated over a 30-minute period under a temperature of 25°C. The emission spectra of the particles before and after exposure to TATP vapors were measured using both Hamamatsu C10082CA mini-spectrometer and Edimburgh FLS980 Spectrometer in order to evaluate the performance of the Hamamatsu C10082CA mini-spectrometer and verify that the results are comparable to those obtained in the experiments carried out to date. The experimental conditions in the case of the Hamamatsu devise were acquisition time = 100000 μs (default value) and LED intensity = 2 %. Edimburgh instrument parameters were λexc = 370 nm, Δλexc = 0.30 nm, Δλem = 0.15 nm, integration time 0.3 s/step and step of 1 nm for all samples. A comparative table of the results is shown below in **Table S7**, in order of increasing distance from the TATP source (10 – 25 – 50 – 75 – 100 – 150 – 200 – 300 cm).

HAMAMATSU C10082CA MINI-SPECTROMETER	EDIMBURGH FLS980 SPECTROMETER
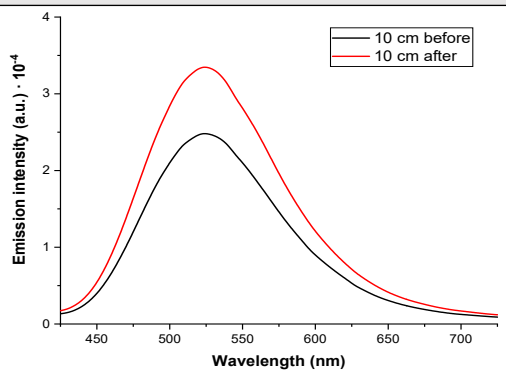	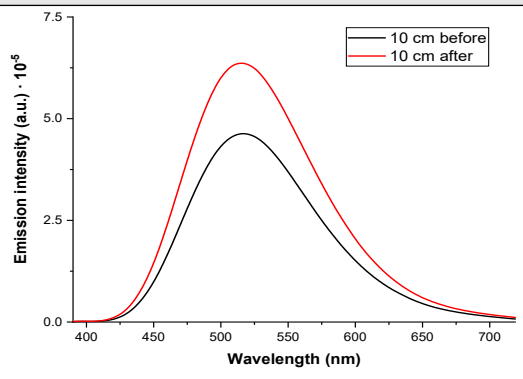

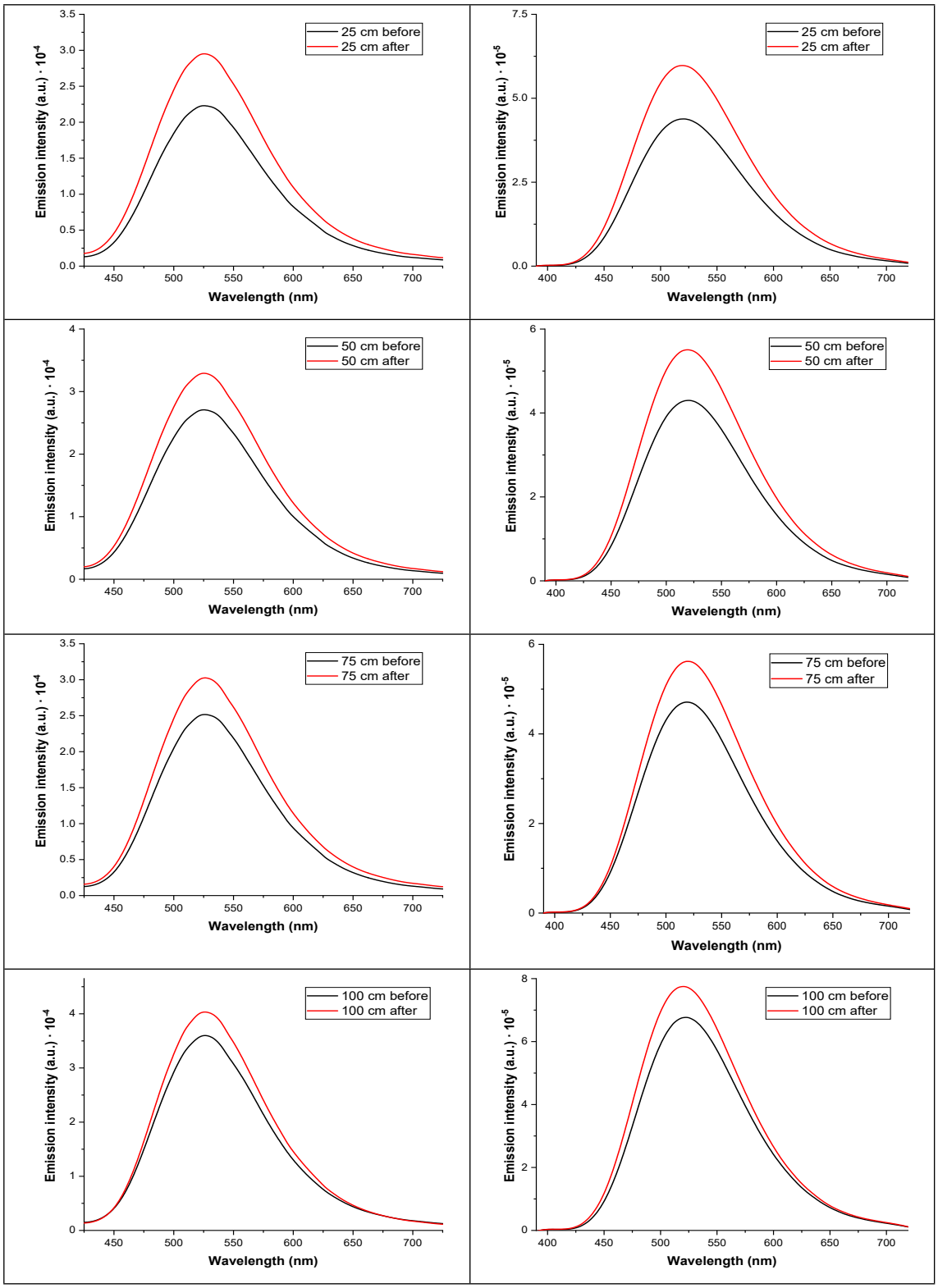
25 cm before
25 cm after
Emission intensity (a.u.) · 10⁻⁴
Wavelength (nm)
25 cm before
25 cm after
Emission intensity (a.u.) · 10⁻⁵
Wavelength (nm)
50 cm before
50 cm after
Emission intensity (a.u.) · 10⁻⁴
Wavelength (nm)
50 cm before
50 cm after
Emission intensity (a.u.) · 10⁻⁵
Wavelength (nm)
75 cm before
75 cm after
Emission intensity (a.u.) · 10⁻⁴
Wavelength (nm)
75 cm before
75 cm after
Emission intensity (a.u.) · 10⁻⁵
Wavelength (nm)
100 cm before
100 cm after
Emission intensity (a.u.) · 10⁻⁴
Wavelength (nm)
100 cm before
100 cm after
Emission intensity (a.u.) · 10⁻⁵
Wavelength (nm)

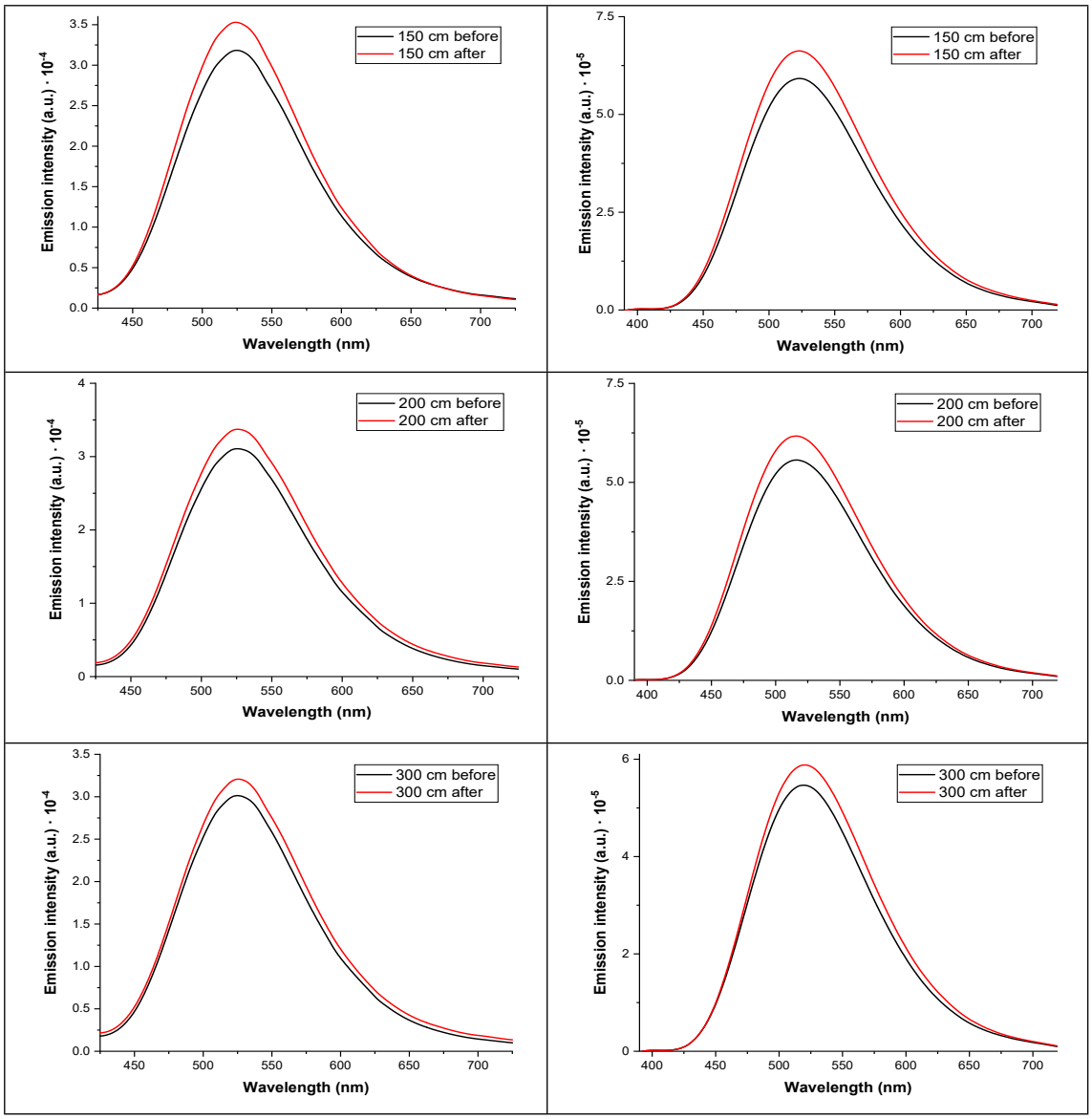

Table S7*. Emission spectra of the particles before and after a 30-minute exposure to TATP vapors in order of increasing distance from the TATP source measured by a Hamamatsu C10082CA mini-spectrometer (left) and an Edimburgh FLS980 Spectrometer (right).*

In both cases the maximum emission is placed around 525 nm. The histogram in the **Table S8** represents the maximum emission peak (λem max = 525 nm) before and after exposure to TATP vapors as a function of distance from the TATP source, once again comparing both spectrometers.

HAMAMATSU C10082CA MINI-SPECTROMETER	EDIMBURGH FLS980 SPECTROMETER

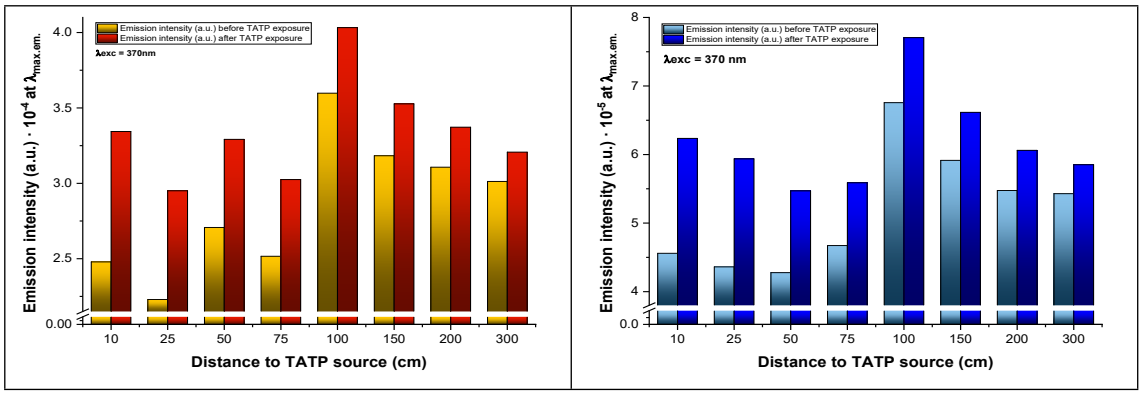

Table S8. *Histogram plotting the peak emission before and after a 30-minute exposure to TATP vapors as a function of distance from the TATP source measured by a Hamamatsu C10082CA mini-spectrometer (left) and an Edimburgh FLS980 Spectrometer (right).*

Photographs under UV light before and after exposure to TATP vapors were also taken and are shown below (Figure S20).

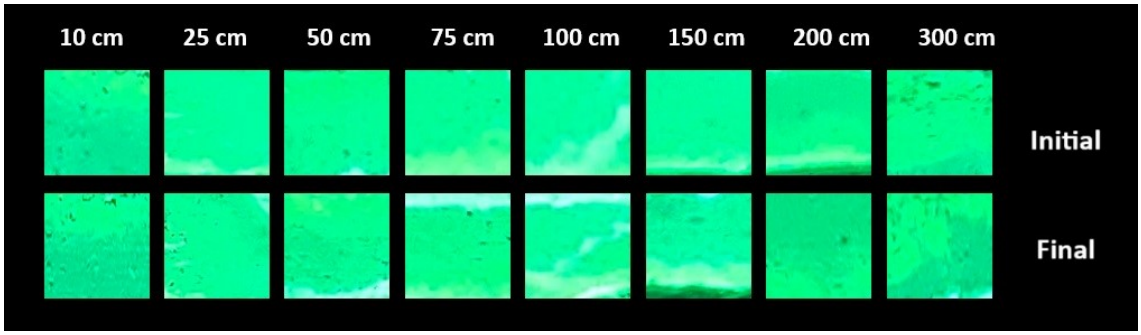

Figure S20. *Comparative photograph taken under UV light before and after a 30-minute exposure to TATP vapors.*

To make the comparison of the results obtained in the different experiments easier, the variation in the fluorescence emission intensity has been referenced to the following parameters: 30 minutes duration of the experiment, 5 mg of TATP evaporated per experiment.

Graphs in **Table S9** have been made, representing emission intensity variation before and after exposure to TATP vapours versus distance to the TATP source (up) and emission intensity proportionality factor versus distance to the TATP source (down) measured using both Hamamatsu C10082CA mini-spectrometer (left) and Edimburgh FLS980 Spectrometer (right), for homogenized experiments lasting 30 minutes and 5 mg of evaporated TATP.

HAMAMATSU C10082CA MINI-SPECTROMETER	EDIMBURGH FLS980 SPECTROMETER

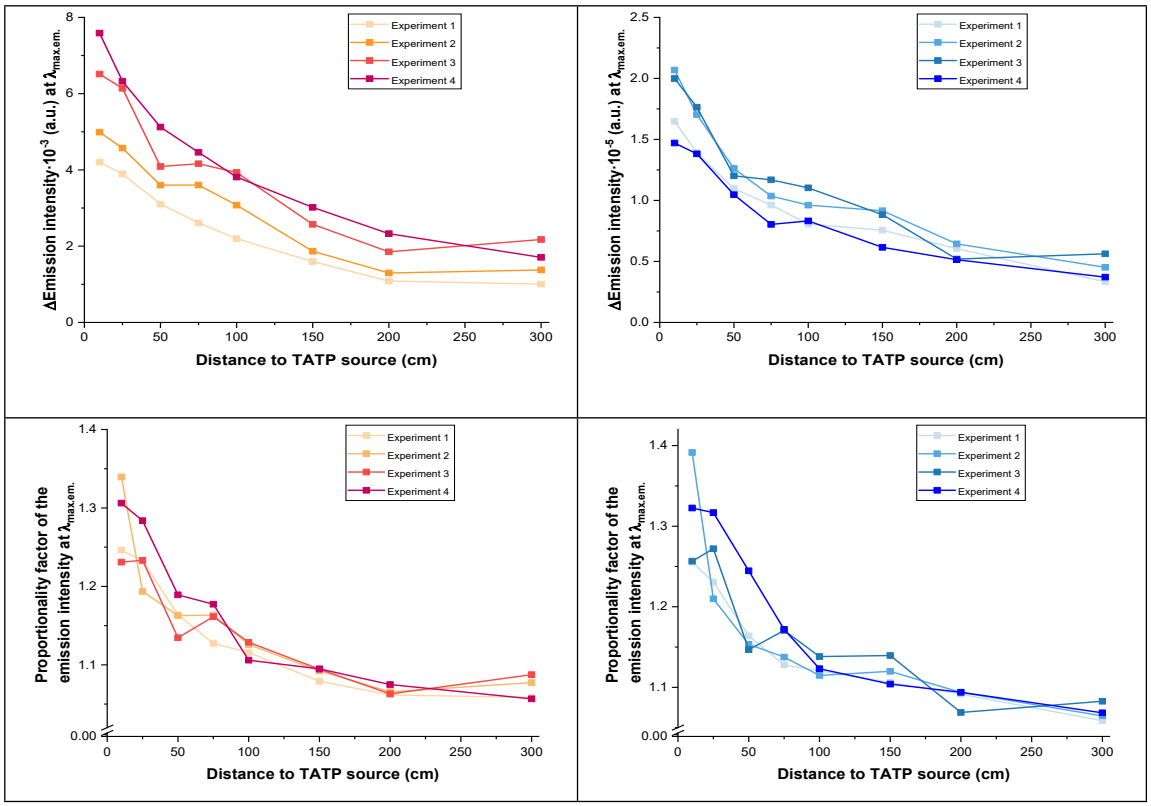

***Table S9**. Emission intensity variation before and after exposure to TATP vapours versus distance to the TATP source (up) and emission intensity proportionality factor versus distance to the TATP source (down) measured using both Hamamatsu C10082CA mini-spectrometer (left) and Edimburgh FLS980 Spectrometer (right).*

The average increase in emission intensity:

- <u>In Experiment 1:</u>
  - For particles located **75 cm or less** from the TATP source was **119.2 %** if measured with the **Hamamatsu C10082CA mini-spectrometer** and **119.4%** if measured with the **Edimburgh FLS980 Spectrometer**. While the figure for particles located 1 m or more is only **107.9 %** if measured with the **Hamamatsu C10082CA mini-spectrometer** and **109.4 %** if measured with the **Edimburgh FLS980 Spectrometer**, as shown in **Table 10**.

SENSING PARTICLE POSITION	HAMAMATSU C10082CA MINI-SPECTROMETER	EDIMBURGH FLS980 SPECTROMETER
10 cm	124.6 %	125.5 %
25 cm	123.2 %	123.1 %
50 cm	116.4 %	116.4 %
75 cm	112.7 %	112.8 %
100 cm	111.6 %	112.1 %
150 cm	107.9 %	110.6 %
200 cm	106.2 %	109.1 %
300 cm	105.8 %	105.9 %

***Table S10.** Increment in fluorescence emission intensity of sensing particles as a function of their distance from the TATP source using data from a Hamamatsu C10082CA mini-spectrometer (middle) and an Edimburgh FLS980 Spectrometer (right).*

- <u>In Experiment 2:</u>

- For particles located **75 cm or less** from the TATP source was **121.4 %** if measured with the **Hamamatsu C10082CA mini-spectrometer** and **122.3 %** if measured with the **Edimburgh FLS980 Spectrometer**. While the figure for particles located 1 m or more is only **109.1%** if measured with the **Hamamatsu C10082CA mini-spectrometer** and **109.8 %** if measured with the **Edimburgh FLS980 Spectrometer**, as shown in **Table S11**.

SENSING PARTICLE POSITION	HAMAMATSU C10082CA MINI-SPECTROMETER	EDIMBURGH FLS980 SPECTROMETER
10 cm	133.9 %	139.1%
25 cm	119.3 %	121.0 %
50 cm	116.2%	115.3 %
75 cm	116.3%	113.8 %
100 cm	112.6%	111.5 %
150 cm	109.2 %	112.0 %
200 cm	106.6 %	109.4 %
300 cm	107.8 %	106.5 %

Table S11. *Increment in fluorescence emission intensity of sensing particles as a function of their distance from the TATP source using data from a Hamamatsu C10082CA mini-spectrometer (middle) and an Edimburgh FLS980 Spectrometer (right).*

- In Experiment 3:
  - For particles located **75 cm or less** from the TATP source was **119.0 %** if measured with the **Hamamatsu C10082CA mini-spectrometer** and **121.1 %** if measured with the **Edimburgh FLS980 Spectrometer**. While the figure for particles located 1 m or more is only **109.4 %** if measured with the **Hamamatsu C10082CA mini-spectrometer** and **110.7 %** if measured with the **Edimburgh FLS980 Spectrometer**, as shown in **Table S12**.

SENSING PARTICLE POSITION	HAMAMATSU C10082CA MINI-SPECTROMETER	EDIMBURGH FLS980 SPECTROMETER
10 cm	123.1 %	125.7 %
25 cm	123.3 %	127.2 %
50 cm	113.5 %	114.7 %
75 cm	116.1 %	117.1 %
100 cm	112.9 %	113.8 %
150 cm	109.5 %	113.9 %
200 cm	106.3 %	106.9 %
300 cm	108.7 %	108.3 %

Table S12. *Increment in fluorescence emission intensity of sensing particles as a function of their distance from the TATP source using data from a Hamamatsu C10082CA mini-spectrometer (middle) and an Edimburgh FLS980 Spectrometer (right).*

- In Experiment 4:

- For particles located **75 cm or less** from the TATP source was **123.9 %** if measured with the **Hamamatsu C10082CA mini-spectrometer** and **126.4 %** if measured with the **Edimburgh FLS980 Spectrometer**. While the figure for particles located 1 m or more is only **108.3 %** if measured with the **Hamamatsu C10082CA mini-spectrometer** and **109.7 %** if measured with the **Edimburgh FLS980 Spectrometer**, as shown in **Table S13**.

SENSING PARTICLE POSITION	HAMAMATSU C10082CA MINI-SPECTROMETER	EDIMBURGH FLS980 SPECTROMETER
10 cm	130.6 %	132.3 %
25 cm	128.4 %	131.7 %
50 cm	118.9 %	124.5 %
75 cm	117.7 %	117.2 %
100 cm	110.6 %	112.3 %
150 cm	109.5 %	110.4 %
200 cm	107.5 %	109.4 %
300 cm	105.7 %	106.8 %

Table S13. *Increment in fluorescence emission intensity of sensing particles as a function of their distance from the TATP source using data from a Hamamatsu C10082CA mini-spectrometer (middle) and an Edimburgh FLS980 Spectrometer (right).*

Maximum emission intensity data are organized according to the distance to the TATP source; representing, on the one hand, emission before contact with TATP vapors and, on the other hand, emission after contact with said vapors. Data are also normalized with respect to the maximum emission from each experiment (**Table S14**).

HAMAMATSU C10082CA MINI-SPECTROMETER	EDIMBURGH FLS980 SPECTROMETER
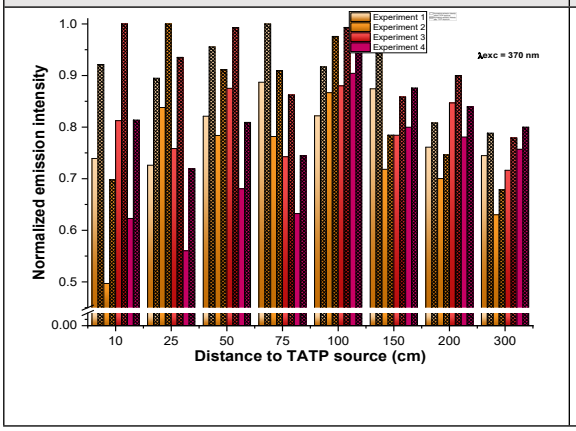	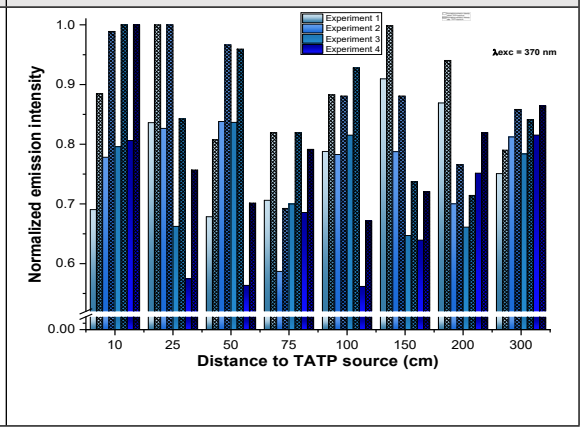

Table S14*. Normalized emission intensity before and after exposure to TATP vapours as a function of the distance to the TATP source measured using both Hamamatsu C10082CA mini-spectrometer (left) and Edimburgh FLS980 Spectrometer (right).*

After this, a common initial emission level is established using the lowest value measured for the particles prior to the exposure to TATP vapours (**Table S15 up**). And finally, the subtraction is made between the final and initial emission, generating **Table S15 down** that contains a graph of emission variation as a function of the distance to the TATP source. **Table S16** contains a 3D representation of this same information.

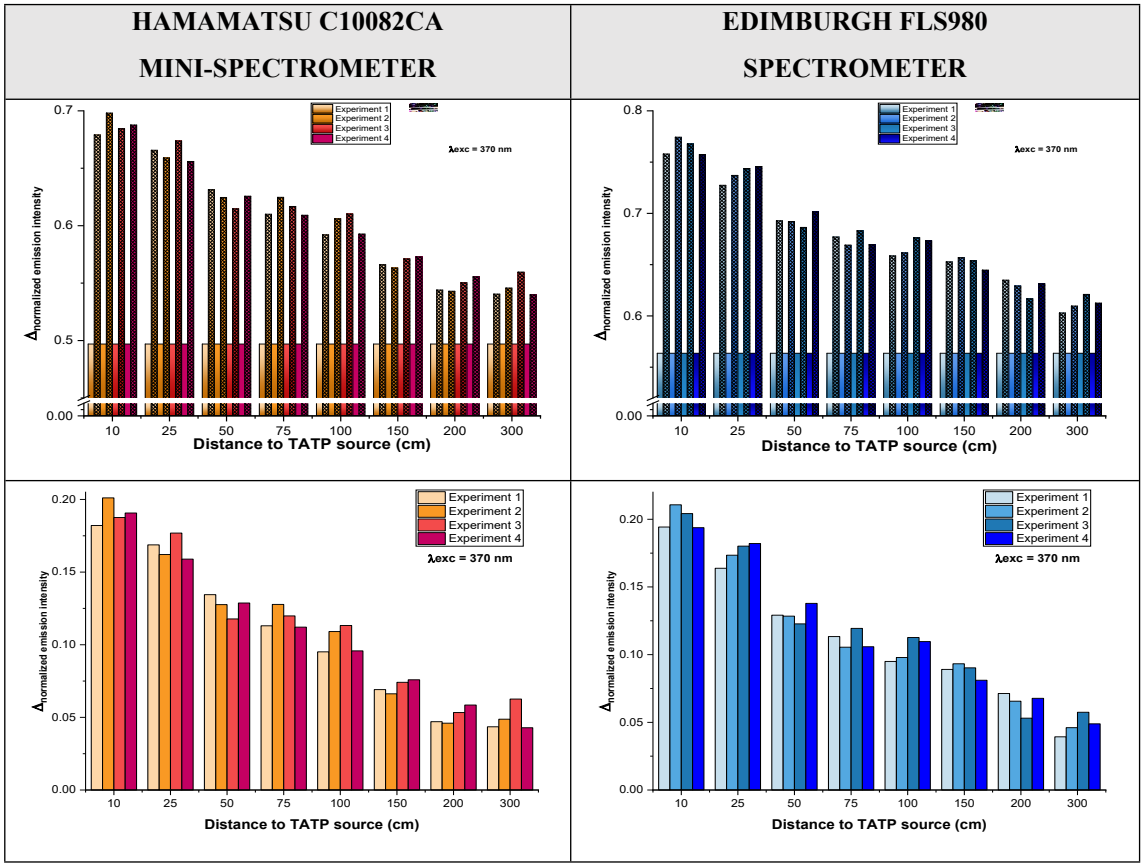

***Table S15**. Normalized emission intensity setting a common initial particulate emission level before and after exposure to TATP vapours as a function of the distance to the TATP source (up) and variation of the normalized emission intensity as a function of the distance to the TATP source (down) measured using both Hamamatsu C10082CA mini-spectrometer (left) and Edimburgh FLS980 Spectrometer (right).*

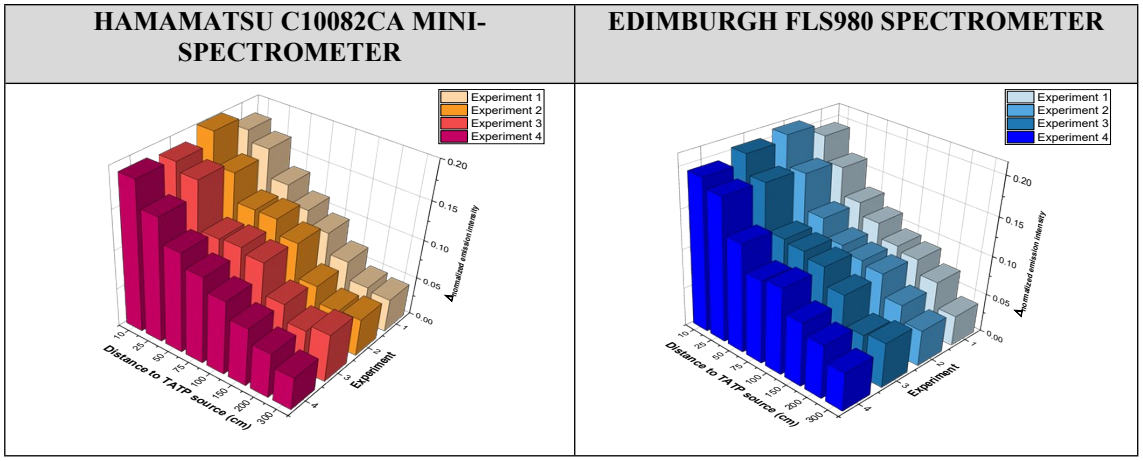

***Table S16.** 3D representation of the variation of the normalized emission intensity as a function of the distance to the TATP source measured using both Hamamatsu C10082CA mini-spectrometer (left) and Edimburgh FLS980 Spectrometer (right).*

As a last step, a Column + Label graph representing the mean and error of the variation of the fluorescence emission (%) as a function of the distance to the TATP source in Experiments 1, 2, 3 and 4 is created for each of the measuring systems (**Table S17**).

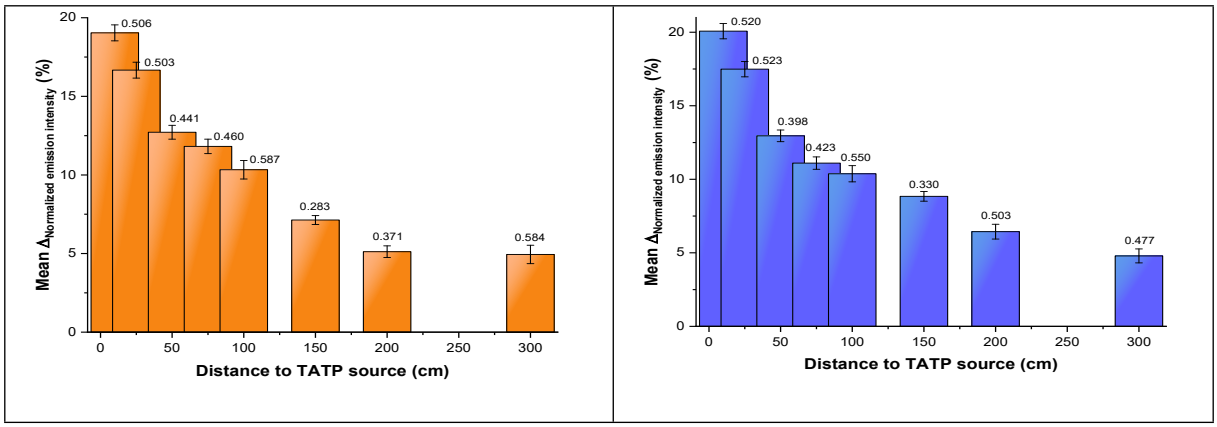

Table S17*. Mean and error of the normalized variation of the fluorescence emission (%) as a function of the distance to the TATP source using both Hamamatsu C10082CA mini-spectrometer (left) and Edimburgh FLS980 Spectrometer (right).*

The mobile platform for the detection of volatile explosive TATP: DESCRIPTION OF THE MECHANICAL PARTS.

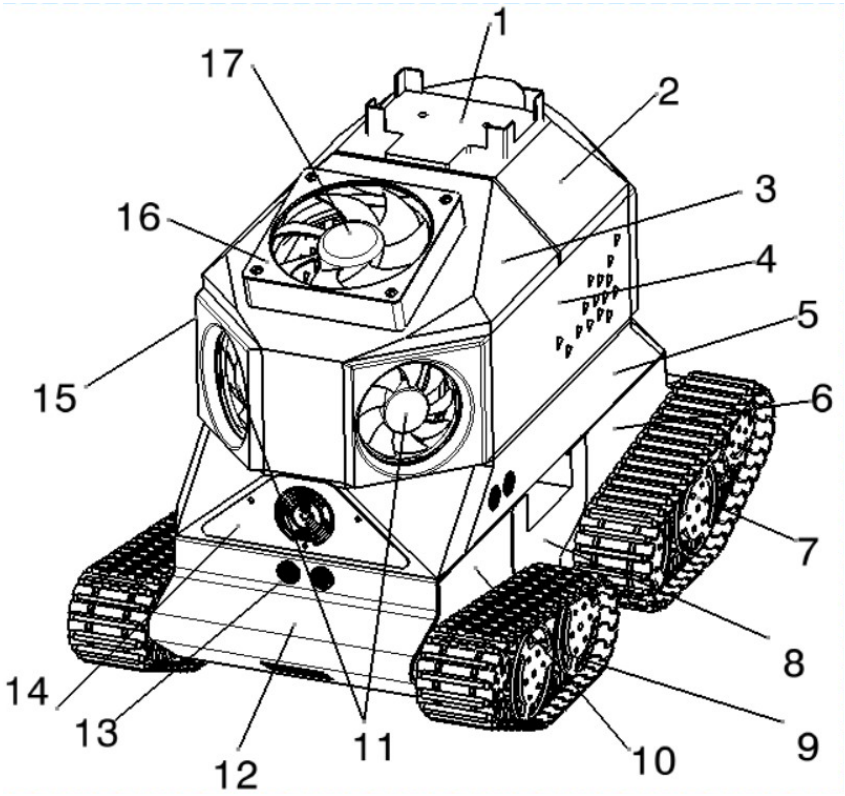

FIGURE S21. EXTERIOR VIEW. FRONT

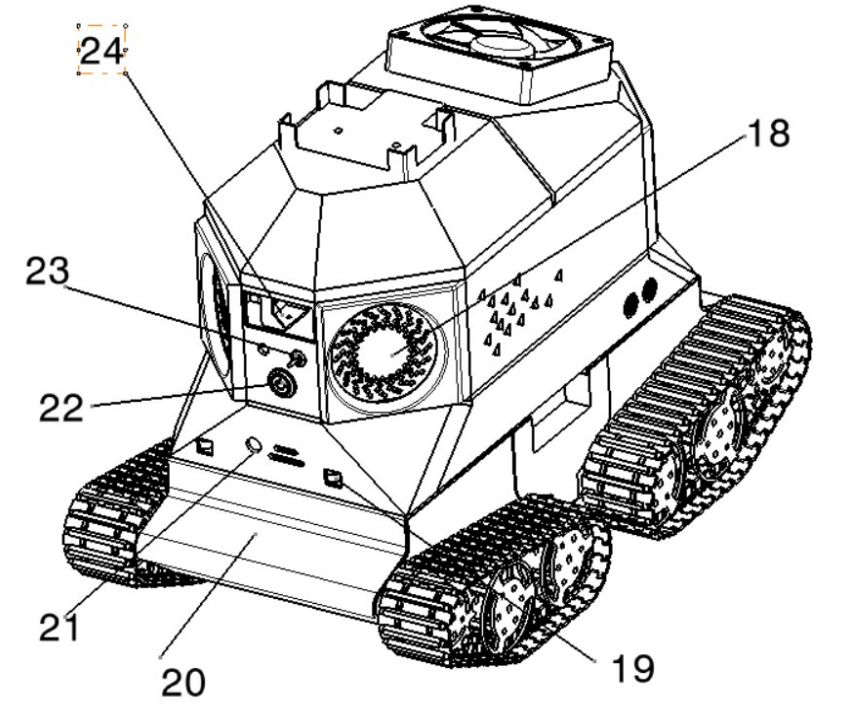

FIGURE S22. EXTERIOR VIEW. REAR

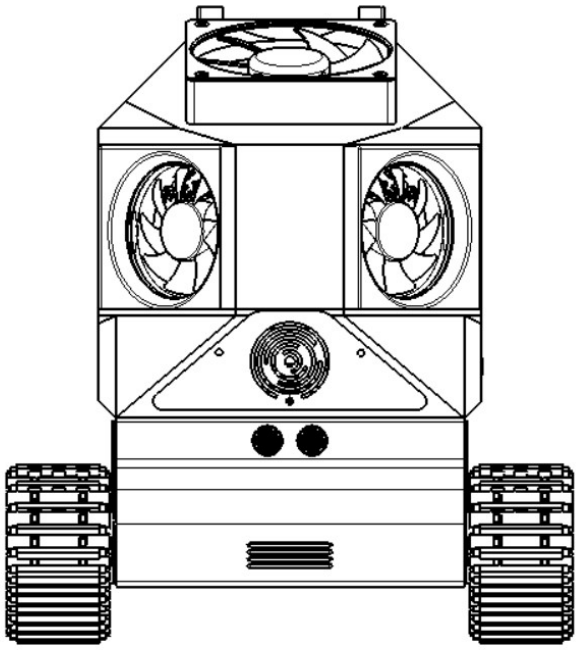

FIGURE S23. ELEVATION

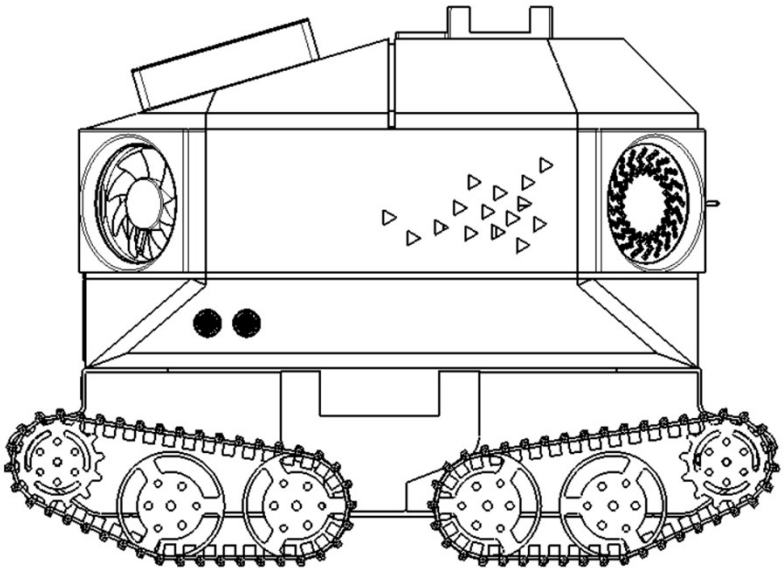

FIGURE S24. PROFILE

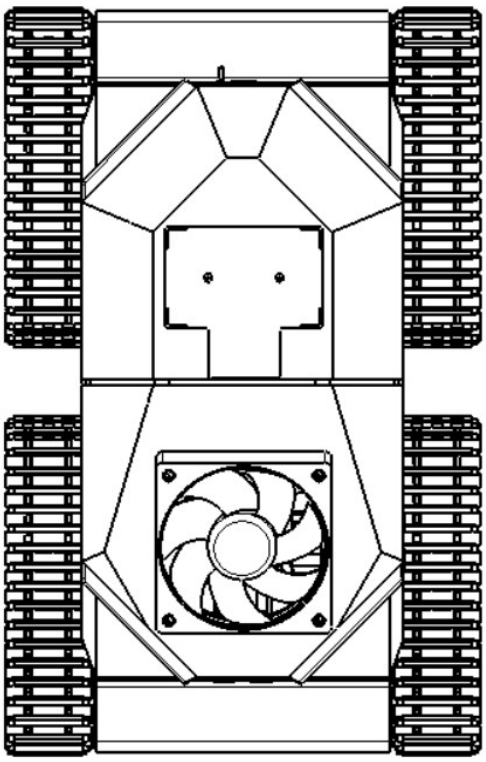

FIGURE S25. PLAN VIEW

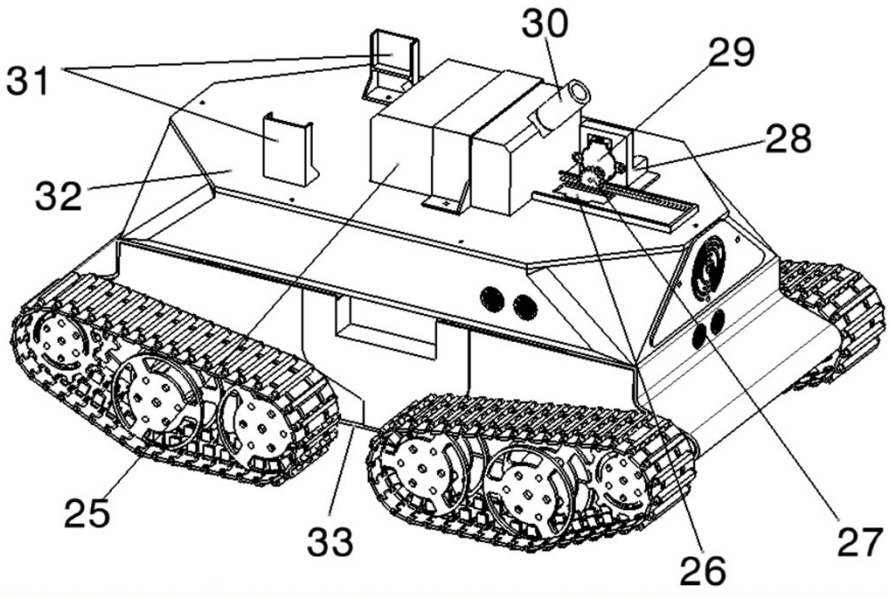

FIGURE S26. INTERIOR PART

The robot is capable of detecting explosive traces of TATP in the environment and warning of their presence, moving through the terrain manually using a control transmitter or autonomously using an automatic guidance system, and whose operating mode can be selected on demand by activating the switch (23).

The aforementioned robot acquires air from the outside by means of a suction system composed of two auxiliary aspirators (11), two lateral suction nozzles (15), an upper suction nozzle (16) and a main aspirator (17). The sucked air is subsequently evacuated through the air outlet nozzles (18) and the holes in the robot's fairing (4). The main aspirator (17) of outside air can be activated manually from the operator's operating control or automatically by means of the vehicle's internal programming. By means of the manual control command, the operator can move the vehicle around the terrain at his/her request, and activate both the initial comparative analysis of the sample deposited inside the robot on the sample cart (26), as well as the subsequent analysis once the outside air suction time has concluded, and which will determine whether the result is positive or negative.

The geometry of the robot's top cover (3) is designed in such a way that it directs, for a certain time, the air flow on a reagent sample that is positioned on the sample cart (26). The time can be controlled on demand by the operator in manual mode or has a certain duration in stand-alone mode.

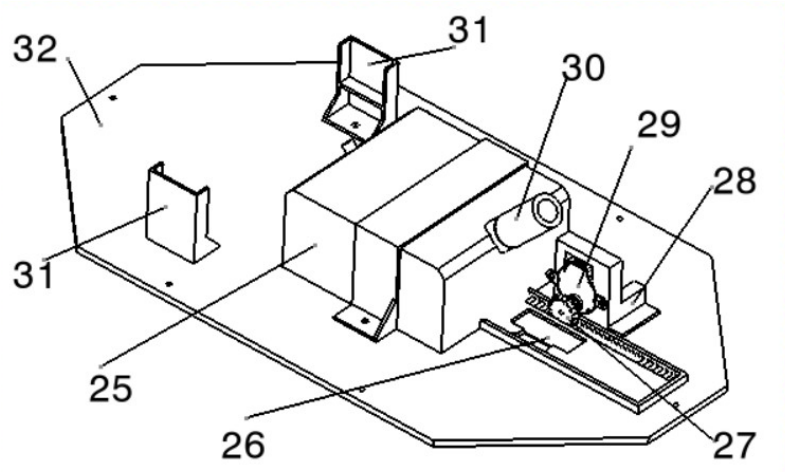

FIGURE S27. SAMPLING AND ANALYSIS SYSTEM.
SAMPLE CAR OUTSIDE

Once this time has elapsed, the sample cart (26) together with the reagent moves within the guide base (32) until it is introduced into the analysis chamber (25).

The geometry and arrangement of the analysis chamber (25), the sample carriage (26) and the guide base (32) ensure that once the sample is inside the analysis chamber (25), its interior remains within certain ranges of light intensity that allow the analysis of the sample placed in the sample carriage (26). The sample remains inside the analysis chamber (25) for a programmed time, and after that time, the sample carriage (26) together with the reagent sample, returns to the initial position, sliding on the guide base (32).

The movement of the sample cart (26) is carried out by means of the action of a toothed wheel (27), the rack of the sample cart (26) and a motor (29) housed on a support (28), and controlled by its corresponding hardware and programming. The configuration and specific geometric

design of the previous elements together with its hardware and programming, make that both the sample cart (26), as well as the reagent sample placed on it, always move between two fixed points, initial point and final point, such that the analysis carried out inside the analysis chamber (25), is always executed in the same position, thus allowing a comparative analysis to be carried out on the same point of the sample, before and after the vehicle has been moving through the terrain and aspirating the ambient air of that terrain.

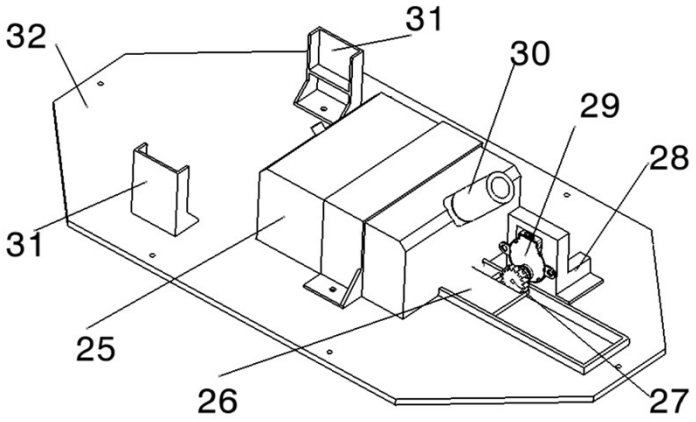

FIGURE S28. SAMPLING AND ANALYSIS SYSTEM. SAMPLE CART INSIDE THE CAMERA OBSCURA

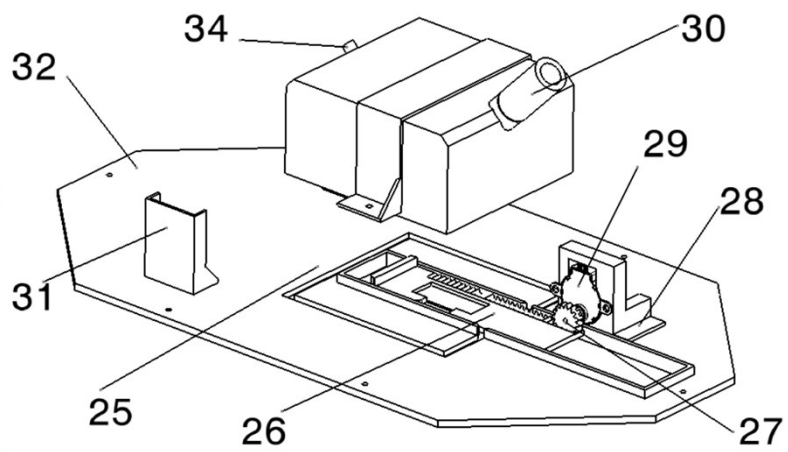

FIGURE S29. EXPLODED VIEW OF THE SAMPLING AND ANALYSIS SYSTEM. SAMPLE CART INSIDE THE CAMERA OBSCURA

Once the analysis is complete, if it is positive, the vehicle emits an alarm sound and displays a red message on a mobile device located on the operator's control station. If the analysis is negative, a green message is displayed. Communication between the robot and the mobile device located on the control station is carried out wirelessly via a modem housed in the communication support (1).

The sample acquisition, sampling and analysis system composed of a guide base (25), sample carriage (26), gear wheel (27), motor support (28), electric motor (29), cylindrical coupling (30), UV supports (31) and guide base (32), together with the measuring devices (minifluorometer, UV light emitter) and data management device, are located inside the upper fairing, composed of the upper cover for samples (2), the upper cover for measuring devices (3) and the middle fairing (4).

The UV emitter is anchored and positioned on the guide base (32) by means of the UV supports (31) and is connected to the analysis chamber (25) through the cylindrical coupling (30). These elements, due to their specific geometry, allow the measuring devices to remain in position.

The movement of the vehicle is carried out through the traction system composed of caterpillar wheels (7), (9) and their symmetrical ones, and by four electric motors (35), located inside the lower fairing of the vehicle, composed of the side covers (6), (8), (10) and their symmetrical ones, the front fairing (12), the rear fairing (20), and the underbody (33).

The fairing has charging connections for the batteries (21) and communication connections with the hardware (19). Both the middle fairing (5) and the front fairing (12) have mapping sensors (13) that allow the vehicle to be guided when it is in autonomous mode.

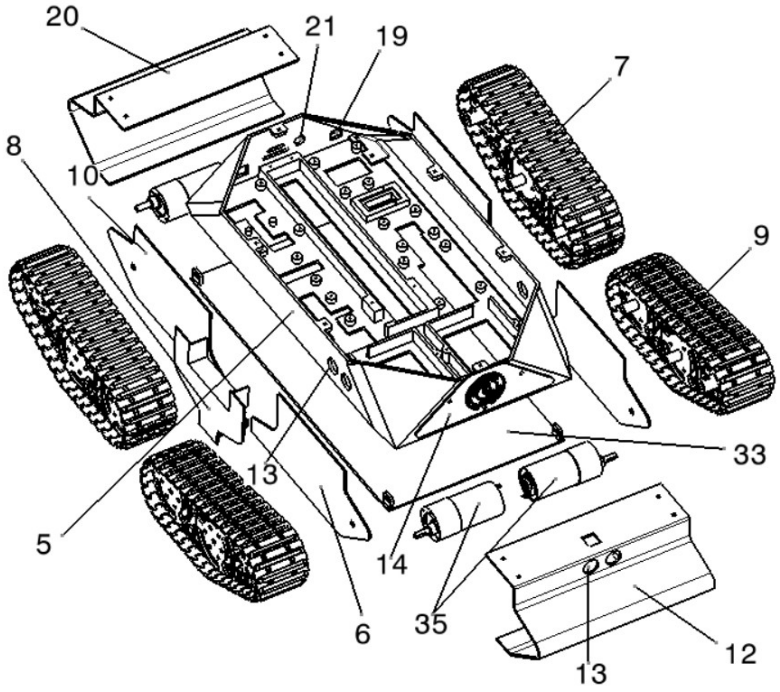

FIGURE S30. EXPLODED VIEW OF THE TRACTION SYSTEM AND MIDDLE AND LOWER FAIRING

This traction system, whether in manual mode (control transmitter) or autonomous mode, is actuated and controlled by the hardware and its internal programming, which is located within the middle fairing (5), as are the power batteries. The middle fairing (5) has a configuration that allows the various hardware and power elements to be secured.

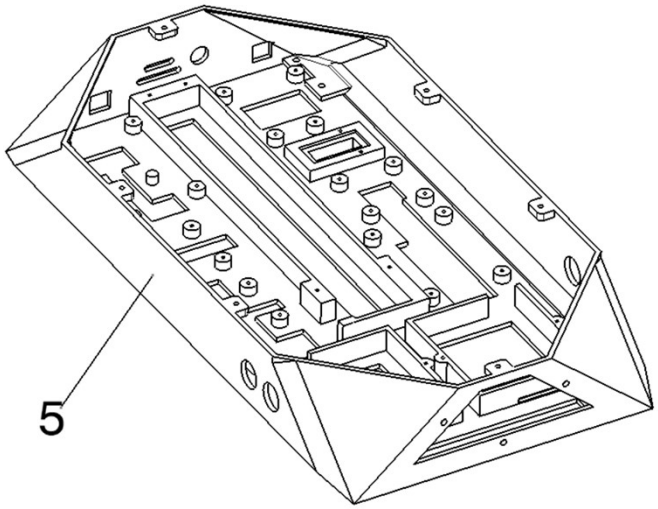

FIGURE S31. FAIRING FOR HOUSING
THE HARDWARE AND POWER SUPPLY

The system connects to the robot via a wireless local area network (WLAN), using standard communication protocols (e.g., TCP/IP) to establish a data transmission channel. This connection allows access to the user interface of the Hamamatsu mini-fluorometer, the device that performs fluorescent measurements. The data obtained from these measurements are exported and stored in an Excel file (.xls), using functions integrated into the fluorometer software for direct export.

Subsequently, an Excel macro, developed in Visual Basic for Applications (VBA), is executed. This macro functions as an API, interacting with the Excel files previously generated by the mini fluorometer. The API accesses two specific worksheets within the .xls file, using objects and methods from the Excel object model (Workbook, Worksheet, Range, etc.) to read and manipulate the data.

The API process includes a routine for comparing data between the two worksheets. Depending on the result of this comparison, the conditional logic implemented in VBA (using structures like If...Then...Else) determines whether the result is positive or negative. If the result is positive, an additional procedure is executed that triggers a sound alert, using a function from the Windows API (Beep or PlaySound).

DETECTION OF TATP BY USING THE ROBOTIC SYSTEM IN THE EXPERIMENTS

Figure S32. *Preparing the mobile platform for the TATP detection experiments.*

MEASUREMENT PROCEDURE

The support (consisting of glass + a layer of Sylgard-184 + a layer of silica nanoparticles with adsorbed dye) is placed on the sample cart (Figure S33).

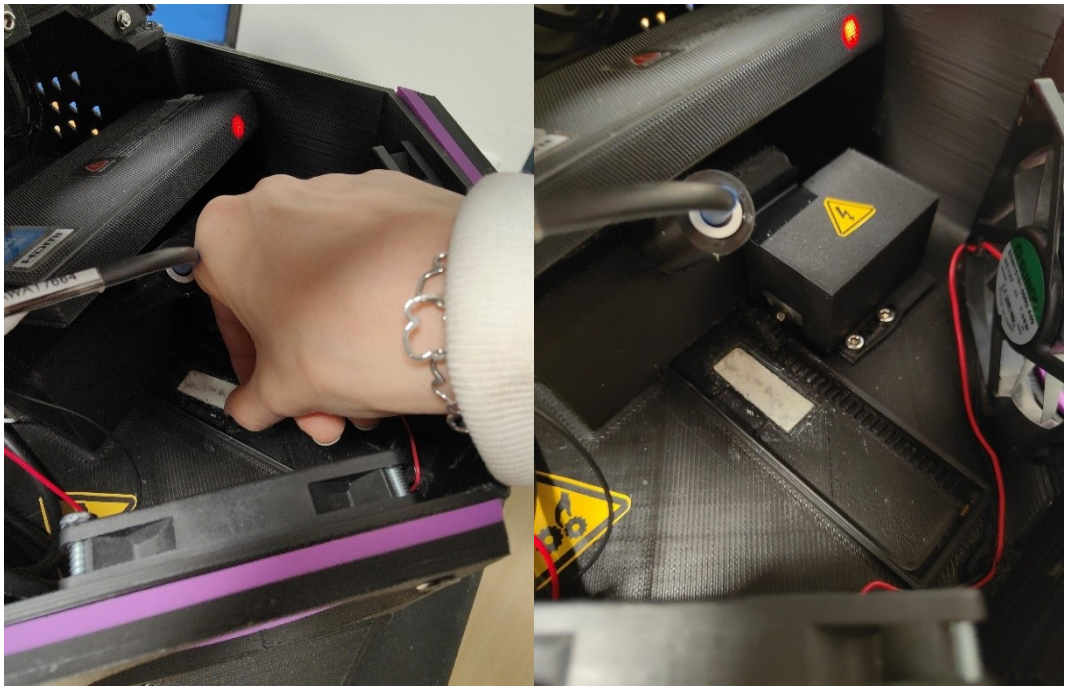

Figure S33. *Support (glass + layer of Sylgard-184 + layer of silica nanoparticles with adsorbed GC2/AR82s) being placed (left) and positioned in its final position (right) inside the sample cart.*

Using the transmitter that controls the robot's movement (Flysky FS-i6 AFHDS 2A 2.4 GHz 6CH Radio System Transmitter for RC helicopter glider with FS-iA6B 6Ch receiver, PPM output with iBus port), the movement of the sample cart within the guidance base is activated until it enters the analysis chamber (Figure S34).

Figure S34. *Flysky FS-i6 Radio System Transmitter with mobile device mounting bracket + OPPO Find X3 Pro mobile phone.*

Using the internet coverage generated by a TP-Link M7350 4G Mobile Hotspot mounted on the robot's top surface, a MeLE PCG02 Pro Stick mini PC (Windows 11 Pro J4125 8GB 128GB, USB-C PD3.0, SSD support, Dual HDMI 4K-HD), and using standard communication protocols (e.g., TCP/IP), a data transmission channel is established between the robot and a remote desktop, via an OPPO Find X3 Pro mobile phone (Figure S35).

Figure S35. *TP-Link M7350 4G Mobile Hotspot on the robot (left), MeLE PCG02 Pro Stick mini PC (center), and OPPO Find X3 Pro mobile phone (right).*

This connection allows access to the user interface of the TOKUSPEC mini-spectrometer software version 1.3 from Hamamatsu Photonics (Figure S35).

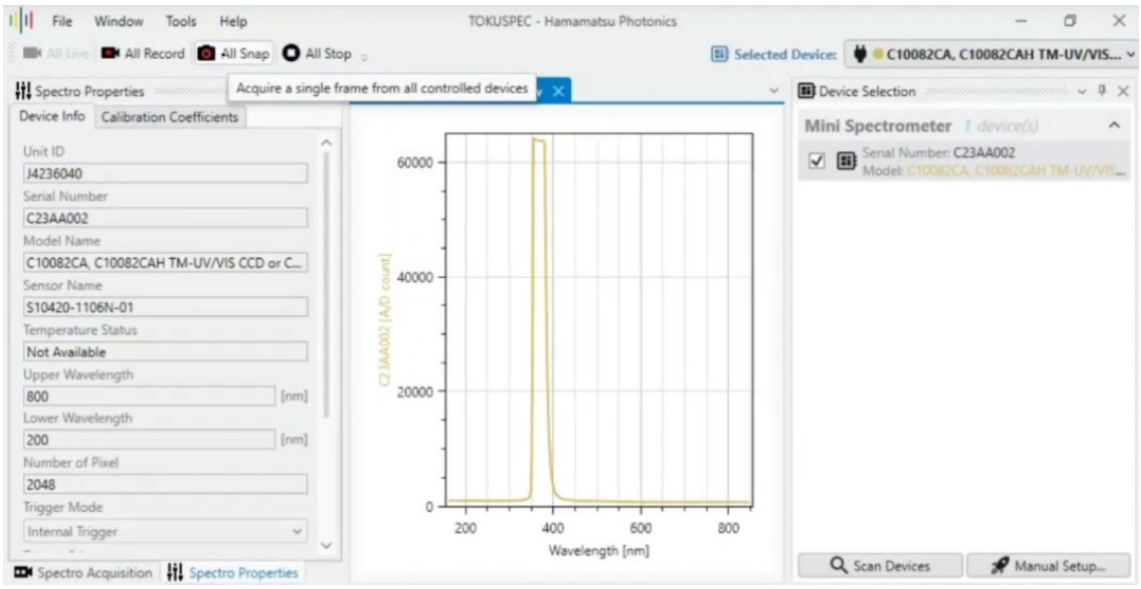

Figure S35. *Measurement screen of the TOKUSPEC mini-spectrometer software version 1.3.*

This software controls the operation of a Hamamatsu C10082CA mini-spectrometer for UV and near-infrared (200 to 800 nm) and high sensitivity, a device that performs the fluorescence emission measurements that support the measurement system (Figure S36).

Figure S36*. Hamamatsu C10082CA mini-spectrometer.*

The system also includes:

• LED light source + controller model L14310-115 (Image 6), mounted condenser lens E11923-015, focal length 15 mm, radiation area (*3) approx. φ6, wavelength 365 / 385 / 405 nm and UV radiation (*4) 6500 mW/cm² from Hamamatsu Photonics, used to excite the sample (Figure S37).

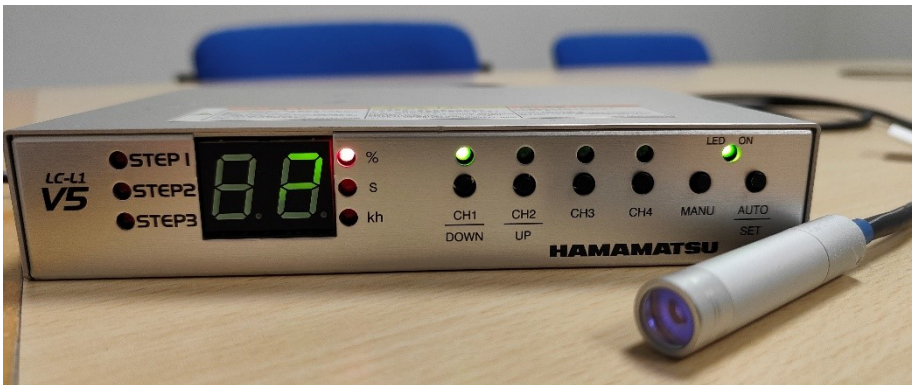

Figure S37. *LED light source and controller model L14310-115.*

• UV-Vis A15362-01 UV-resistant optical fiber, core diameter 600 µm, NA 0.22, length 1.5 m with both ends terminated in SMA905D connectors from Hamamatsu Photonics, captures and transmits the signal to the software (Figure S38).

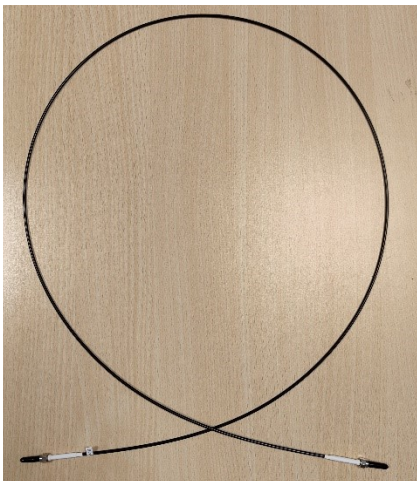

Figure S38. *Optical fiber type A15362-01.*

The measurement parameters set are:

• LED controller model L14310-115:

- LED source at 2% of its total capacity.
- Connection channel 1 (CH01).
- Manual Radiation Mode (MANU).

• TOKUSPEC mini-spectometer software version 1.3:

- No temperature control.
- Wavelength range: 200 - 800 nm.
- Pixel number: 2048.
- Trigger Mode: Internal Trigger.
- Trigger Edge: Rising Edge.
- Gain Mode: None.
- Integration time: 100000 µs.

An initial measurement of the substrate's emission intensity is performed. This measurement is exported and stored in an Excel (.xls) file as “1”, using the fluorometer software's built-in functions for direct export (Figure S39).

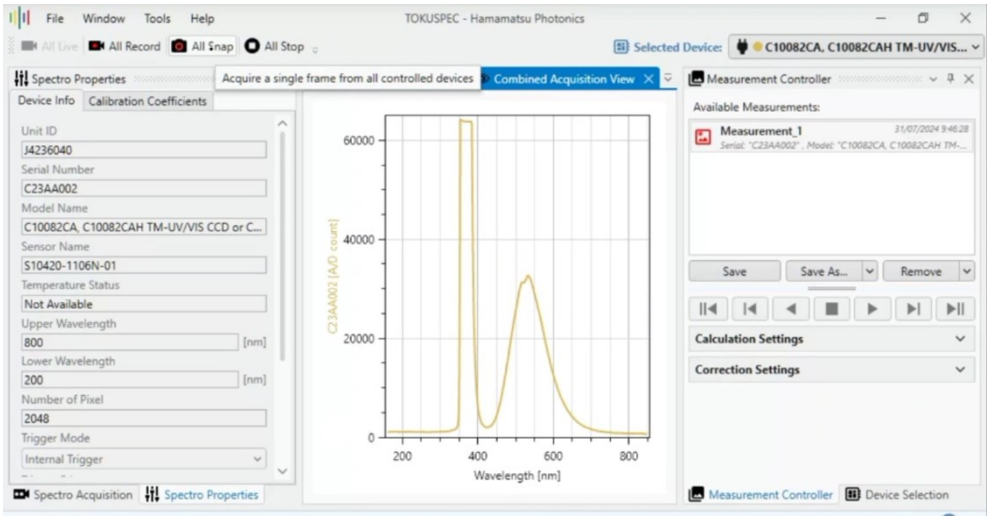

Figure S39. *Measurement screen of the TOKUSPEC mini-spectrometer software version 1.3 during measurement “1”.*

The sample holder remains inside the analysis chamber for a programmed 15 seconds, during which the measurement is taken. After this time, the sample carriage, along with the holder, returns to its initial position, sliding along the guide base. Following this, the robot automatically begins drawing in air from the outside using a suction system consisting of a main aspirator, two auxiliary aspirators, two side suction nozzles, and a top suction nozzle. During this air intake process (and the intake of any TATP vapors present), the robot can remain stationary or move, either manually using a control transmitter or autonomously using an automatic guidance system. Once the desired intake time has elapsed, the sample carriage is reactivated using the control transmitter, which then places the holder back into the analysis chamber. The support remains inside the analysis chamber for 15 seconds, during which time the second measurement is taken. This measurement (saved as “2”) is exported and stored in an Excel file (.xls) (Figure S40).

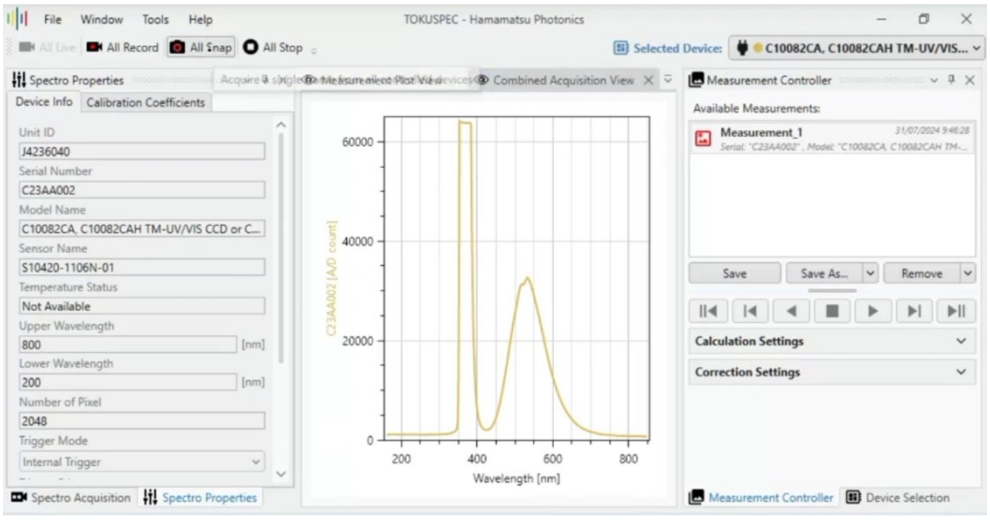

Figure S40. *Screenshot of the TOKUSPEC mini-spectrometer software version 1.3 during measurement “2”.*

After this time, the sample carriage, along with the support, returns to its initial position, sliding along the guide base. The specific configuration and geometric design of the robot's components ensure that both the sample carriage and the support mounted on it always move between two fixed points (initial and final points). In this way, the analysis performed inside the analysis chamber is always carried out in the same position, allowing for a comparative analysis of the same point on the sample, before and after the support has been exposed to the TATP vapors present in the air captured during its movement. Subsequently, an Excel macro, developed in VBA (Visual Basic for Applications), is executed. This macro functions as an API, interacting with the Excel files previously generated by the mini spectrometer. The API accesses two specific worksheets within the .xls file (measurements “1” and “2”), using objects and methods from the Excel object model (Workbook, Worksheet, Range, etc.) to read and manipulate the data. The Excel macro is structured in two main areas. The upper area has a data comparison table on the left and a warning panel on the right. This panel initially appears with an orange background and displays the message “Analysis Pending”. The following buttons can be seen in the lower half:

- Analyze: to proceed with the analysis of the data loaded into the program.

- Update reading: to update measurement files “1” and “2” that the software will compare.

- Delete: to delete the previous data loaded into the macro.

- Exit: to disconnect and safely exit the data comparison macro.

The API process includes a data comparison routine between the two spreadsheets. The emission values in the 527 to 531 nm range (the region of the spectrum where the maximum emission of the sensor compound is found) of measurement “1” (initial measurement) and measurement “2” (final measurement) are compared. Depending on the result of this comparison, the conditional logic implemented in VBA (using structures such as If...Then...Else) determines whether the result is positive or negative. If the fluorescence emission values of sample “2” for the studied spectral region are the same as those of sample “1”—that is, if the sensor's fluorescence emission intensity remains stable after the air sampling process—the result is negative for the presence of TATP vapors. This results in a change in the Excel macro interface, which displays a green square with the message “Negative Result”. If the fluorescence emission values of sample “2” for the studied spectral region are higher than those of sample “1”—that is, if there is an increase in the sensor's fluorescence emission intensity after the air sampling process—the result is positive for the presence of TATP vapors. This results in a change to the Excel macro interface, which now displays a red square with the message “Explosives Detected”. Additionally, an extra procedure is executed that triggers an audible alert, using a Windows API function (Beep or PlaySound), and an alarm signal begins playing through the robot's built-in sound system.

<u>EXPERIMENT 1.</u> 30-minute exposure to **TATP. Newly synthesized compound, silica particles, compound adsorbed one day before. Acquisition time 100000 µs (default value). LED intensity = 2%.**

The fluorescence emission spectra collected by the robot during the experiment are shown in **Table S18**.

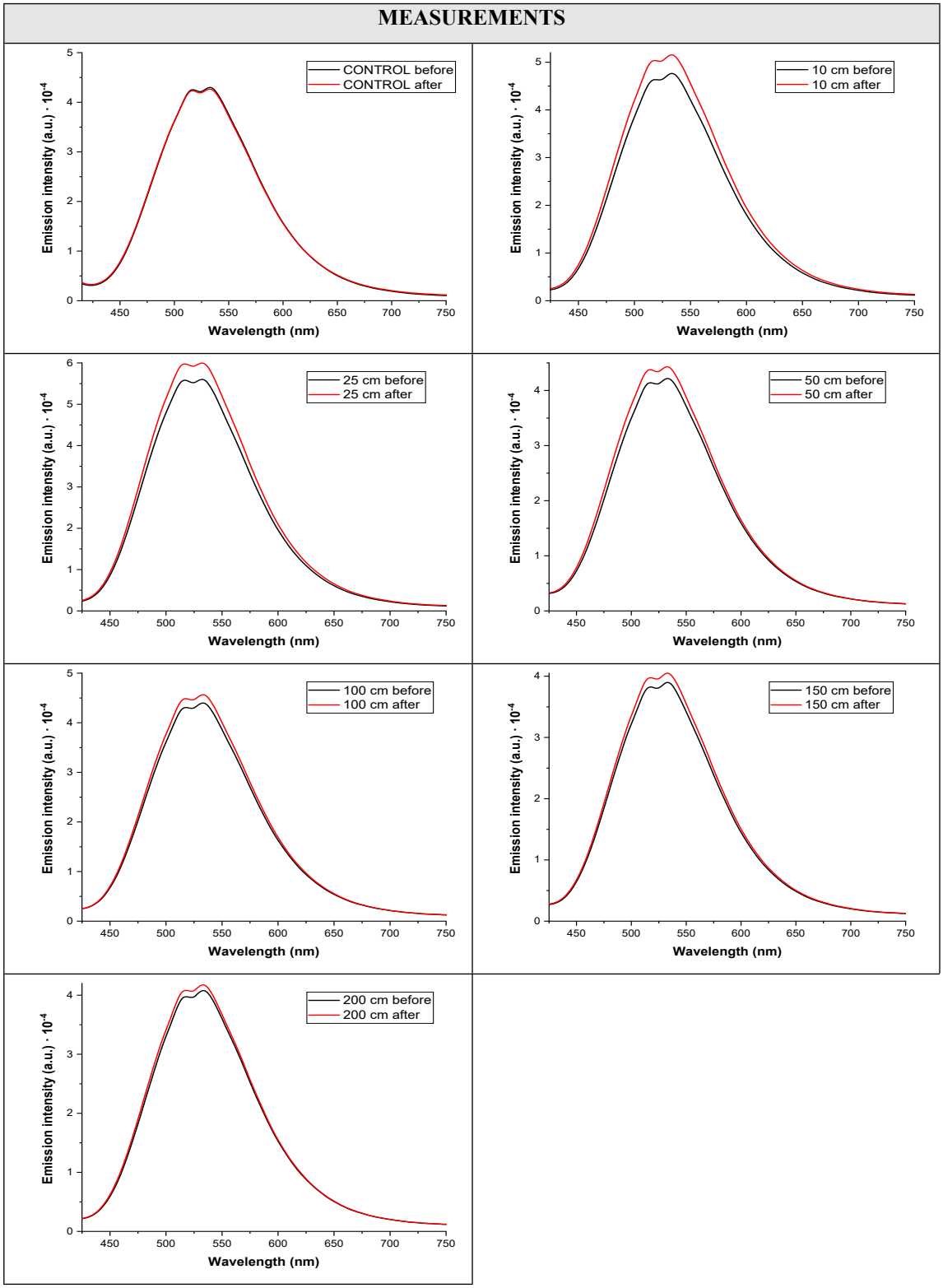

Table S18. *Emission spectra of the sensing particles before and after exposure to TATP vapors in order of increasing distance from the TATP source.*

<u>EXPERIMENT 2.</u> 30-minute exposure to **TATP. Newly synthesized compound, silica particles, compound adsorbed one day before. Acquisition time 100000 µs (default value). LED intensity = 2%.**

The fluorescence emission spectra collected by the robot during the experiment are shown in **Table S19**.

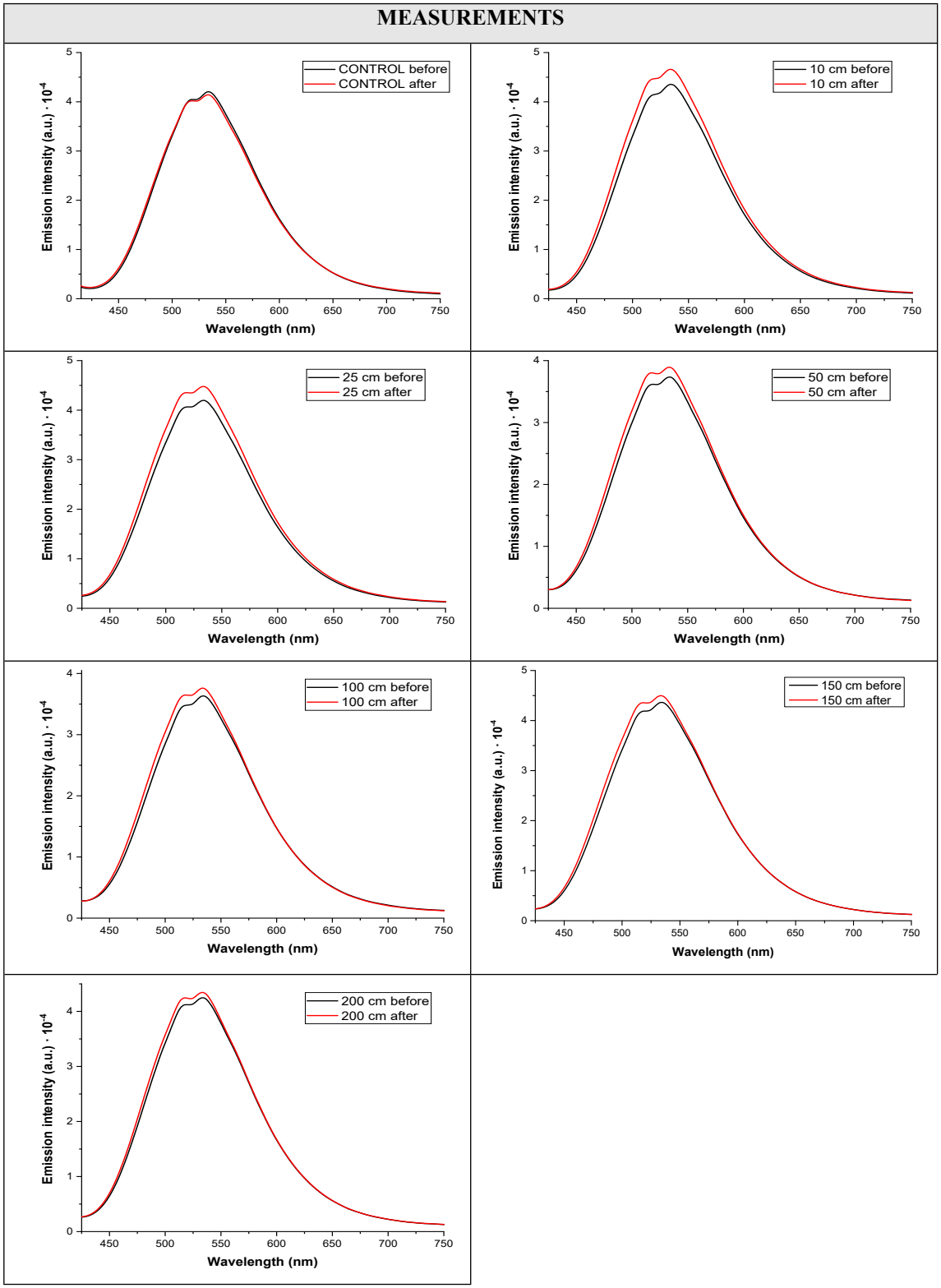

Table S19. *Emission spectra of the sensing particles before and after exposure to TATP vapors in order of increasing distance from the TATP source.*

<u>EXPERIMENT 3.</u> 30-minute exposure to **TATP. Newly synthesized compound, silica particles, compound adsorbed one day before. Acquisition time 100000 µs (default value). LED intensity = 2%.**

The fluorescence emission spectra collected by the robot during the experiment are shown in **Table S20**.

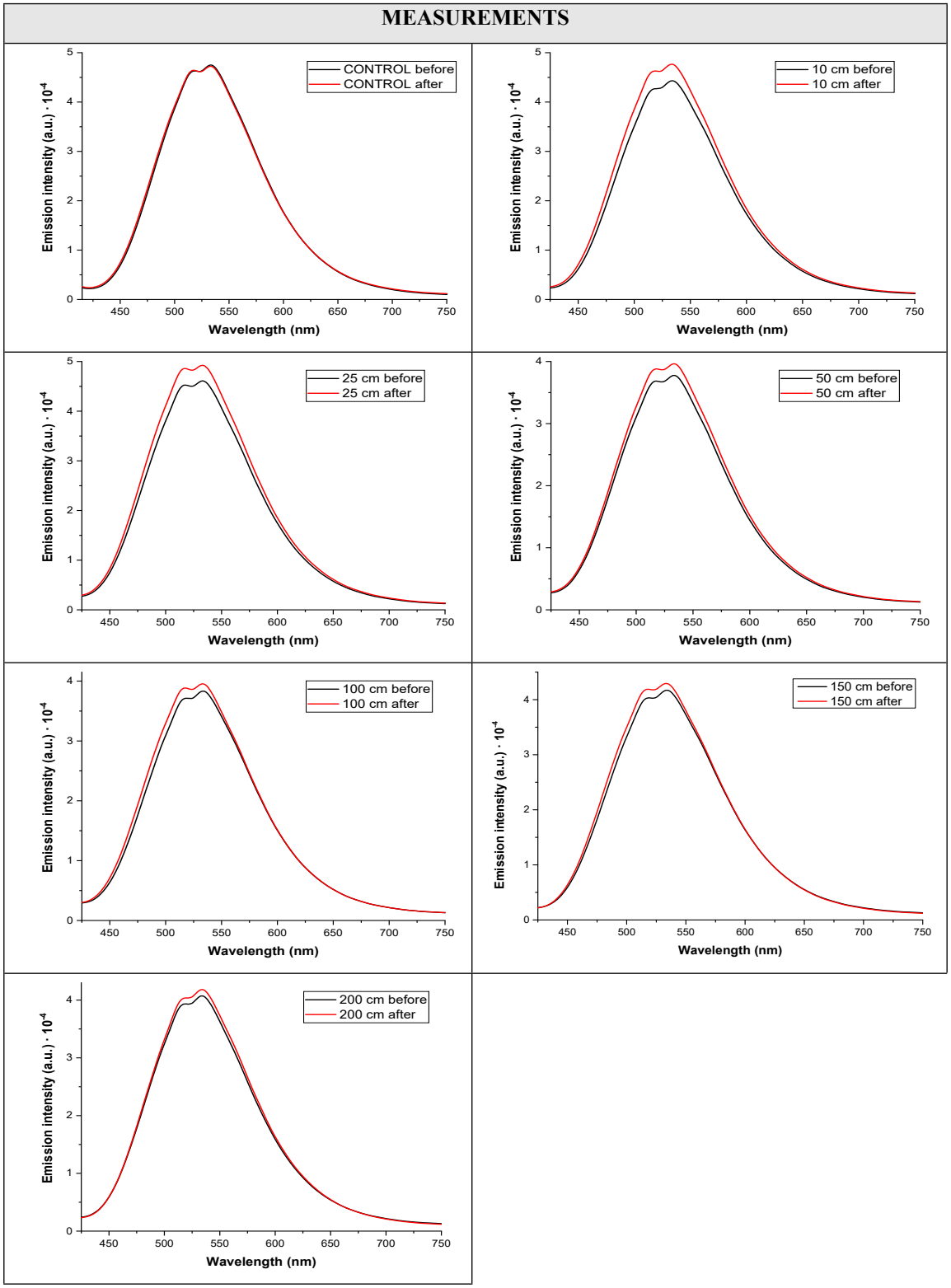

Table S20. *Emission spectra of the sensing particles before and after exposure to TATP vapors in order of increasing distance from the TATP source.*

<u>EXPERIMENT 4.</u> 30-minute exposure to **TATP. Newly synthesized compound, silica particles, compound adsorbed one day before. Acquisition time 100000 µs (default value). LED intensity = 2%.**

The fluorescence emission spectra collected by the robot during the experiment are shown in **Table S21**.

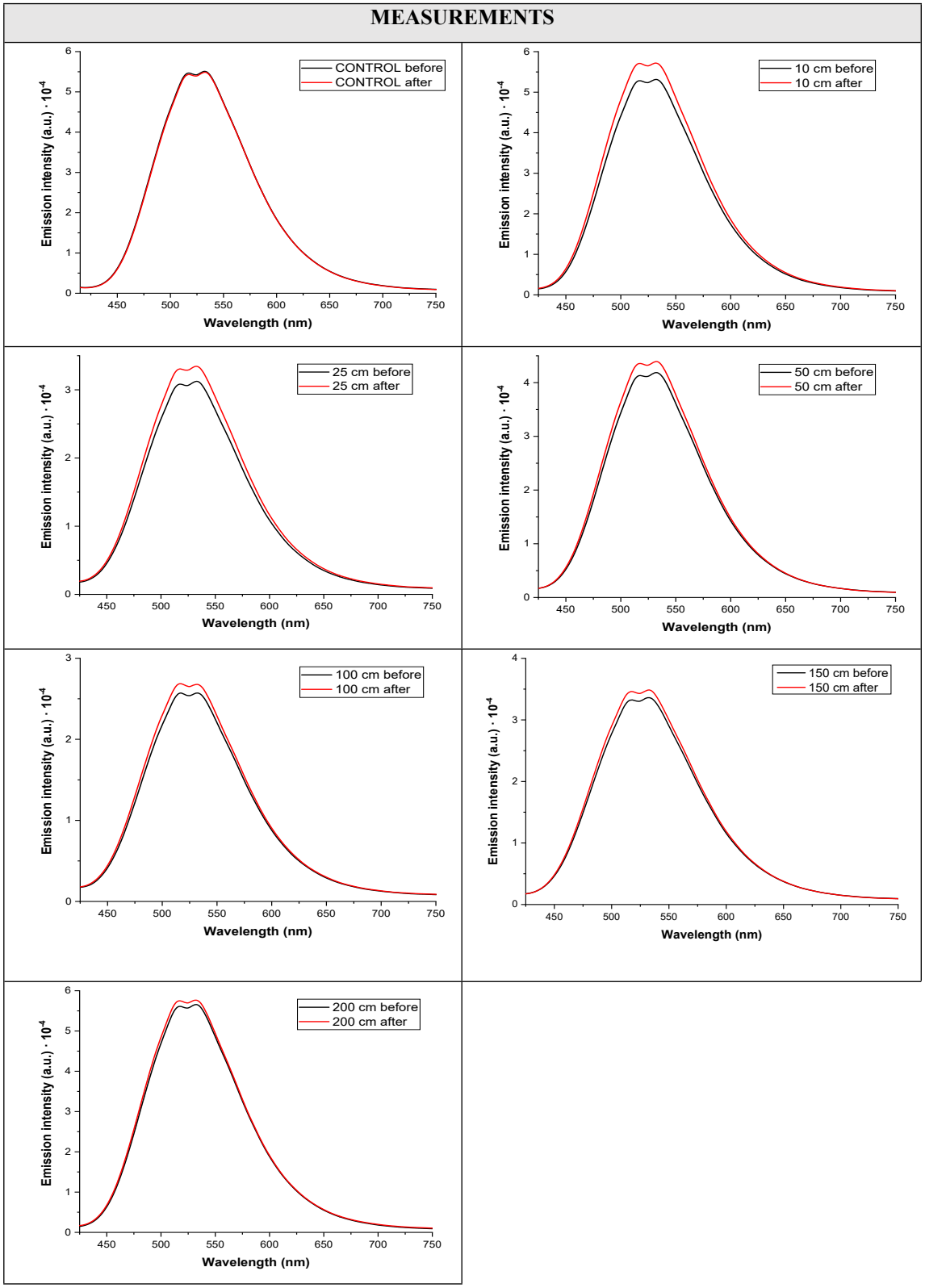

Table S21. *Emission spectra of the sensing particles before and after exposure to TATP vapors in order of increasing distance from the TATP source.*

<u>EXPERIMENT 5.</u> 30-minute exposure to **TATP. Newly synthesized compound, silica particles, compound adsorbed one day before. Acquisition time 100000 µs (default value). LED intensity = 2%.**

The fluorescence emission spectra collected by the robot during the experiment are shown in **Table S22**.

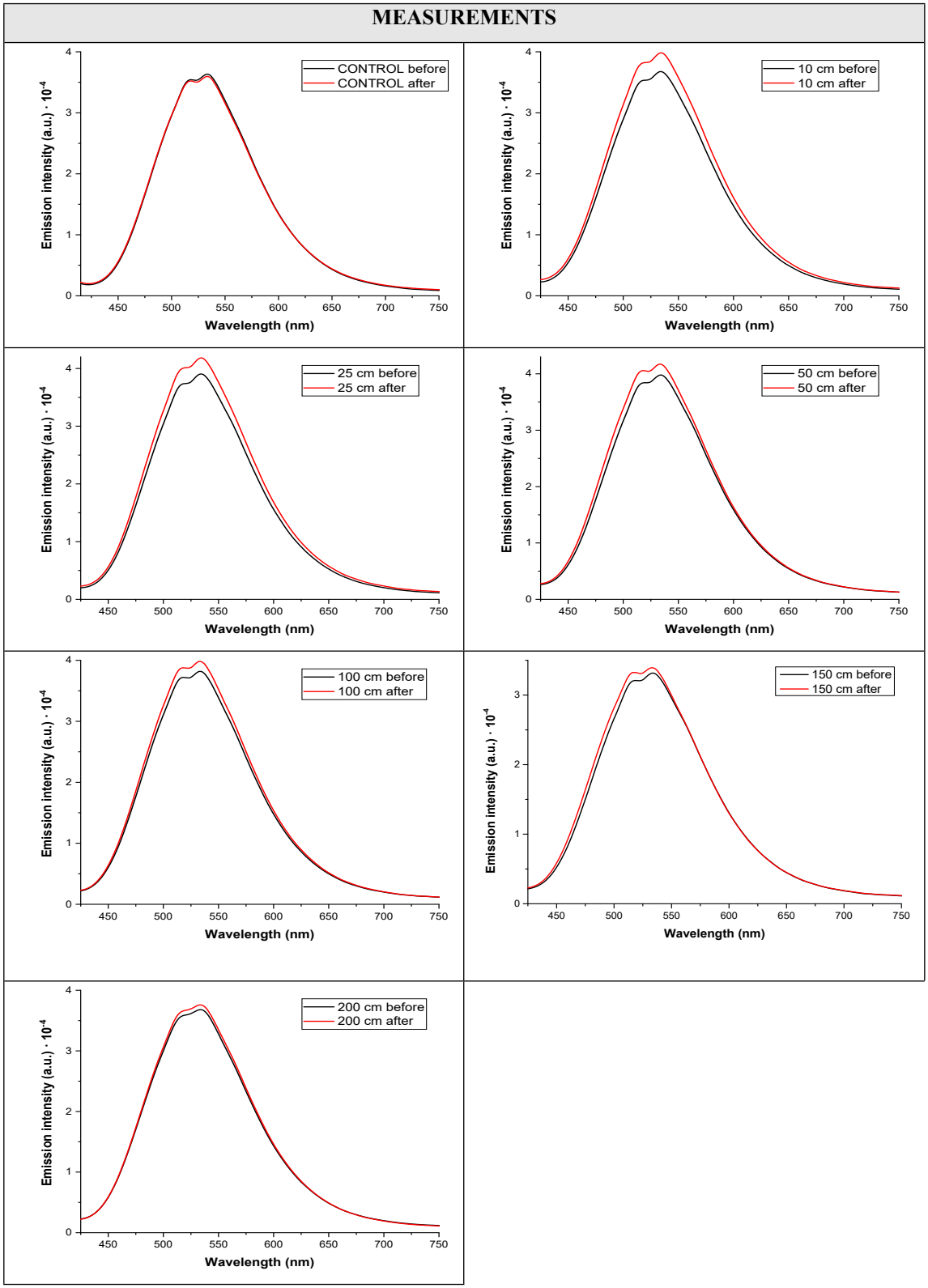

Table S22. *Emission spectra of the sensing particles before and after exposure to TATP vapors in order of increasing distance from the TATP source.*

<u>EXPERIMENT 6.</u> 30-minute exposure to **TATP. Newly synthesized compound, silica particles, compound adsorbed one day before. Acquisition time 100000 µs (default value). LED intensity = 2%.**

The fluorescence emission spectra collected by the robot during the experiment are shown in **Table S23**.

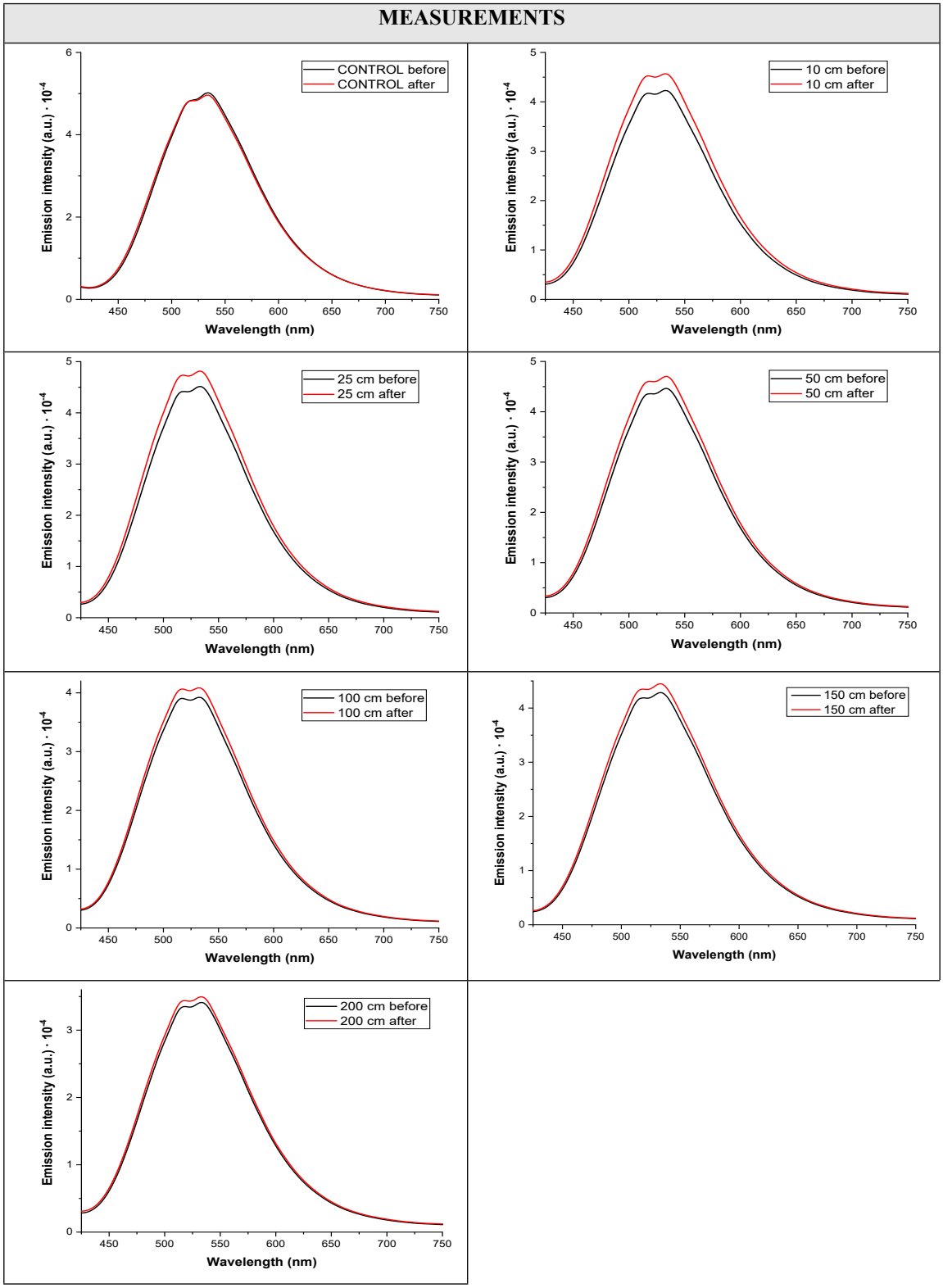

Table S23. *Emission spectra of the sensing particles before and after exposure to TATP vapors in order of increasing distance from the TATP source.*

<u>EXPERIMENT 7.</u> 30-minute exposure to **TATP. Newly synthesized compound, silica particles, compound adsorbed one day before. Acquisition time 100000 µs (default value). LED intensity = 2%.**

The fluorescence emission spectra collected by the robot during the experiment are shown in **Table S24**.

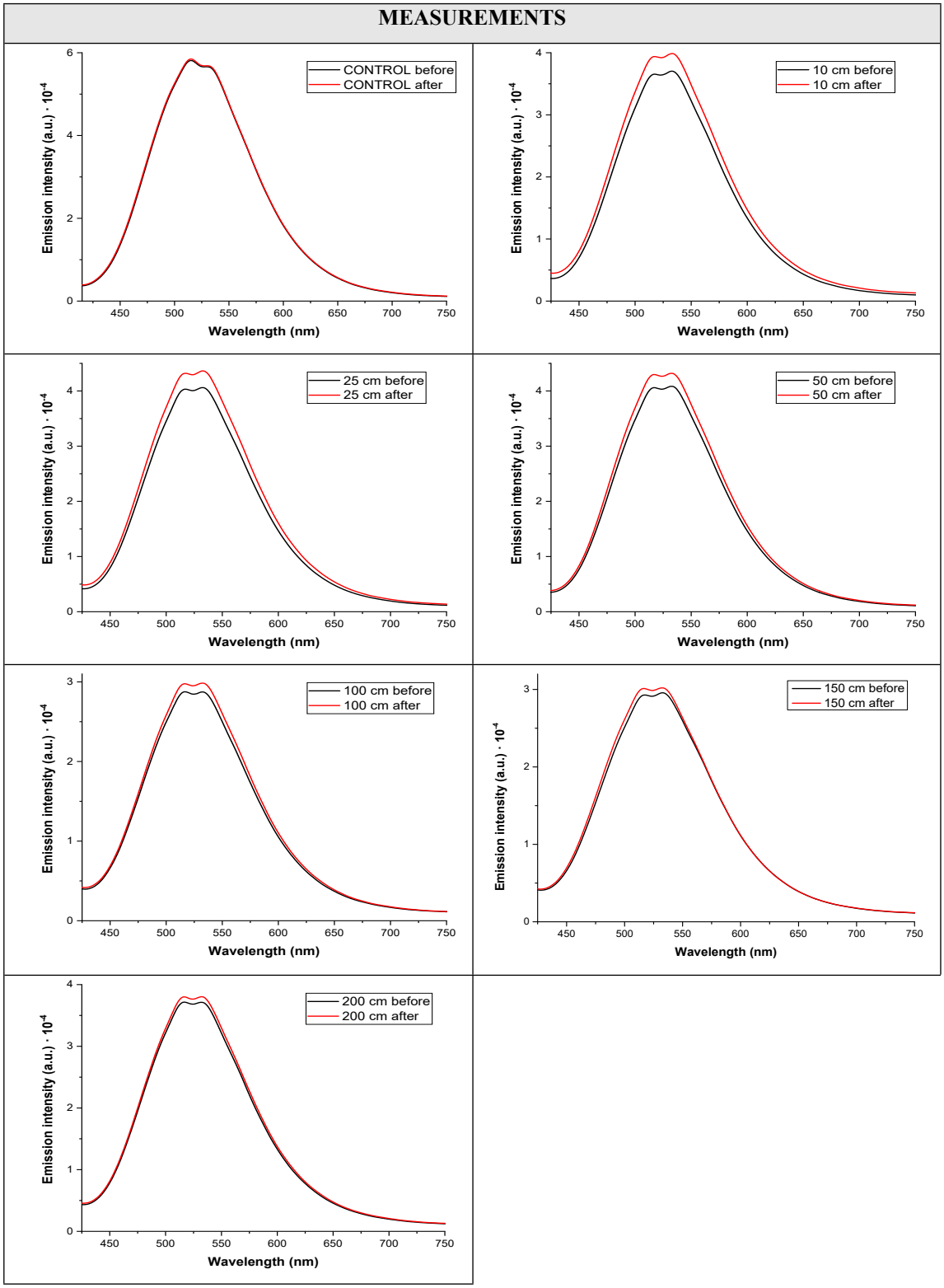

Table S24. *Emission spectra of the sensing particles before and after exposure to TATP vapors in order of increasing distance from the TATP source.*

<u>EXPERIMENT 8.</u> 30-minute exposure to **TATP. Newly synthesized compound, silica particles, compound adsorbed one day before. Acquisition time 100000 µs (default value). LED intensity = 2%.**

The fluorescence emission spectra collected by the robot during the experiment are shown in **Table S25**.

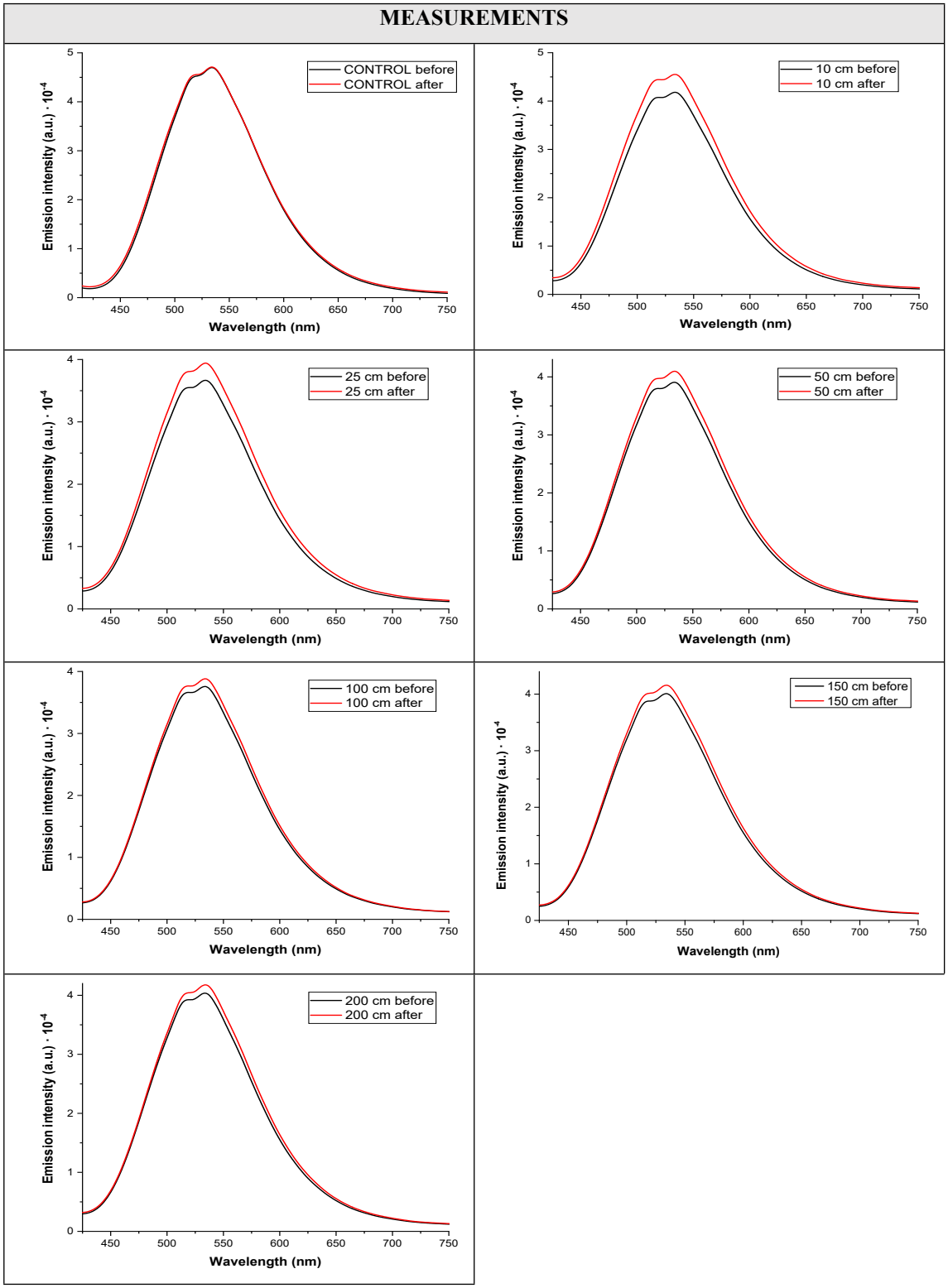

Table S25. *Emission spectra of the sensing particles before and after exposure to TATP vapors in order of increasing distance from the TATP source.*

<u>EXPERIMENT 9.</u> 30-minute exposure to **TATP. Newly synthesized compound, silica particles, compound adsorbed one day before. Acquisition time 100000 µs (default value). LED intensity = 2%.**

The fluorescence emission spectra collected by the robot during the experiment are shown in **Table S26**.

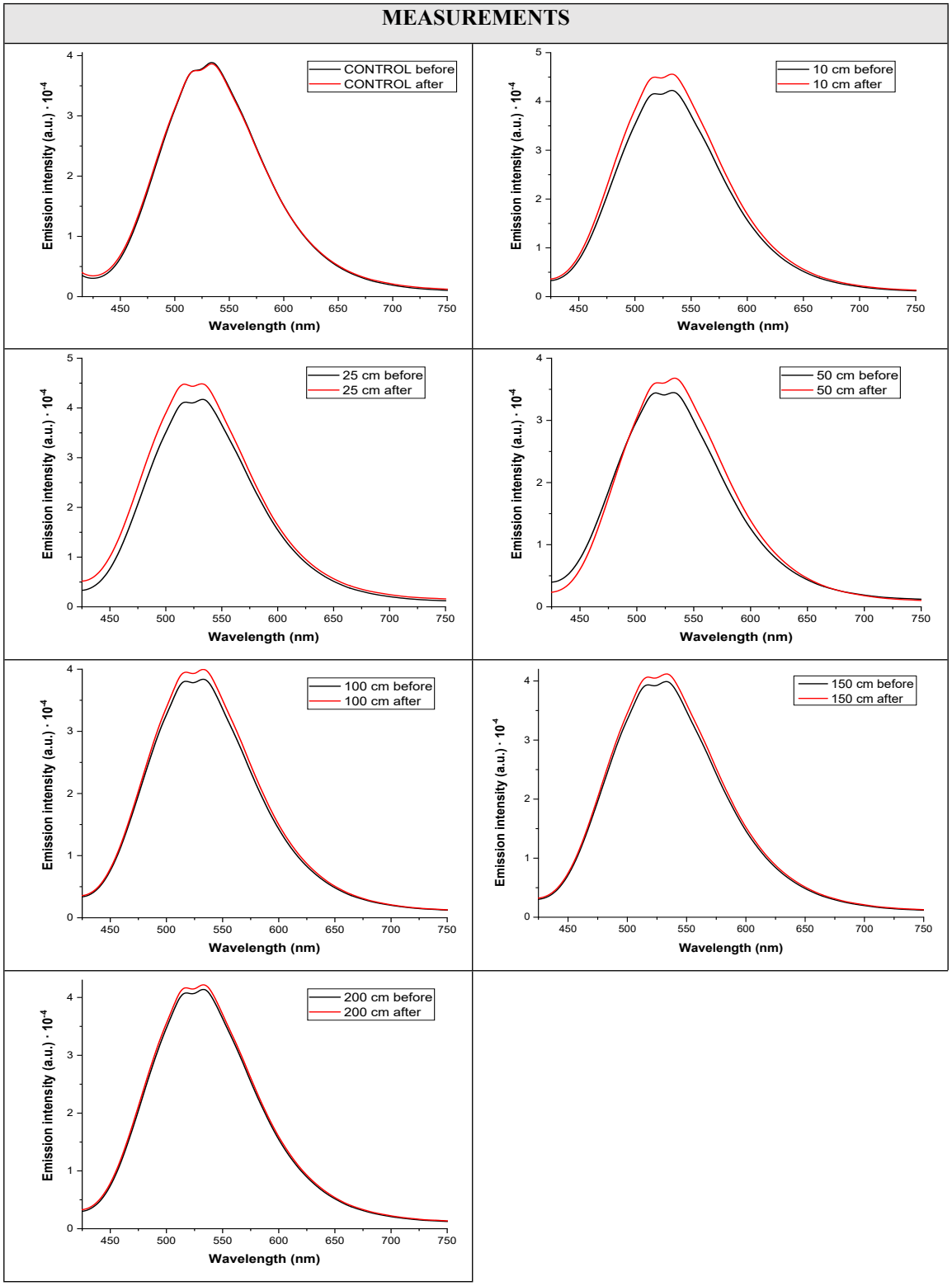

Table S26. *Emission spectra of the sensing particles before and after exposure to TATP vapors in order of increasing distance from the TATP source.*

<u>EXPERIMENT 10.</u> 30-minute exposure to **TATP. Newly synthesized compound, silica particles, compound adsorbed one day before. Acquisition time 100000 µs (default value). LED intensity = 2%.**

The fluorescence emission spectra collected by the robot during the experiment are shown in **Table S27**.

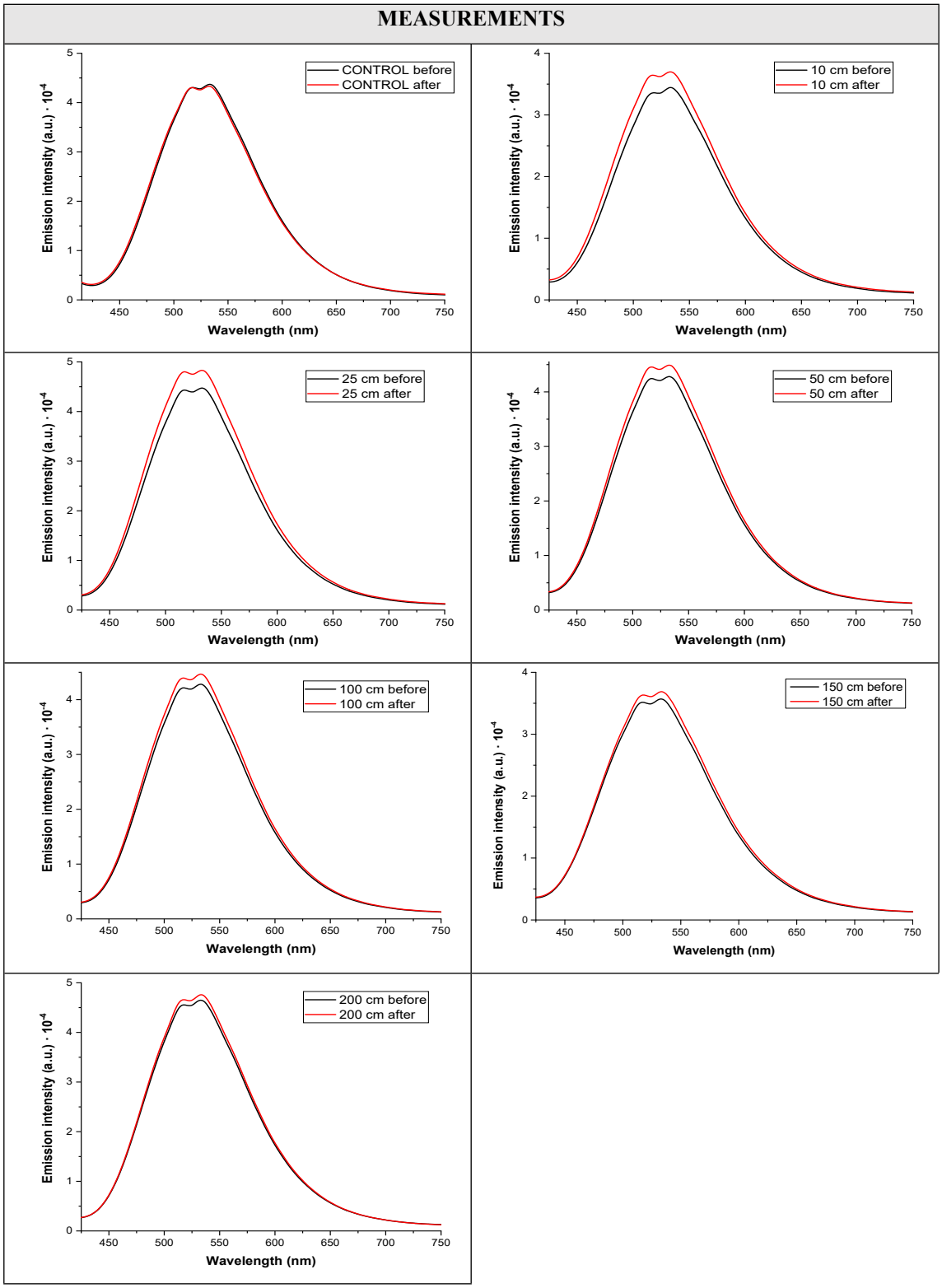

Table S27. *Emission spectra of the sensing particles before and after exposure to TATP vapors in order of increasing distance from the TATP source.*

<u>EXPERIMENT 11.</u> 30-minute exposure to **TATP. Newly synthesized compound, silica particles, compound adsorbed one day before. Acquisition time 100000 µs (default value). LED intensity = 2%.**

The fluorescence emission spectra collected by the robot during the experiment are shown in **Table S28**.

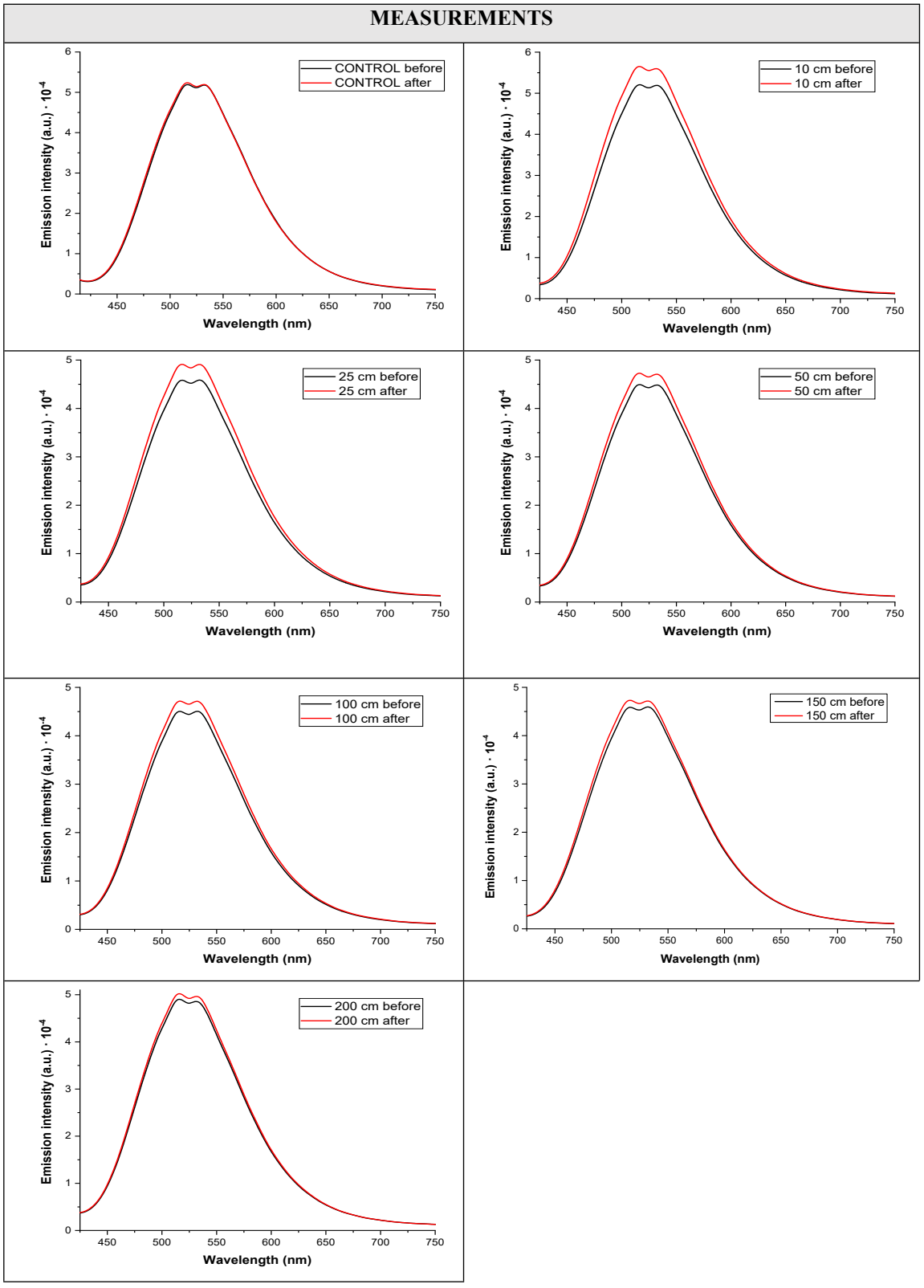

Table S28. *Emission spectra of the sensing particles before and after exposure to TATP vapors in order of increasing distance from the TATP source.*

<u>EXPERIMENT 12.</u> 30-minute exposure to TATP. Newly synthesized compound, silica particles, compound adsorbed one day before. Acquisition time 100000 µs (default value). LED intensity = 2%.

The fluorescence emission spectra collected by the robot during the experiment are shown in **Table S29**.

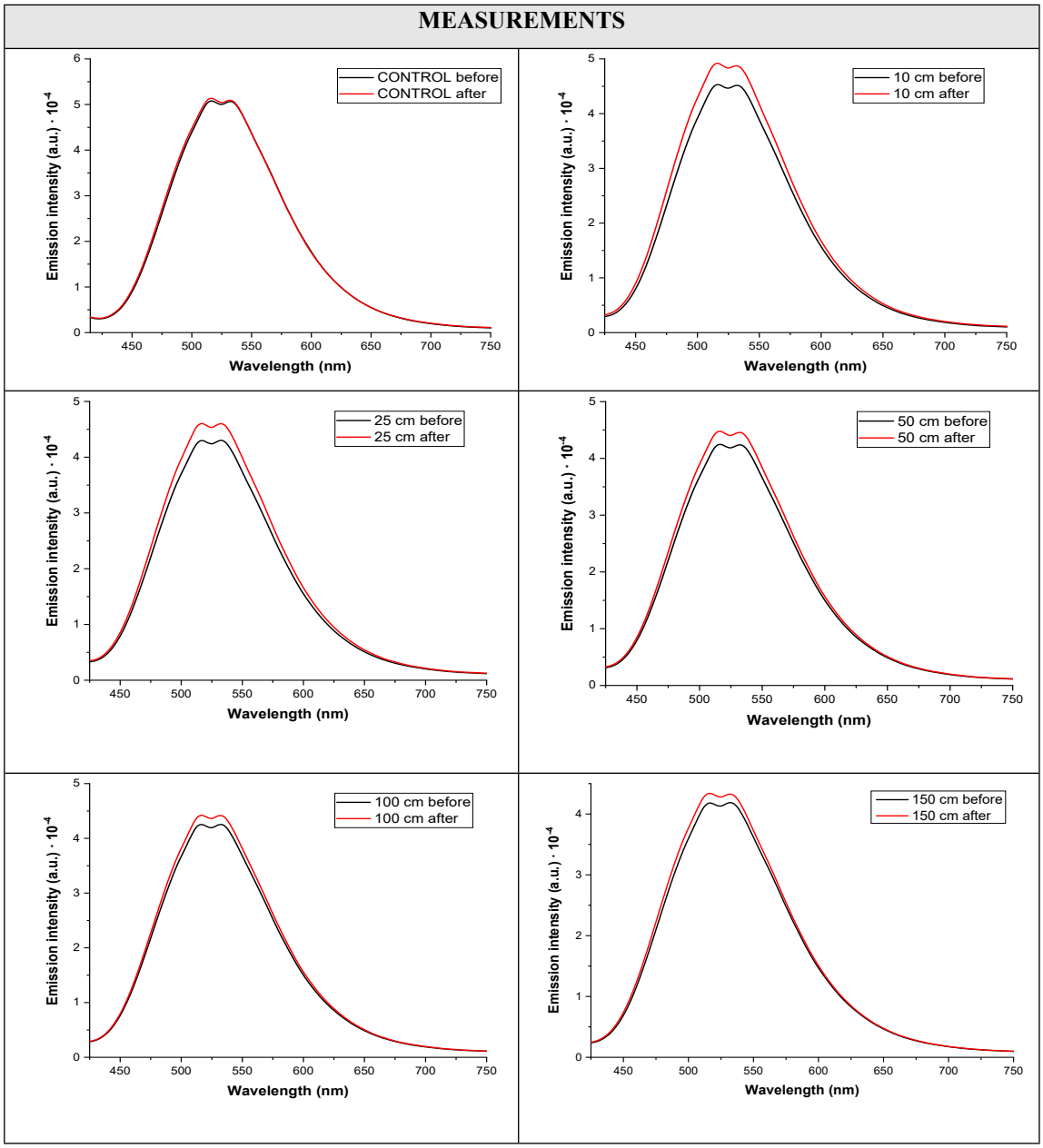

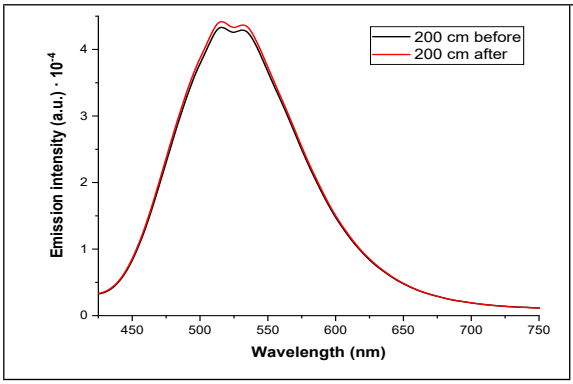

Table S29. *Emission spectra of the sensing particles before and after exposure to TATP vapors in order of increasing distance from the TATP source.*

RESULTS SUMMARY

Finally, variation of the fluorescence emission at the wavelength of maximum emission (525 nm) is calculated for each experiment and distance to the TATP source. It's then joint represented so as to obtain conclusions. The graphs shown in **Table S30** were obtained:

SUMMARY
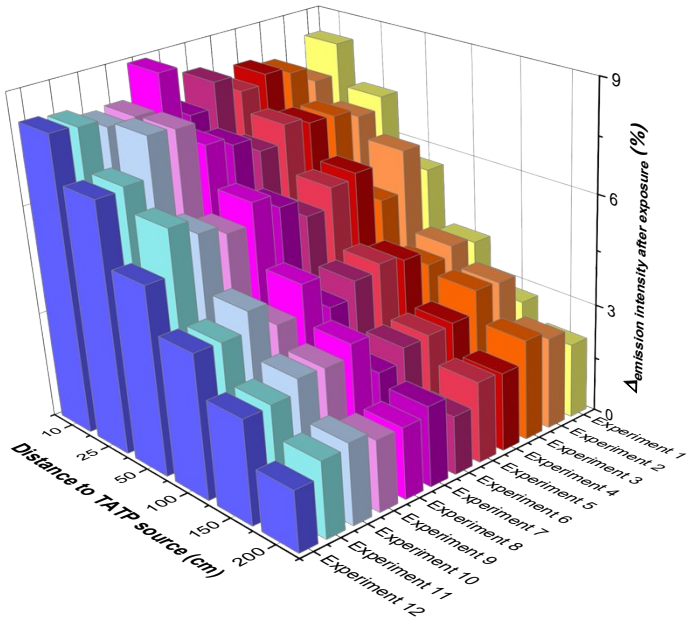
3D bar chart representing the variation (%) of the fluorescence emission of the robot sensing particles as a function of the distance to the TATP source in Experiments 1 to 12.

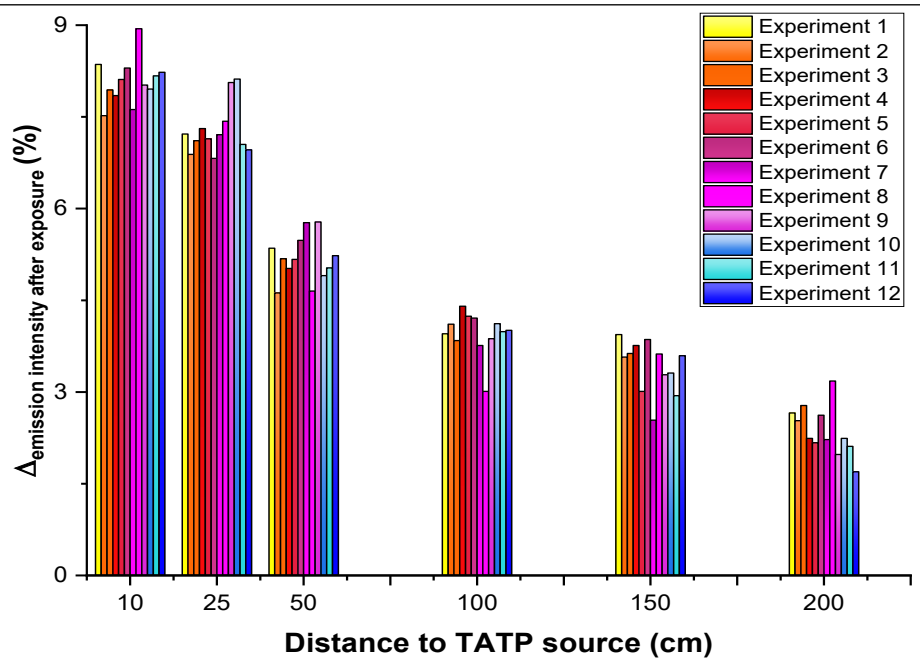

2D bar chart representing the variation (%) of the fluorescence emission of the robot sensing particles as a function of the distance to the TATP source in Experiments 1 to 12.

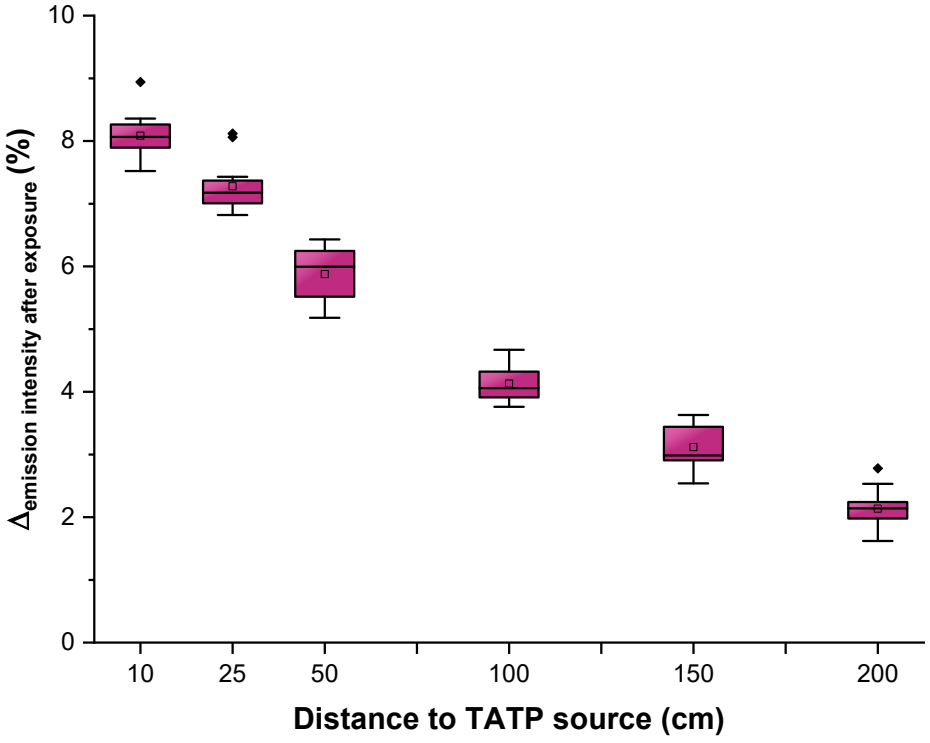

Box and Whisker plot representing the variation (%) of the fluorescence emission of the robot sensing particles as a function of the distance to the TATP source in Experiments 1 to 12.

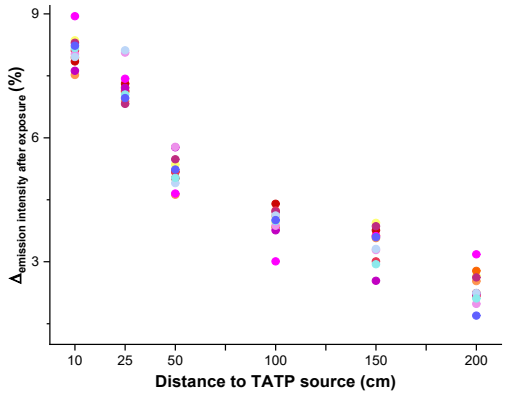	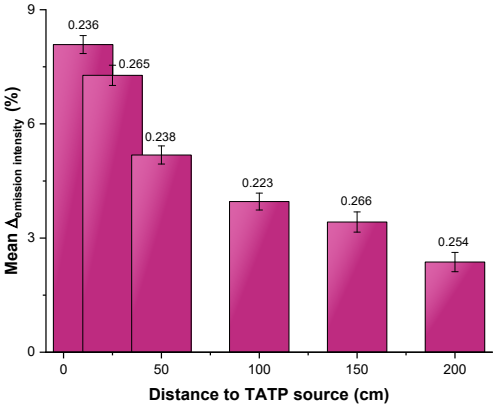
Column scatter plot representing the variation (%) of the fluorescence emission of the robot sensing particles as a function of the distance to the TATP source in Experiments 1 to 12.	Column + Label plot representing the mean and error of the variation (%) of the fluorescence emission of the robot sensing particles as a function of the distance to the TATP source in Experiments 1 to 12.

Table S30. *Joint representations of the data corresponding to Experiments 1 to 12.*

Additionally, a set of 5 experiments was carried out consisting of driving the robot inside the room containing TATP and causing the device to move around the entire room while passing at different distances from the TATP source for a period of 30 minutes.

Fluorescence measurements of the sensing particles are acquired before and after the robot moves through the room in which the TATP is placed, as well as control measurements of the fluorescence of the sensing particles themselves after an identical route in a room lacking TATP.

<u>EXPERIMENT 1.</u> 30-minute exposure to **TATP. Newly synthesized compound, silica particles, compound adsorbed one day before. Acquisition time 100000 µs (default value). LED intensity = 2%.**

The fluorescence emission spectra collected by the robot during the experiment are shown in **Table S31**.

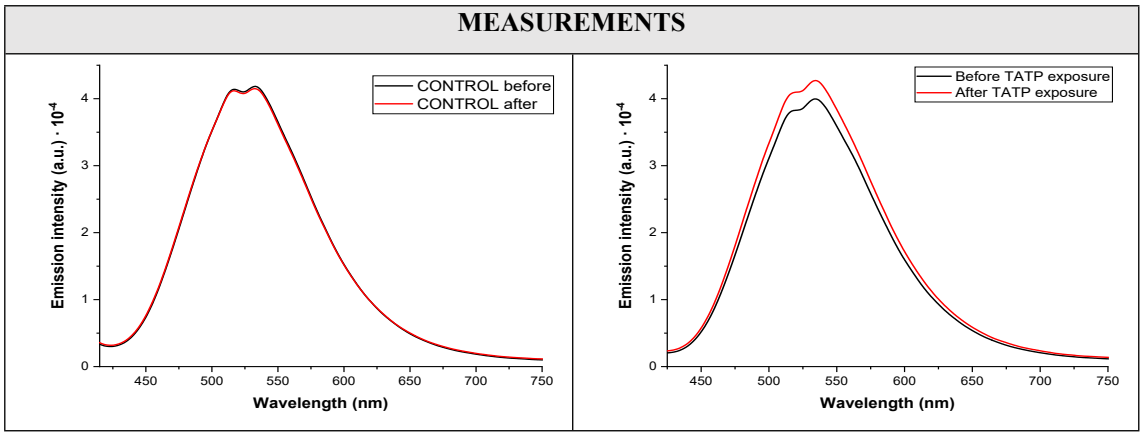

Table S31. *Control measure spectrum of the sensing particles emission (left) and emission spectrum of the particles before and after exposure to TATP vapors (right) in Experiment 1.*

<u>EXPERIMENT 2.</u> 30-minute exposure to **TATP. Newly synthesized compound, silica particles, compound adsorbed one day before. Acquisition time 100000 µs (default value). LED intensity = 2%.**

The fluorescence emission spectra collected by the robot during the experiment are shown in **Table S32**.

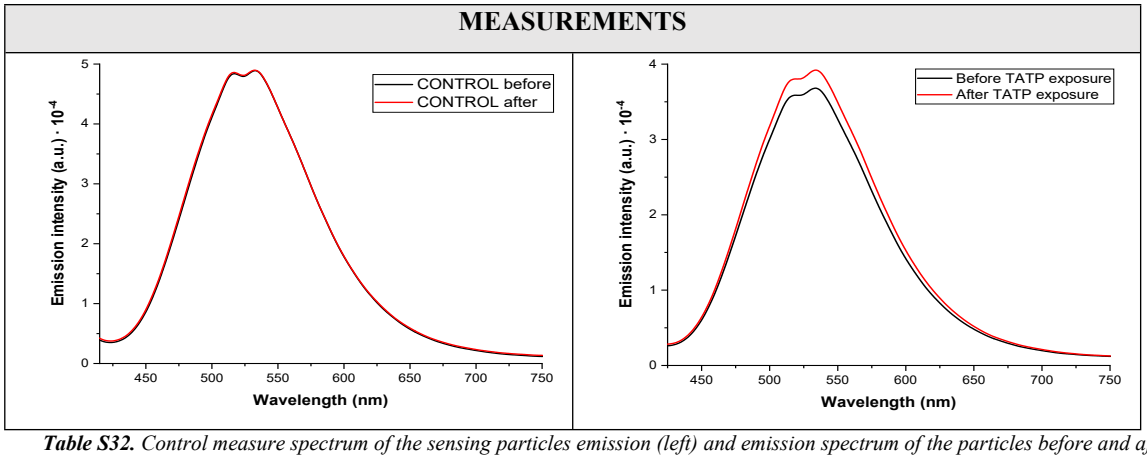

Table S32. *Control measure spectrum of the sensing particles emission (left) and emission spectrum of the particles before and after exposure to TATP vapors (right) in Experiment 2.*

<u>EXPERIMENT 3.</u> 30-minute exposure to **TATP. Newly synthesized compound, silica particles, compound adsorbed one day before. Acquisition time 100000 µs (default value). LED intensity = 2%.**

The fluorescence emission spectra collected by the robot during the experiment are shown in **Table S33**.

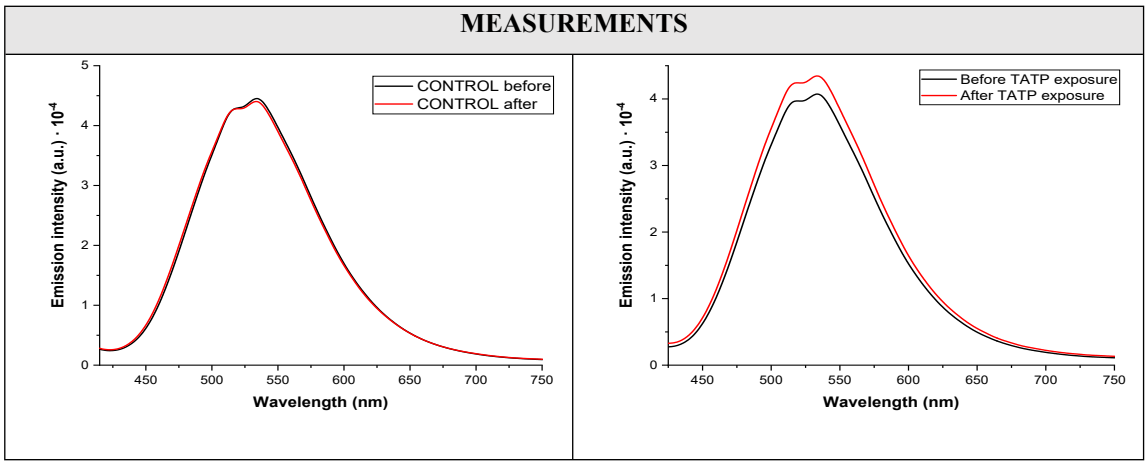

Table S33. *Control measure spectrum of the sensing particles emission (left) and emission spectrum of the particles before and after exposure to TATP vapors (right) in Experiment 3.*

<u>EXPERIMENT 4.</u> 30-minute exposure to **TATP. Newly synthesized compound, silica particles, compound adsorbed one day before. Acquisition time 100000 µs (default value). LED intensity = 2%.**

The fluorescence emission spectra collected by the robot during the experiment are shown in **Table S34**.

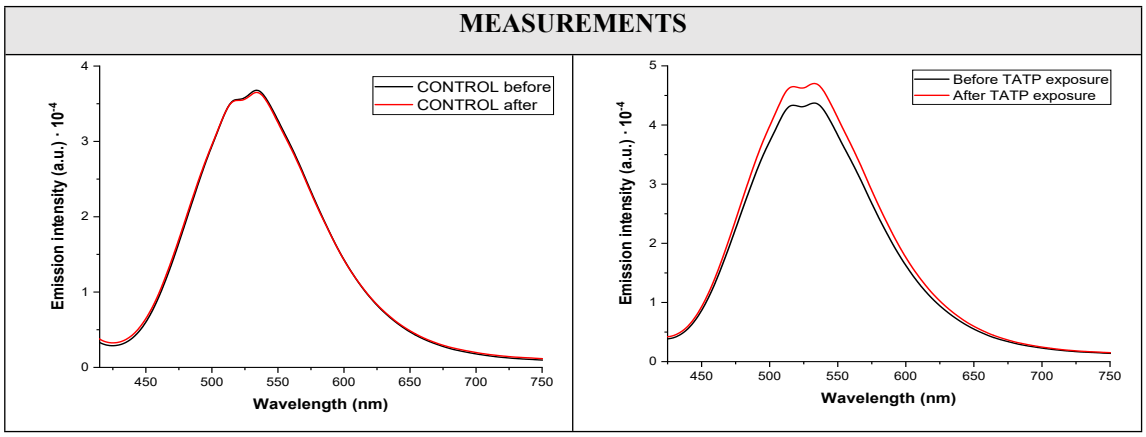

Table S34. *Control measure spectrum of the sensing particles emission (left) and emission spectrum of the particles before and after exposure to TATP vapors (right) in Experiment 4.*

<u>EXPERIMENT 5.</u> 30-minute exposure to **TATP. Newly synthesized compound, silica particles, compound adsorbed one day before. Acquisition time 100000 µs (default value). LED intensity = 2%.**

The fluorescence emission spectra collected by the robot during the experiment are shown in **Table S35**.

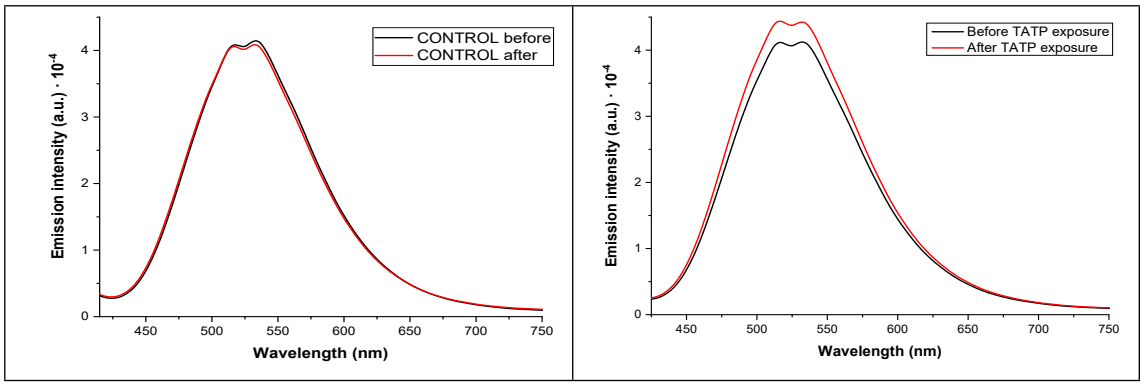

Table S35 *Control measure spectrum of the sensing particles emission (left) and emission spectrum of the particles before and after exposure to TATP vapors (right) in Experiment 5.*

RESULTS SUMMARY

Finally, variation of the fluorescence emission at the wavelength of maximum emission (525 nm) is calculated for each experiment. The emission of the sensing particles increased by an average of **6.945 ± 0.659 %** over the 5 experiments, with a standard deviation of 0.530.

The graphs shown in **Table S36** were obtained as a graphic representation of the conclusions:

SUMMARY	
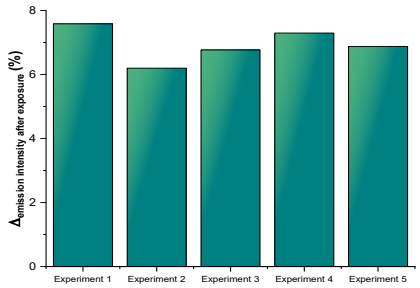	2D bar chart representing the variation (%) of the fluorescence emission of the robot sensing particles in Experiments 1 to 5.
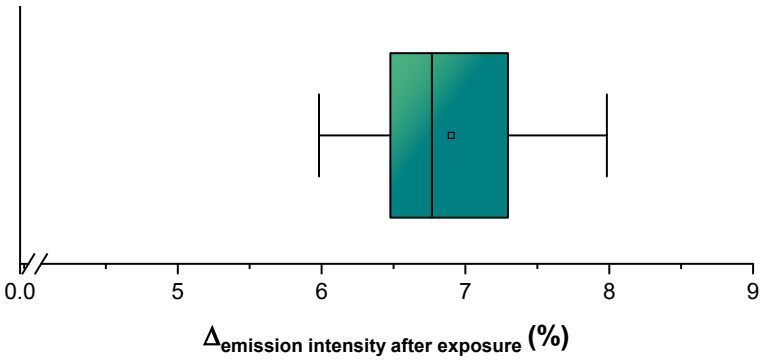	Box and Whisker plot representing the variation (%) of the fluorescence emission of the robot sensing particles in Experiments 1 to 5.

Table S36*. Joint representations of the data corresponding to Experiments 1 to 5.*